731

334
3/26

MASTER

SNAP-21 PROGRAM, PHASE II

DEEP SEA RADIOISOTOPE-FUELED THERMOELECTRIC GENERATOR POWER SUPPLY SYSTEM

QUARTERLY REPORT NO. 10

Space and Defense Products
ELECTRICAL PRODUCTS GROUP
3-M CENTER, ST. PAUL, MINN. 55101, PH 633-9400
3M COMPANY

DISCLAIMER

Report No. MMM 3691-44

AEC RESEARCH AND DEVELOPMENT REPORT

This report has been prepared under Contract AT(30-1)3691
with the U. S. Atomic Energy Commission

SNAP-21 PROGRAM, PHASE II

DEEP SEA RADIOISOTOPE-FUELED THERMOELECTRIC GENERATOR POWER SUPPLY SYSTEM

QUARTERLY REPORT NO. 10

Period Covered

October 1, 1968 to December 31, 1968

Prepared by

SNAP-21
Technical Staff

Approved by

J. Brandt
Manager,
SNAP-21 Program

Issued by

Space and Defense Products

MINNESOTA MINING AND MANUFACTURING COMPANY

ST. PAUL, MINNESOTA 55101

page blank

LEGAL NOTICE

page blank

DISTRIBUTION LIST

	No. of Copies
U.S. Atomic Energy Commission Division of Reactor Development and Technology Washington, D.C. 20545 Attn: S.J. Seiken	5
U.S. Atomic Energy Commission New York Operations Office 376 Hudson Street New York, New York 10014 Attn: L. Wasser	2
U.S. Atomic Energy Commission NY Patents Group Upton, New York 11973	1
Director, Nuclear Engineering Division Naval Facilities Engineering Command Washington, D.C.	1
U.S. Atomic Energy Commission RDT Site Office, 3M Company 2501 Hudson Road Space Center, Building 551 St. Paul, Minnesota 55119 Attn: John J. Stefano	1
Isotopes Development Center ORNL Post Office Box X Oak Ridge, Tennessee 37830 Attn: R.A. Robinson	2
Hittman Associates, Inc. Technical Information Department 9190 Red Branch Road Columbia, Maryland 21043	1

TID-4500
Category UC-33

page blank

TABLE OF CONTENTS

TABLE OF CONTENTS (Continued)

LIST OF FIGURES

LIST OF FIGURES (Continued)

LIST OF FIGURES (Continued)

page blank

LIST OF TABLES

1.0 SUMMARY

The most significant technical accomplishments on the SNAP-21 Program during this period were:

- System S10D2 put on long-term test
- Completed environmental testing and post-environmental analysis of System S10D3
- Completed assembly of Systems S10P1 and S10P2
- Initiated assembly of Systems S10P3 and S10P4
- Completed fueling of Systems S10P1 and S10P2
- Biological shields (11 and 12) were received and inspected by 3M Company, then shipped to Linde
- Completed encapsulation and evaluation of two radiation plugs
- Completed engineering analysis of B10D4, Topical Report (MMM 3691-40)
- Completed assembly and testing of B10DL1, B10DL2, and B10DL3
- Completed assembly of Insulation System B10DL4 and partial assembly of B10DL5
- Modification to generators A10P2, A10P3, A10P4, and A10P5 was completed
- Completed Final Development Test Plan for fueled systems

2.0 TASK I – 10-WATT SYSTEM

2 1 SYSTEMS

2 1 1 System S10D2

System S10D2 is the first electrically heated system which contains all Phase II design components. The objective of this unit is to have a system on long-term test and thereby have a "standard" of comparison with future SNAP-21 systems.

The planned test sequence for this unit is as follows:

a) Electrical and Thermal Performance

b) Dynamic Test

c) Electrical and Thermal Performance

d) Hydrostatic Pressure Test

e) Electrical and Thermal Performance

f) Long-Term Test

Following is the effort expended on this system during this report period.

After completing the shipping container's optimum ventilation test last quarter, System S10D2 was allowed to stabilize at BOL input power (with generator short circuited and with the upper and center cooling fin assemblies attached). The lower fin assembly was used for System S10D3.

Two additional tests were conducted prior to initiation of long-term performance testing. The first test was designed to determine the maximum system handling

time. For this test the cooling fins were removed with the system on the test stand. Temperatures were recorded at 15 minute intervals until the average cold junction approached the maximum safe temperature of 180°F.* For this cold junction temperature, the average hot junction temperature was 1100°F.

The temperature data is found in Table 2-1 and the average cold junction heat-up curve is shown in Figure 2-1. Refer to Figure 2-2 for thermocouple locations.

The data supports the conclusion that the system will not be endangered if the cooling fins are removed when the room ambient temperature is approximately 72°F or less, and if the thermopile is short circuited. In later systems, those in which the generator has nickel plated cold caps, the maximum cold junction temperature is increased to 225°F. This has the effect of increasing the safety factor when removing the cooling fins in a 72°F ambient room temperature.

The system was then immediately placed into a water tank and the short circuit load resistor across the thermopile was removed. Temperatures were monitored and recorded at 30-minute intervals under open circuit conditions. The average hot junction maximum temperature was to be the open circuit test limiting point. After seven hours at open circuit, the average hot junction temperature had risen to 1034°F, as shown in Figure 2-3 and and Table 2-2.

Because of the slow increase in average hot junction temperature, the test was terminated after seven hours and a rated load resistor (57.6 ohms) was connected across the system output. The decrease in average hot junction temperature is also shown in Figure 2-3 and Table 2-2.

From the open circuit testing, the conclusion was drawn that the average hot frame temperature would not reach the maximum limit of 1100°F if the load resistor were to burn out (system open circuit condition) while in the environmental water tank during long- or short-term testing.

Following the termination of the open circuit testing, long-term performance testing was initiated on October 18, 1968. Long-term testing continued for the balance of this report period.

*Cold caps in generator A10D4 are not nickel plated.

Table 2-1. System S10D2 Interim Handling Time-Test with Generator Short Circuited

224 Watts Input	Seg. Ring at Pressure Vessel	Cold Frame Center	Average Cold Junction	Average Hot Junction	Average Hot Frame (Ext)	Emitter Center	Ambient
Stabilization	98	118	150	926	996	1250	72
Cooling Fins Removed	99	118	151	926	996	1250	72
15 minutes	102	122	154	930	998	1250	72
30 minutes	105	125	157	932	999	1250	72
45 minutes	106	128	160	934	1000	1251	72
60 minutes	110	130	162	935	1001	1252	72
75 minutes	112	132	164	936	1002	1252	72
90 minutes	114	134	166	937	1003	1252	72
105 minutes	115	135	168	938	1005	1253	72
120 minutes	118	138	169	939	1006	1254	72
135 minutes	118	140	171	940	1007	1254	72
150 minutes	118	140	171	940	1007	1254	72
165 minutes	119	140	172	941	1007	1254	72
180 minutes (Placed in Water Tank)	61	90	125	905	970	1221	72

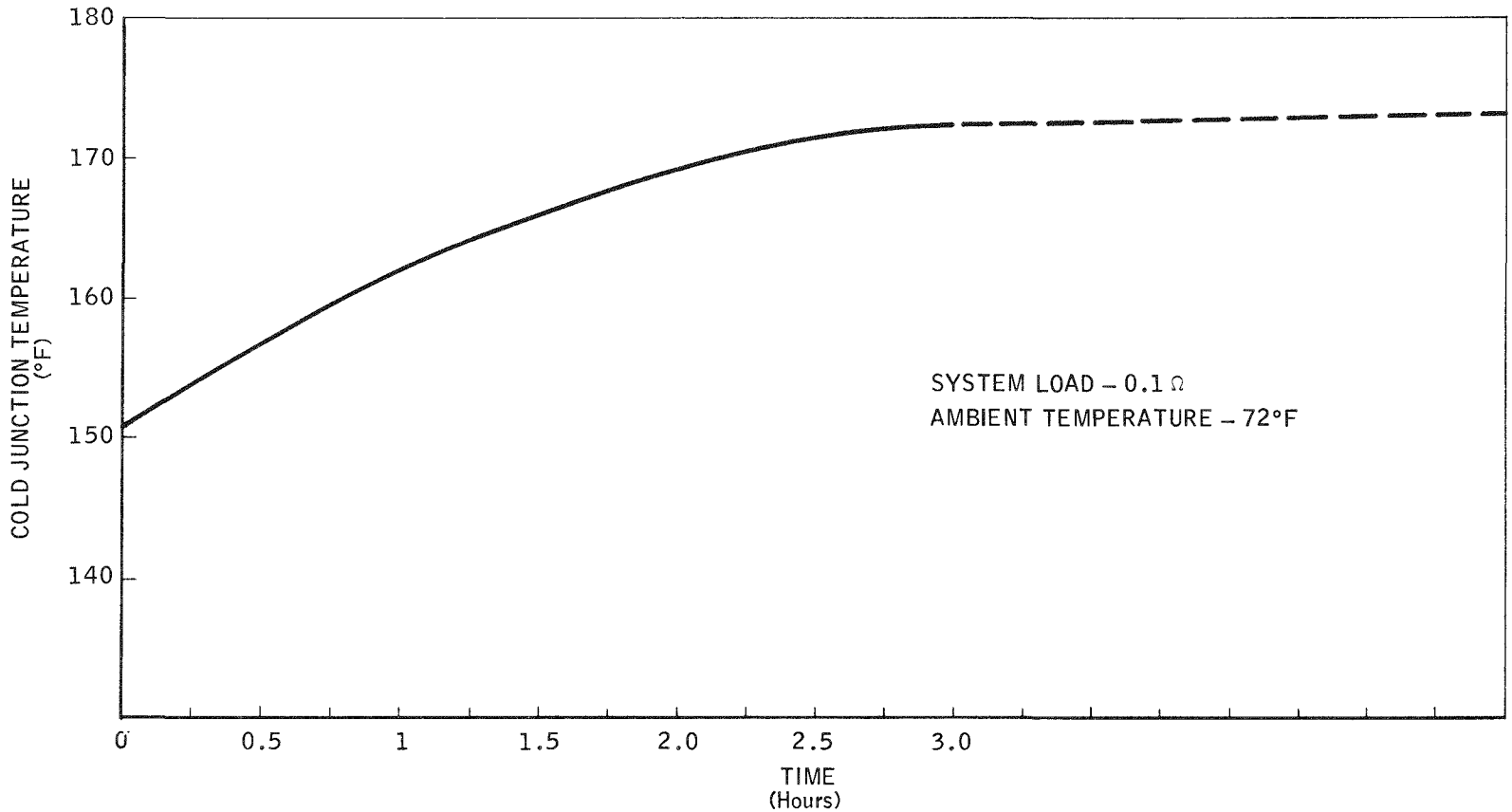

Figure 2-1. SNAP-21 System S10D2 – Heat-Up with Fins Removed

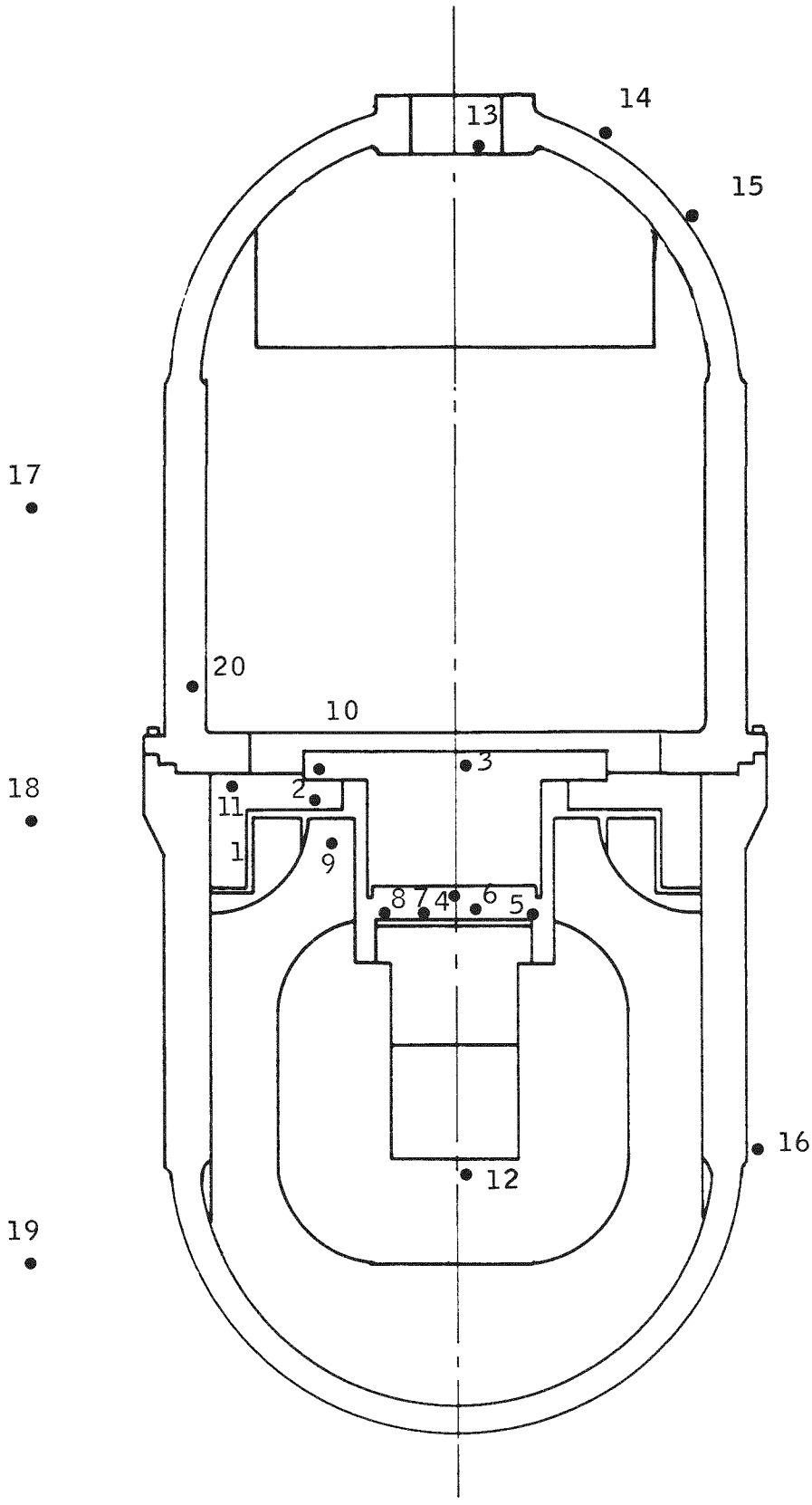

Figure 2-2. System S10D2 Instrumentation

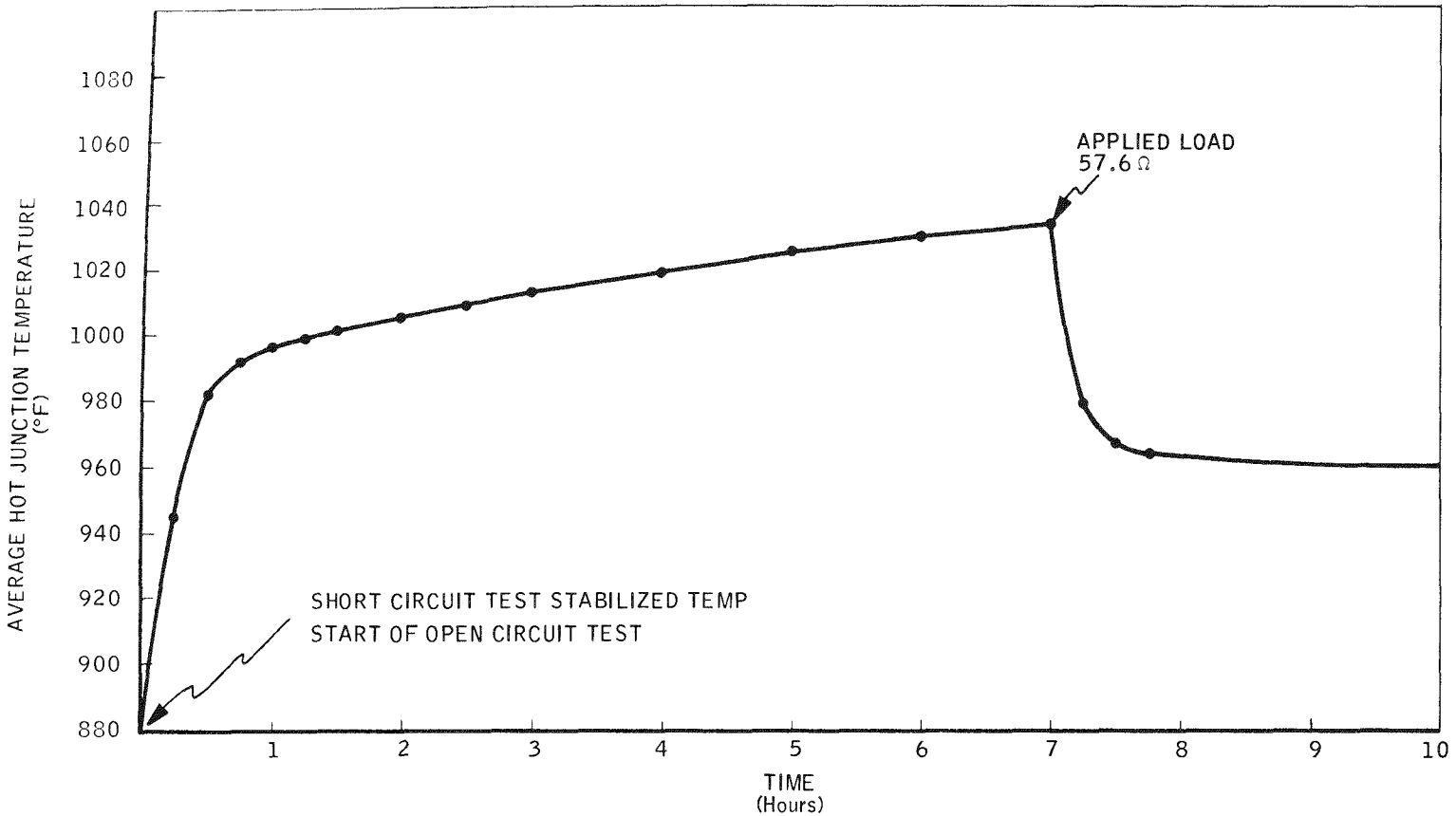

Figure 2-3. SNAP-21 System S10D2 – Open Circuit Test

Table 2-2. System S10D2 Open Circuit Test in Water Tank

224 Watts Input	Seg. Ring at Pressure Vessel	Cold Frame Center	Average Hot Frame (Ext)	Average Hot Button	Emitter
Short Circuit in Water Tank	40	62	953	880	1226
Open Circuit Test	40	62	953	880	1226
15 minutes				945	
30 minutes	41	58	1057	982	1254
45 minutes				992	
1 hour	42	59	1073	997	1263
1 hour 15 minutes				999	
1 hour 30 minutes	42	59	1077	1002	1266
2 hours	43	60	1081	1005	1270
2 hours 30 minutes				1009	
3 hours	42	61	1088	1013	1276
4 hours	43	61	1095	1019	1282
5 hours	41	60	1101	1025	1287
6 hours	42	60	1106	1030	1292
7 hours (applied load 57.6 ohms)	43	61	1113	1034	1299
15 minutes				979	
30 minutes				967	
1 hour				963	

Tables 2-3, 2-4 and 2-5 show typical performance data for the system. Figure 2-4 shows TEG and system performance. Shown on Figure 2-37 are the ratios of experimental to theoretical: Seebeck voltage, resistance,* and matched load power. From the data it can be seen that the performance for the system has been stable this past report period.

Further analysis of the data for System S10D2 has indicated that the emissive coating of the emitter plate might have come off the emitter plate. As was reported in SNAP-21 Quarterly No. 8, the emitter temperature increased about 20°F after it was shipped from 3M Company to Sandia for shock and vibration. This corresponds to an emittance change from 0.88 to 0.73. This change in emitter temperature appears to have only a slight effect on system performance. The system has been stable since the occurrence.

Conclusive proof as to whether or not a loss of emissive coating caused the change in emitter temperature can only be established by disassembly of the system A decision on this has not been made

2 1 2 System S10D3

System S10D3 is the second electrically heated system assembled using all Phase II design components The objective of this unit is to obtain long-term test data to evaluate the effect of time on system performance

The planned test sequence for this unit is as follows:

a) Electrical and Thermal Performance

b) Dynamic Test

c) Electrical and Thermal Performance

d) Hydrostatic Pressure Test

e) Electrical and Thermal Performance

f) Long-Term Test

Following is the effort expended on this system during this report period

*Theoretical resistance includes only material resistance

Table 2-3. System S10D2 Temperature Profile in Water

Thermocouple Location (See Figure 2-)	Identification	Pre-Dynamic Test 4/28/68 (°F)	Post-Hydro Test 9/4/68 (°F)	Long-Term Test 11/15/68
1	Segmented Ring at Pressure Vessel Wall	39	43	45
2	TEG Mounting Plate (inner)	50	54	56
3	TEG Cold Frame Center (external)	58	63	65
4	TEG Hot Frame Center (external)	1042	1040	1041
5	TEG Hot Frame Edge (external)	1047	1046	1046
6	Emitter Center	1254	1277	1278
7	Emitter Midway	1262	1287	1287
8	Emitter Edge	1305	1332	1332
9	Insulation System Upper	97	103	103
10	TEG Cold Frame Outer (external)	53	59	60
11	TEG Mounting Plate Male	42	47	49
12	Heater Block Bottom	1435	1470	1471
13	Power Conditioner Base	44	41	-
14	Pressure Vessel, Cover Upper	40	40	41
15	Pressure Vessel, Cover Center	40	41	40
16	Pressure Vessel Body Lower	40	41	40
	TEG Hot Frame (internal) – Edge	1012	1014	1009
	TEG Hot Frame (internal) – Center	999	998	993
	Hot Electrode – Edge	999	1001	996
	Hot Electrode – Center	976	976	971
	Cold Electrode – Edge	95	98	96
	Cold Electrode – Center	91	94	93

Table 2-3. System S10D2 Temperature Profile in Water (Continued)

Thermocouple Location (See Figure 2-)	Identification	Pre-Dynamic Test 4/28/68 (°F)	Post-Hydro Test 9/4/68 (°F)	Long-Term Test 11/15/68
	Cold Frame (internal) – Edge	82	83	82
	Cold Frame (internal) – Center	74	72	72
	Follower – Edge	81	84	83
	Follower – Center	80	81	81
17	Water – Top	40	40	39
18	Water – Middle	40	40	39
19	Water – Bottom	39	40	39

Table 2-4. System S10D2 Electrical Performance

Item	4/24/68	9/4/68	11/15/68
System Power Input (corrected-watts)	218*	218*	220*
Generator Primary Load Voltage (vdc)	5.32	5.29	5.30
Generator Bias Load Voltage (vdc)	0.739	0.734	0.736
Generator Primary Load Current (amperes)	2.89	2.80	2.78
Generator Bias Load Current (amperes)	0.142	0.138	0.136
Generator Primary Power Output (watts)	15.30	14.81	14.73
Generator Bias Power Output (watts)	0.105	0.101	0.100
Generator Total Power Output (watts)	15.405	14.91	14.83
Conditioner Primary Voltage Input (vdc)	5.31	5.26	5.27
Conditioner Bias Voltage Input (vdc)	0.734	0.724	0.726
Conditioner Primary Current Input (amperes)	2.89	2.80	2.78
Conditioner Bias Current Input (amperes)	0.142	0.138	0.136
Conditioner Primary Power Input (watts)	15.25	14.73	14.65
Conditioner Bias Power Input (watts)	0.104	0.099	0.098
Conditioner Total Power Input (watts)	15.35	14.82	14.74
System Load Voltage (vdc)	24.6	24.5	24.48
System Load Current (amperes)	0.428	0.426	0.426
System Load (ohms)	57.48	57.38	57.5
System Power Output (measured)* (watts)	10.53	10.46	10.43
Test Hours	233.0	1771	3502

*Actual power input after watts transducer was recalibrated and lead losses subtracted.

Table 2-5. Thermoelectric Performance, Generator A10D4 in System S10D2

Parameter	4/24/68	9/4/68	11/15/68
Primary Open Circuit (volts)	9.46	9.40	9.30
Primary Load Voltage (volts)	5.32	5.29	5.30
Primary Load Current (amps)	2.87	2.80	2.78
Bias Open Circuit (volts)	1.39	1.37	1.37
Bias Load Voltage (volts)	0.739	0.734	0.736
Bias Load Current (amps)	0.142	0.138	0.136
Internal Resistance (ohms)	1.43	1.46	1.43
Total Power Output (watts)	15.40	14.91	14.83

Environmental testing and post-environmental analysis was completed this past quarter. Table 2-6 gives the test sequence for System S10D3.

Table 2-6. System S10D3 Test Sequence

Test	Facility	Comments
Short-Term Performance	3M Company	Water tank with the temperature of the water at 38°F – 42°F
System Check-Out	3M Company	Cooling manifold used to maintain cold end temperatures
System Check-Out and Shock and Vibration	Sandia	Shock and vibration to specification
Check-Out and Hydrostatic	Southwest Research Institute	Hydrostatic test to specification
Post-Environmental Analysis	3M Company	Min-K 1999 in radiation gap and spalling of emissive coating cause for degradation
Long-Term Test	3M Company	Awaiting decision on re-assembly

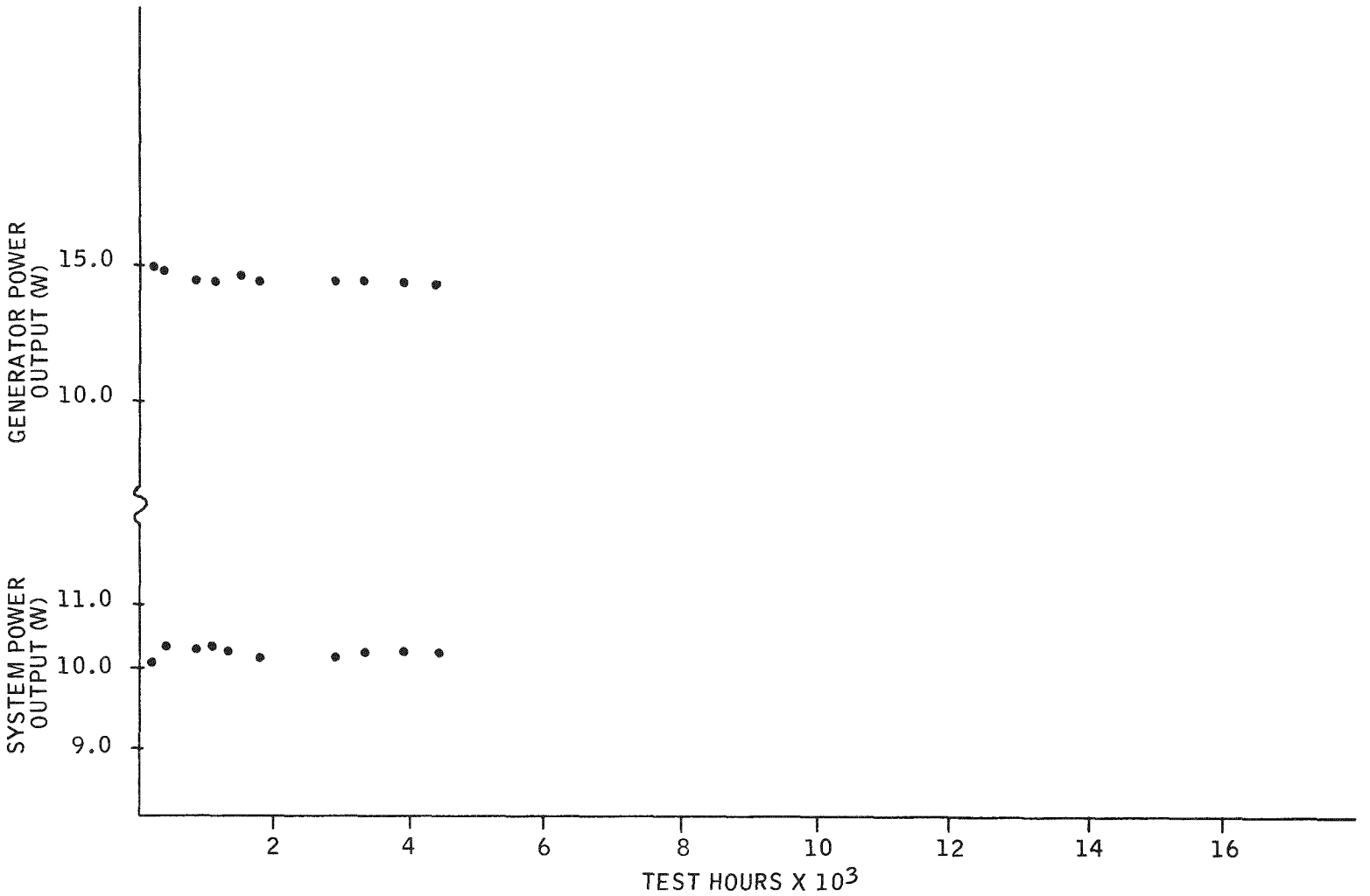

Figure 2-4. System S10D2 Performance

The system showed higher emitter plate temperatures, and lower hot frame temperatures while undergoing vibration in the X axis. The primary cause for this change in thermal profile was the migration of Min-K 1999 between the emitter and collector, and secondary cause was the spalling of the emissive coating from the emitter plate. The system is presently disassembled and a decision will be made early next quarter on the disposition of the system.

Following are the results of the environmental testing and post-test analysis:

2 1 2 1 Shock and Vibration

The shock and vibration was conducted at Sandia Test Laboratories from October 11, 1968 through October 14, 1968.

Upon arrival at the test facility, the system and equipment were unpackaged and inspected for transportation damage. The cooling manifolds were attached, the monitoring and controlling instrumentation connected, and heat-up was initiated.

During the heat-up period, a dummy load equal to system weight was placed in the shock and vibration fixture and attached to the vibration machine. Vibration control instrumentation was calibrated and adjusted to give the optimum pulse for shock testing. This information was recorded on tape to be played back during the system shock testing. This calibration was conducted in the three test axes.

After three days of system heat-up, the test unit was transferred to the shock and vibration fixture and was allowed to stabilize. The system was subjected to the required levels and durations for vibration and shock, as indicated below:

Vibration

5-6 Hz at 0.7 in. displacement

6-26 Hz at 1.3 g peak acceleration

26-40 Hz at 0.036 in. displacement

40-50 Hz at 3.0 g peak acceleration

Sweep three times 5-50-5 Hz in three axes in a period of 45 minutes per axis.

Shock

Terminal peak sawtooth wave pulse with a magnitude of 6 g and a duration of 6 milliseconds.

Three shock pulses in each direction of the three major axes (total 18 shocks).

System performance readings were taken before and after each axis of vibration and each three shock pulses. See Table 2-7. Figure 2-5 shows the emitter plate and average hot frame temperatures versus time throughout the shock and vibration testing.

The system successfully completed the vibration and shock requirements in the vertical (Z) axis. During and following the vibration in the two horizontal axes (X and Y), the hot frame temperatures decreased and the thermoelectric generator output dropped. The heater plate (emitter) temperature also increased until the temperature difference between the average hot frame and heater plate (emitter) had increased from 230°F to 322°F.

The changes in temperatures did not begin until after the higher frequency (above 20 Hz) phase of vibration in the X axis. The strongest indication, however, was that Min-K entered the gap between the emitter and the collector during the vibration sequence of dynamic testing. Very little Min-K is necessary to cause this temperature difference. The amount necessary to cause the temperature distribution finally attained is only enough to make a thin film over the emitter to block 38 percent of the radiant heat transfer.

The shock testing in the horizontal axes (X and Y) was completed and did not seem to contribute to the performance degradation. Following the vibration and shock testing, the system was allowed to restabilize before input power was terminated and cool-down initiated. It was decided to continue on with hydrostatic testing.

Table 2-7. Shock and Vibration, System S10D3

214 Watts Input	Seg Ring at Pressure Vessel	Cold Frame	Hot Frame Center	Hot Frame Edge	Emitter	Room Ambient	Receptacle Ref	Vgbr (V DC)	Vgpr (V DC)	Egbo (V DC)	Vgbl (V DC)	Egpo (V DC)	Vgpl (V DC)	Vsr (V DC)	Eso (V DC)	Vsl (V DC)	Pgp (Watts)	Pgb (Watts)	Pg (Watts)	Rg (Ohms)	Pso (Watts)	Rsl (Ohms)	Test Hours
Stabilization	71	90	1020	1030	1260	76	73	0 0059 0 118	0 0103 2 63	1 33	0 674	9 07	4 98	0 0426	9 07	24 5	13 10	0 0795	13 180	1 644	10 44	57 51	300 4
Before Z Axis Vibration	70	90	1020	1030	1260	77	73	0 0059 0 118	0 0103 2 63	1 33	0 674	9 07	4 98	0 0426	9 07	24 5	13 10	0 0795	13 180	1 644	10 44	57 51	301 4
After Z Axis Vibration	70	90	1022	1032	1256	79	8	0 0059 0 118	0 0106 2 69	1 33	0 673	9 11	4 99	0 0426	9 11	24 6	13 22	0 0804	13 279	1 644	10 48	57 75	302 6
Before Z Axis Shock	70	90	1019	1029	1254	81	73	0 0059 0 118	0 0106 2 69	1 33	0 643	9 06	4 98	0 0426	9 08	24 6	13 20	0 0794	13 279	1 644	10 48	57 75	304 9
After Z Axis Shock	70	90	1019	1029	1254	83	74	0 0059 0 118	0 010 2 63	1 32	0 672	9 07	4 98	0 0426	9 07	24 5	13 10	0 0793	13 179	1 644	10 44	57 51	306 1
After Z Axis Shock	70	90	1018	1028	1253	82	8	0 0059 0 118	0 0106 2 69	1 33	0 672	9 07	4 98	0 0426	9 08	24 6	13 17	0 0803	13 249	1 644	10 48	57 75	306 9
System Transfer (After)	70	88	1018	1029	1251	80	74	0 0059 0 118	0 010 2 63	1 32	0 643	9 07	4 98	0 0426	9 07	24 5	13 10	0 0794	13 179	1 644	10 44	57 51	371 9
Before Y Axis Vibration	68	88	1018	1029	1252	80	73	0 0059 0 118	0 010 2 63	1 33	0 643	9 07	4 98	0 0426	9 07	24 5	13 10	0 0794	13 179	1 515	10 44	57 51	373 2
After Y Axis Vibration	68	88	988	1000	1251	86	73	0 0059 0 118	0 0093 2 48	1 26	0 6	8 61	4 [illegible]	0 0426	8 62	24 5	12 33	0 0797	12 410	1 457	10 44	57 51	374 4
3 Hours After Y Axis Vibration	68	86	986	998	1252	83	4	0 0059 0 118	0 00 4	1 2	0 6	8 61	4 96	0 0426	8 62	24 5	12 30	0 0797	12 380	1 461	10 44	57 51	377 4
After Y Axis Shock (6 Hours After Vibration)	69	88	988	1000	1253	79	71	0 0059 0 118	0 0093 2 48	1 26	0 643	8 61	4 96	0 0426	8 62	24 5	12 30	0 0797	12 380	1 477	10 44	57 51	380 4
After Y Axis Shock	70	88	990	1002	1254	80	72	0 0059 0 118	0 0093 2 48	1 26	0 674	8 66	4 97	0 0426	8 62	24 5	12 33	0 0797	12 410	1 477	10 44	57 51	380 9
Before X Axis Vibration	70	88	991	1003	1255			0 0059 0 118	0 0100 2 66	1 2	0 6	8 68	4 97	0 0426	8 68	24 5	12 43	0 0797	12 510	1 473	10 44	57 51	381 4
After X Axis Vibration	68	86	942	953	1268	78	2	0 0059 0 116	0 0082 2 30	1 17	0 663	8 01	4 83	0 0413	8 02	23 9	11 11	0 0769	11 190	1 372	9 92	57 39	382 6
After X Axis Shock	70	88	936	947	1268	78	78	0 0057 0 114	0 0081 2 28	1 16	0 6 [illegible]	7 83	4 80	0 0413	7 94	23 7	10 94	0 0751	11 015	1 362	9 79	57 38	383 2
After X' Axis Shock	70	87	936	948	1268	78	5	0 00 0 114	0 0081 2 28	1 17	0 660	[illegible]	4 81	0 0413	7 96	23 8	10 97	0 0752	11 045	1 367	9 83	57 63	383 5
14 Hours After X Axis Shock	70	88	966	978	1245	8	73	0 0060 0 120	0 0084 2 [illegible]	1 22	0 677	8 34	4 [illegible]	0 0426	8 34	24 5	11 63	0 0812	11 711	1 431	10 44	57 51	397 4
18 Hours After X' Axis Shock (Stabilization)	69	88	970	981	1298	80	72	0 0059 0 118	0 0093 2 38	1 23	0 678	8 38	4 9[illegible]	0 0426	8 38	24 5	11 78	0 0800	11 860	1 430	10 44	57 51	401 6

DATA IDENTIFICATION

Vgbr	Voltage generator bias circuit across 0 01 ohm shunt	Vsl	System load voltage
Vgpr	Voltage generator primary circuit across 0 04 ohm shunt	Pgp	Thermoelectric generator primary power output
Egbo	Thermoelectric generator bias open circuit voltage	Pgb	Thermoelectric generator bias power output
Vgbl	Thermoelectric generator bias load voltage	Pg	Thermoelectric generator power output
Egpo	Thermoelectric generator primary open circuit voltage	Rg	Thermoelectric generator internal resistance
Vgpl	Thermoelectric generator primary load voltage	Pso	System power output
Vsr	System shunt voltage (0 1 ohm)	Rsl	System load
Eso	System open circuit voltage		

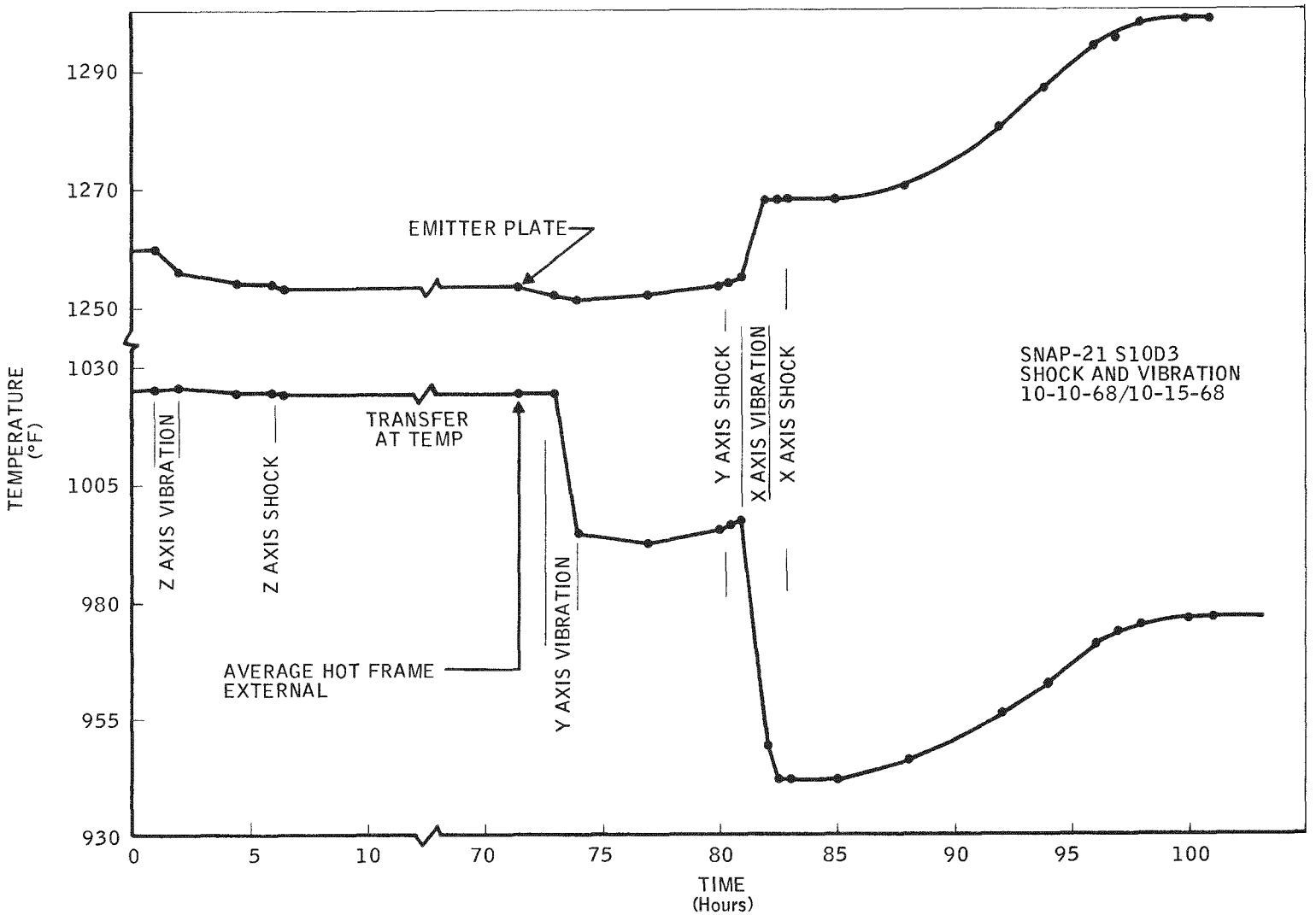

Figure 2-5. Emitter Plate and Average Hot Frame Temperatures versus Time Throughout Dynamic Test of S10D3

Sandia is presently preparing a complete test report on the shock and vibration testing.

2.1 2.2 Hydrostatic Pressure Testing

After completion of dynamic testing the system and equipment were packaged and sent to Southwest Research Institute for hydrostatic pressure testing.

The test system underwent a heat-up in the test stand using the chill rings to establish a reference. It was then placed in a pressure chamber filled with chilled salt water. The chamber was pressurized to 10,000 psi and maintained at that pressure for five hours. System performance was monitored and recorded periodically to determine if any damage had occurred.

Table 2-8 gives pertinent data on the hydrostatic testing of S10D3. As can be seen from the data, the system performance was not affected by the hydrostatic test.

2.1.2.3 Post-Environmental Analysis

The system arrived at 3M Company from Southwest Research Institute on November 4, 1968. The system was disassembled and an analysis was initiated to find the cause for the temperature excursion experienced by S10D3 during shock and vibration.

The upper section of the shipping container was removed, and the X, Y, Z recorder, impactograph, temperature recorders, and charts were examined. It was noted that the paper drive mechanism of the X, Y, Z recorder had not been activated. Even though this did not affect the mechanism from indicating shock, it would be impossible to determine the time. No abnormal excursions were noted on any charts. The recording units and upper half of the shipping container were replaced.

On November 5, 1968, the unit was moved to the fueled system assembly room. The shipping container cover was removed, the recorders checked again, and no adverse movements were noted. The system was removed from the shipping container, and placed in a holding fixture.

Table 2-8. Hydrostatic Test Data Summary

	Prior to Pressurization	After 4.7 hrs. At 10,000 psi	After Pressurization
Segmented Ring at Pressure Vessel	36	34	32
Cold Frame	53	54	54
Hot Frame Center	943	951	942
Hot Frame Edge	954	964	954
Emitter	1282	1284	1281
(Water)	36	34	32
(TEG Bias Current)	0.112	0.114	0.112
(TEG Primary Current)	2.35	2.43	2.38
(TEG Bias Closed Circuit Voltage)	0.682	0.683	0.683
(TEG Primary Closed Circuit Voltage)	4.94	4.95	4.93
(TEG Bias Open Circuit Voltage)	1.19	1.21	1.19
(TEG Primary Open Circuit Voltage)	8.17	8.28	8.16
(TEG Internal Resistance)	1.365	1.369	1.348
Total (TEG Total Power Out)	11.68	12.107	11.806
(System Load Voltage)	24.4	24.4	24.4
(System Power Out)	10.37	10.37	10.35
(System Load Resistance)	57.41	57.41	57.55
Test Hours	564.2	572.4	590.5

The bolts holding the upper half (cover) of the pressure vessel to the lower half (body) were removed. The cover was lifted off and a visual examination indicated no apparent changes from the time it was assembled until disassembly.

An electrical check was made from the pins of the system (Marsh-Marine) external connector to the internal (Blue Ribbon) connectors to check out

instrumentation wiring. The cover was replaced on the body, and electrical checks were made through the system (both male and female Blue Ribbon connectors). No discrepancies were noted in the instrumentation wiring.

After removal of the cover (first time), the body assembly was visually checked. The only item noted was corrosion on the steel bolts which hold the mounting plate to the segmented ring retainer. No apparent changes to the balance of body assembly were noted at this stage of disassembly.

The yellow plastic plugs, the silastic used to hold micro-quartz plugs in position, the micro-quartz plugs, and the Min-K 1999 were removed from the generator cold frame and the generator neck tube annulus. Heater wires, instrumentation wires, ceramic beads and other electrical insulation were removed and cut, as required for disassembly of the generator from the system. The Blue Ribbon connectors were disassembled.

When the copper cold frame was removed from the aluminum mounting plate, moisture was noted at the interface of the two parts. Moisture was also noted later at other metal interfaces when disassembled. This moisture is attributed to condensation from entrapped air in the system during assembly. This moisture will not be present in fueled systems since a desiccant is used to dry up the moisture. All except two generator mounting bolts were removed. By use of a "borescope", lights and mirrors, the annulus between the generator and the neck tube was examined and found to be relatively free of Min-K. Two heater lead cold solder joints were noted.

The body assembly was then turned over in such a manner that the insulation system pressure transducer fitting was 90° to the pivot axis, and followed the rotation so that no load would shift against it as the system was turned over. The remaining two generator mounting screws were removed, and the generator was lowered slowly by use of jacks.

It was noted that loose granular type material of about two tablespoons volume was on the hot frame. This material was analyzed and found to be Min-K.

Discoloration of the micro-quartz around the heater leads and bolt holes of the emitter plate was noted. Yellow Min-K was found in the bolt holes around the

bolts holding the emitter plate to the heater block. Approximately one-third to one-half of the emitter plate surface was scaled off.

2.1.2.4 Evaluation of Disassembled System

An analysis was initiated to find the cause for the temperature excursion experienced by S10D3 during shock and vibration.

Preliminary results indicate that the major cause for the temperature changes were due to the Min-K 1999 which was found between the emitter and hot frame.

It appears that the Min-K entered the radiation gap by a path through the microquartz insulation around the heater and instrumentation leads. Also discovered at the time of teardown was the loss of approximately half of the emissive coating from the upper surface of the radiation disc which exposed the unoxidized base of stainless steel.

Upon examination of the S10D3 radiation disc, there exists two possible explanations. The first is that the oxide coating was too heavy and that the thermal expansion difference between the thick oxide layer and its base metal could not survive thermal cycling. The second possibility is an incompatibility between elements of the system. Even though this seemed remote, the powdered Min-K 1999 that had worked into and around the heater block was analyzed. The results are given in Table 2-9. The analysis indicated varying amounts of stainless steel oxide (a complex nickel-iron-chromium-oxygen compound) dispersed throughout the four samples of Min-K.

In addition, a small amount of Min-K 1999 and anti-seize compound (used on the radiation disc holding bolts) was heated on a sample of oxidized stainless with no deleterious effects to the coating. The only unusual result observed was the change of color of the Min-K from white to yellow. It is suspected that this may be a valence change in the titanium causing a reaction analogous to the zinc oxide transformation.

Table 2-9. Min-K 1999 Analysis

Element %											
Sample	Fe	Cr	Ni	Ti	Si	Mn	Mg	Al	Mo	Cu	O_2
1	0.002	-	-	2	>30	-	0.003	0.01	-	-	Bal.
2	5	1	0.2	3	>30	0.1	0.005	0.03	0.01	0.1	Bal.
3	10	2	0.3	3	>30	0.4	0.005	0.03	0.03	0.2	Bal.
4	8	2	0.8	2	10	0.2	0.003	0.03	0.03	0.2	Bal.
5	20	5	3	0.3	3	0.1	0.003	0.02	0.05	0.3	Bal.

Sample Identification:

1. Min-K 1999 (new)
2. From heater block top – between radiation disc and block
3. Bottom of hot block
4. Under radiation disc next to bolts that hold hot block
5. Hot frame

To check the other possible explanation (that of a thick oxide layer) an attempt to duplicate the failure was made. Five small stainless steel coupons were oxidized at temperatures of 1200, 1400, 1600, 1800 and 2000°F. These samples, along with a new radiation disc (lot 4530), were thermally cycled three times at 1200°F. No effects were observed except in the coupon that was prepared at 2000°F.

This sample lost some of its coating that spalled off upon cooling. No effects were noted on the radiation disc which was subsequently thermally cycled to 1800°F with only a small portion of its coating spalling off. This led to the belief that the radiation disc from lot 4530 and the disc from S10D3 (lot 4601) were not prepared similarly.

Metallographic sections were prepared from both radiation disc in order to determine relative coating thickness. Figures 2-6 and 2-7 indicate a difference in coating thickness of ten to one with the S10D3 disc having the heavier layer. Figure 2-8 shows the edge of the S10D3 radiation disc with its oxide coating that formed while the system was at temperature. The gross difference in coating thickness shows why the radiation disc (lot 4530) retained its coating during thermal cycling and why the disc in S10D3 lost its coating during operation.

Because of the difference noted in the photos, Metallurgical Inc., was contacted to determine any basis for the difference between the oxide coatings. After examination of the heat treat records, it was concluded that the six radiation discs from lot 4601 (S10D3) be treated, two at a time, per 3M specification* in a medium size muffle furnace. Including heat up and cool down time, these discs were at an elevated temperature (>1200°F) for more than an hour. The remaining five discs from this lot are expected to behave similarly to S10D2 where small temperature excursions were noted during moving from 3M to Sandia. However, these temperature changes do not indicate the presence of Min-K between the hot block and radiation disc as in S10D3.

*Specification called for a heat treatment of 0.5 hour at 2000°F. This has been changed to a treatment of about 0.6 hour at about 1550°F.

All Photos 200X

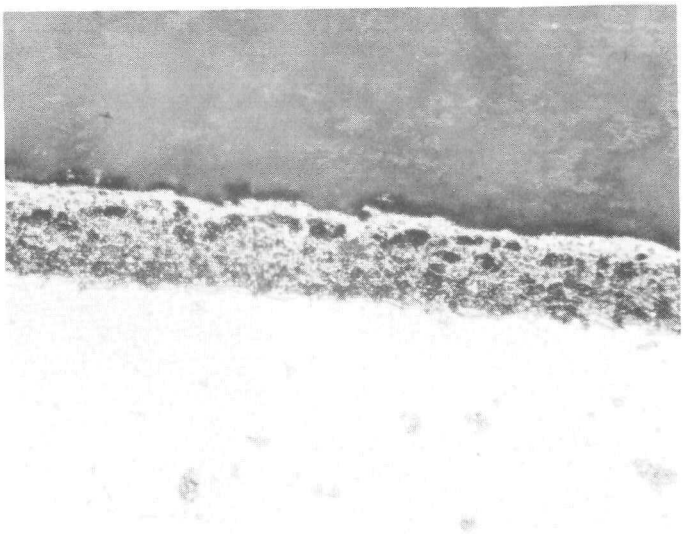

0.005 inch

Figure 2-6. Center Portion of S10D3 Disk

Oxide

Stainless Steel

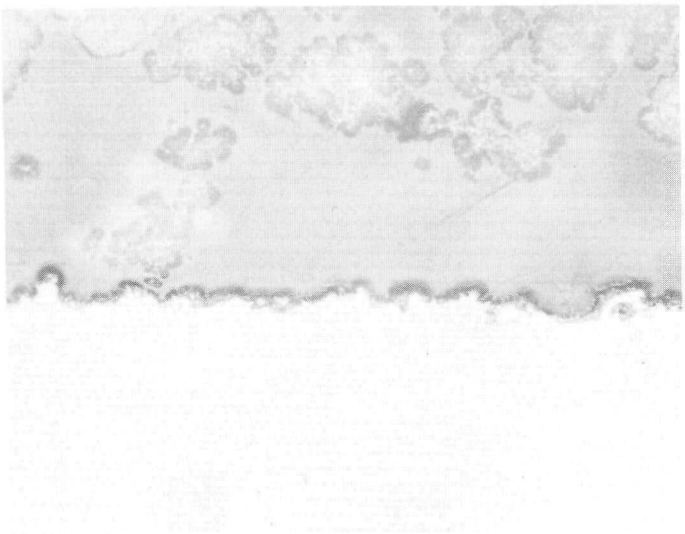

Figure 2-7. Disk from Kit 4539

Oxide

Stainless Steel

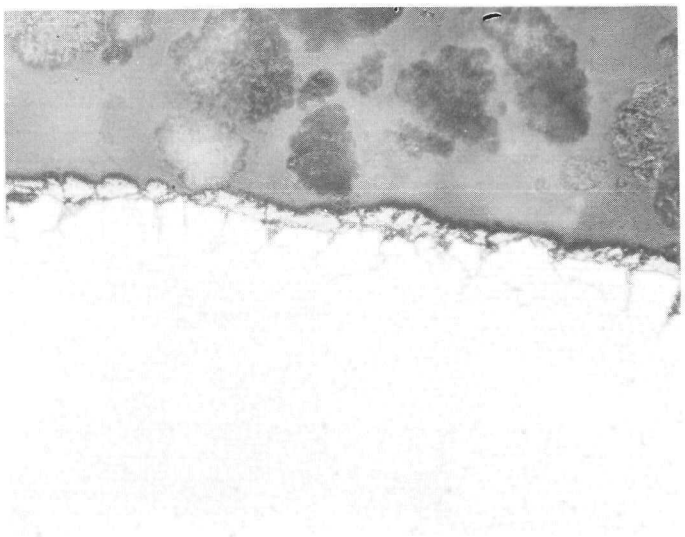

Oxide

Stainless Steel

Figure 2-8. Edge Portion of S10D3 Disk

The six discs from lot 4530 were treated in a very large furnace (20' x 5' x 5') which is often operated under a controlled atmosphere (N_2). It is suspected that lot 4530 was heat treated at 2000°F under a protective atmosphere, and was oxidized only upon placement in the furnace cooling chamber. This process resulted in a thin oxide layer (Figure 2-7). It is unlikely that this process could be exactly duplicated.

It can be concluded that the major cause for the change in thermal profile of S10D3 was the migration of Min-K 1999 into the radiation gap during shock and vibration. A secondary reason for the decrease in performance was the spalling of the oxide coating of the emitter plate. Indications are that thermal cycling was the cause for the spalling of the oxide coating. It appears this happened after the Min-K migration. This cannot be pin-pointed because of the gross disturbance caused by the Min-K in the radiation gap.

From the findings discussed above, the following are recommended:

1) The remaining five radiation discs in lot 4530 may be used in assembly of SNAP-21 systems.

2) The heat treat temperature for future fabrication of radiation discs be lowered from 2000°F to 1500°F.

3) Any remaining discs from lot 4601 should be scrapped.

The Min-K in the radiation gap came from the annulus between the generator case and the neck tube. It entered the radiation gap by filtering past the seal between the end of the generator case and the edge of the radiation disk. This seal consisted of several rings of micro-quartz placed at the bottom of the annulus. The lip on the generator case compresses the rings when installed to make the seal. See Figure 2-9.

It is difficult to maintain a tight seal with an electrically heated system because of the large number of penetrations through the seal. On System S10D3 there were twelve penetrations: 8 heater leads, 1 radiation disk thermocouple and 3 generator hot frame thermocouples. Another factor that made the seal less effective was the counter-bored holes in the radiation disk at the attachment screw locations These counter-bored holes locally relieve compression on the micro-quartz pads and provide an opening for Min-K to enter the radiation gap.

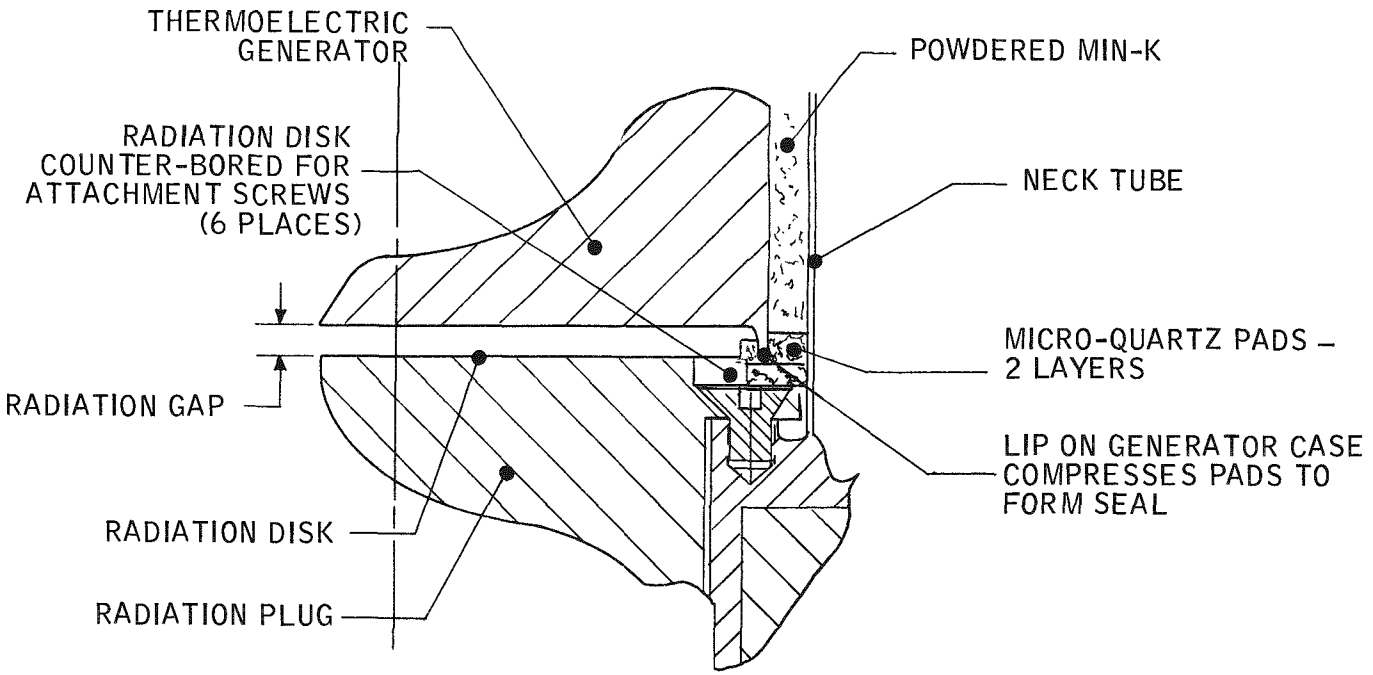

Figure 2-9. Radiation Disk Seal on System S10D3

On a fueled system there will be only three penetrations through the insulation seal (1 radiation disk thermocouple and 2 generator hot frame thermocouples); consequently, the seal problem will be much less severe. To ensure further that the seal will be completely effective, two design changes were incorporated on the fueled systems. First, the counter-bored holes in the radiation disk were filled with stainless steel segments machined to fit the hole and welded to a circular wire that holds them in place. See Figure 2-10.

This assembly is installed over the radiation disk after the attachment bolts are torqued. It makes the outside diameter of the disk continuous and easier to seal.

The second change was to add a double wrap of micro-quartz around the bottom of the generator. This double layer provides a much improved seal against the powdered Min-K (see Figure 2-11). Figure 2-12 is a photograph of the radiation disk with the counter-bored plugs in place and the micro-quartz pads. The double-wrap micro-quartz around the generator (Figure 2-13) is held in place during assembly by cotton thread which burns away when the system reaches operating temperature.

2 1 2 5 Preparation for System Fueling and Shipment

3M was granted a permit, No 5830, from the Department of Transportation to cover over-the-road movement within the country of the SNAP-21 System in its special shipping container

2 1 3 Fueled Systems Assembly

Systems S10P1 through S10P4 are the four isotopic fueled systems All components of all systems will be of the final design All systems will be subjected to environmental and performance tests identical to those performed on S10D3 so that a direct evaluation of fueled versus electrically heated systems can be made After the final electrical and thermal performance tests, three systems will be shipped to the Naval Radiological Defense Laboratory where they will be placed on test in the ocean One system will remain on test in the 3M laboratory

Following is the effort expended on fueled systems during this report period

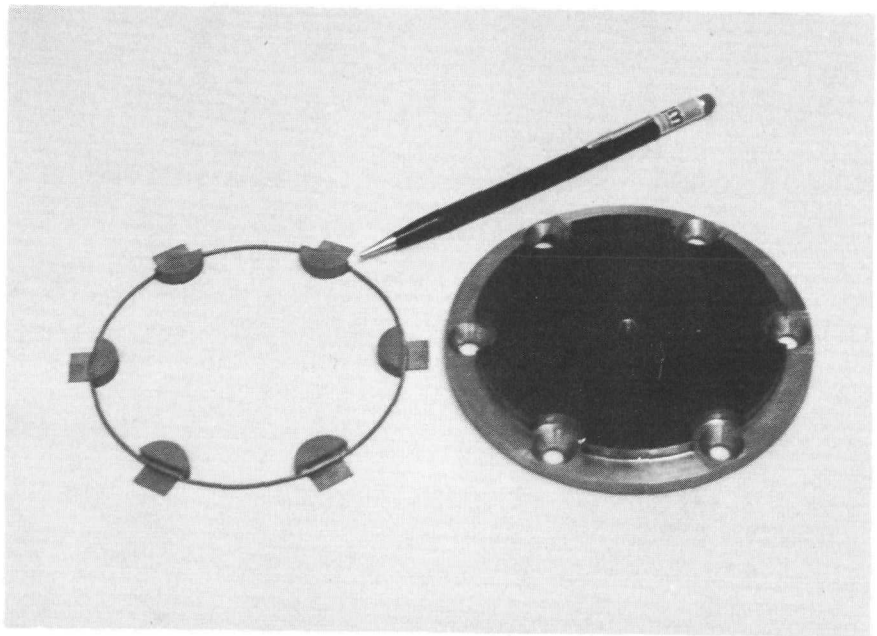

Figure 2-10a. Radiation Disk with Hole Filler Disassembled

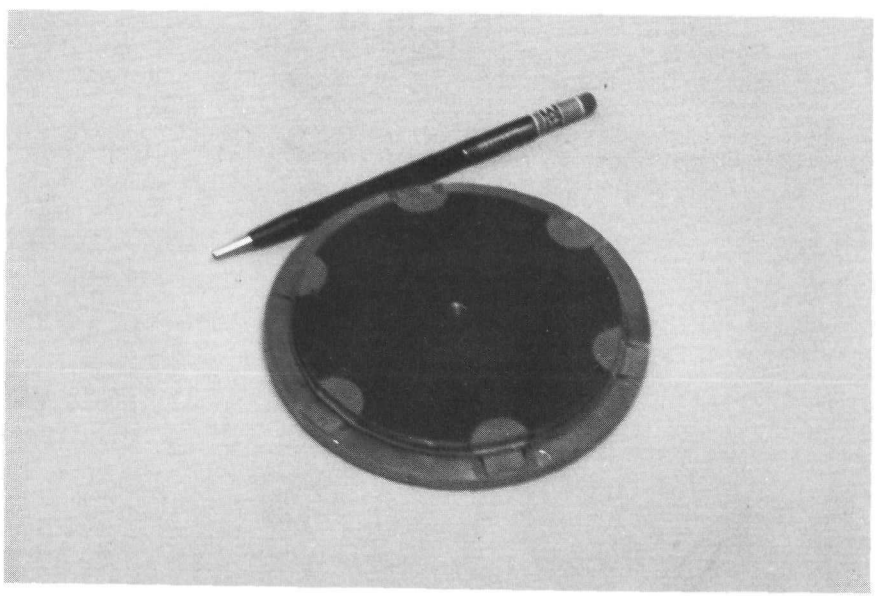

Figure 2-10b. Radiation Disk with Hole Filler Assembled

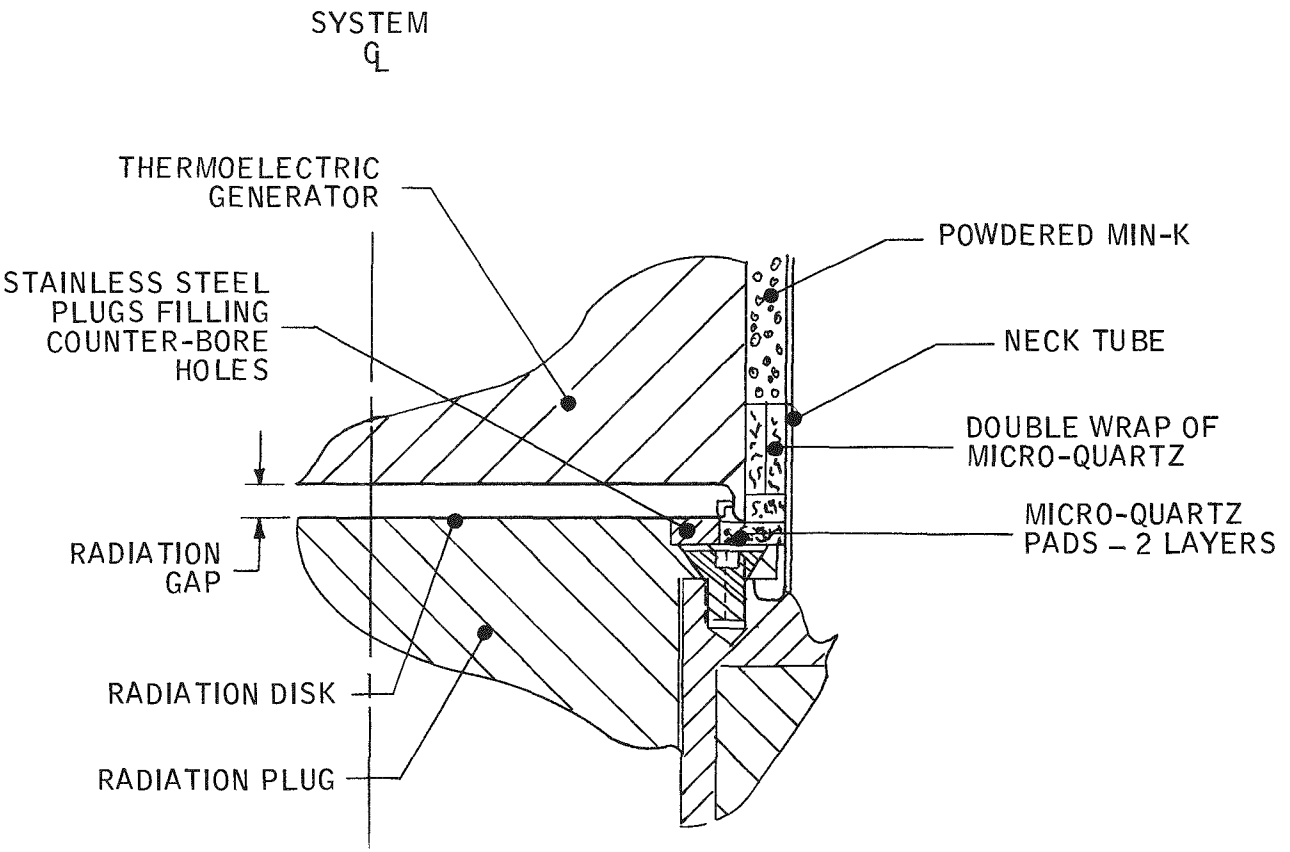

Figure 2-11. Radiation Disk Seal for Fueled Systems

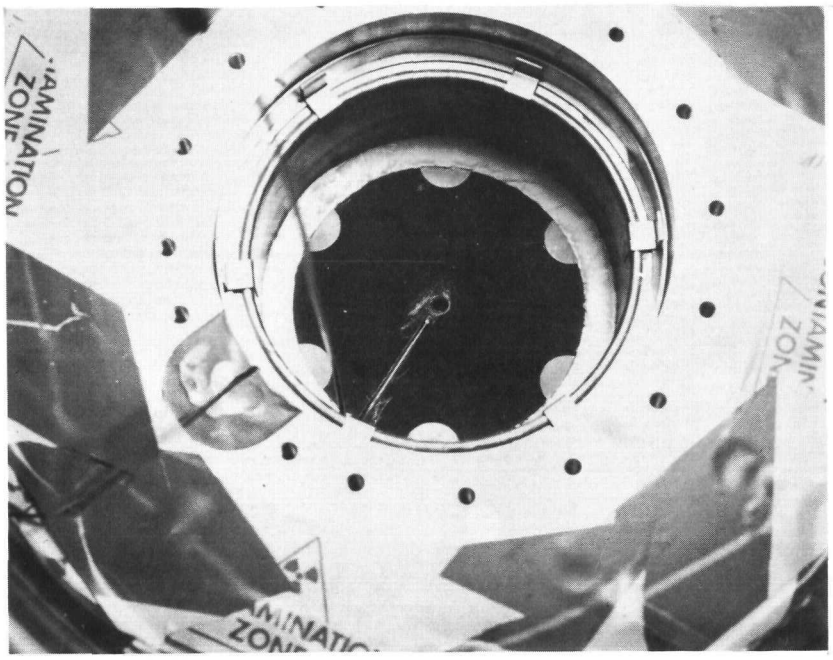

Figure 2-12. Radiation Disk with Counter-Bore Plugs and Micro-quartz Pads in Place

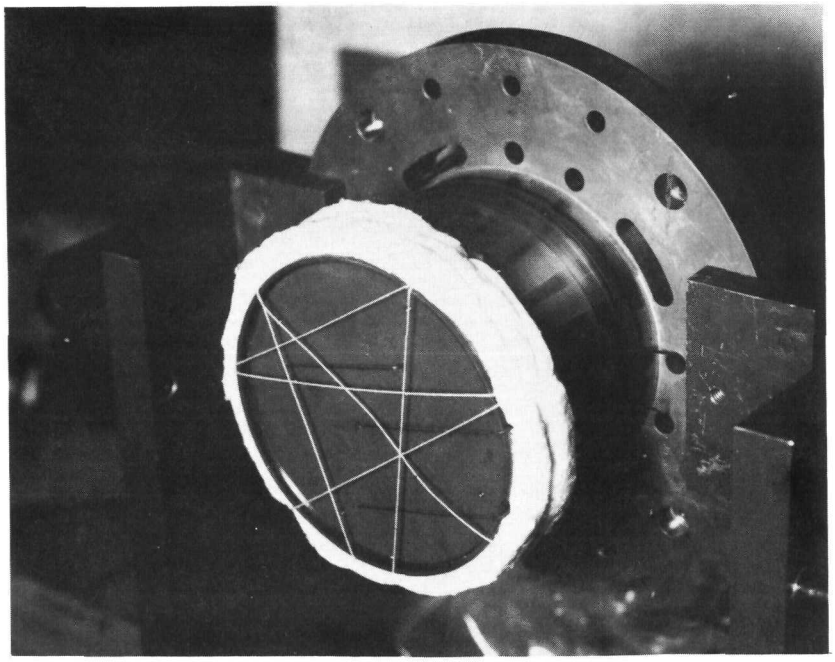

Figure 2-13. Micro-quartz Wrap on Generator Case

Two systems, S10P1 and S10P2, were assembled, and the assembly of the remaining two systems, S10P3 and S10P4, was initiated. With each assembly, the cover of the pressure vessel, which contains the power conditioner, is pre-wired. A cover connects electrically with its pressure vessel body by a receptacle/plug system. The covers of Systems S10P3 and S10P4 are wired and ready for incorporation into their respective systems.

Following wiring of the pressure vessel covers at 3M Company, Systems S10P1 and S10P2 were shipped to Oak Ridge National Laboratory where the remainder of each system assembly was carried out. For shipment, the covers were fastened to empty pressure vessel bodies with the composites secured in the system shipping containers. Shock forces of less than 1 g were encountered on the trips.

The assembly at ORNL is a two-day operation. All steps up to, but excluding, the insertion of the fuel capsule are accomplished the first day. The main steps prior to fueling are: 1) installation of the insulation system into the pressure vessel; 2) assembly and installation of the generator mounting plate and segmented centering ring, and 3) making certain measurements to determine if the radiation disc/hot frame thermal radiation gap will be within specification upon completion of assembly.

Once the fuel capsule is inserted into the shield cavity, the time until completion of system assembly must be kept to a minimum. The system is unable to dump excessive heat efficiently until the pressure vessel cover is firmly in place. To avoid overheating the thermoelectric generator cold end (which could cause thermoelectric leg degradation), the fuel capsule is inserted first; the assembly to completion is not terminated until the pressure vessel cover is in place and some means of cooling (water tank or cooling fins) is provided.

After insertion of the fuel capsule, the shield plug is installed; then the system is removed from the hot cell for the remainder of the assembly. The generator is fastened to the mounting plate, and the annulus between generator long case and insulation system neck tube is insulated by charging Min-K 1999 through ports in the generator cold frame. Once the generator is in place in the system, its cold frame temperature is periodically monitored to watch for any possible thermal excursion. In Systems S10P1 and S10P2, the cold frame temperature

did not rise above 90°F, considerably below the maximum permissible temperature of 180°F.

Following insulation of the generator, the body of the system was wired so that it would mate with the cover to complete the electrical and thermal circuits when the pressure vessel cover was fastened to the body. When the cover of S10P2 was originally installed, several thermocouples failed to register. The cover was removed, the contacts of the plugs and receptacles were cleaned, the cover was replaced, and the thermocouples functioned properly.

With their covers in place, each system was checked out electrically, and then lowered into a refrigerated water tank to establish initial stable reference points for future comparison following static and dynamic testing.

The main components installed in Systems S10P1 and S10P2 are as follows:

System	S10P1	S10P2
Thermoelectric Generator	A10P3	A10P2
Power Conditioner	H10P1	H10P2
Insulation System	B10DL2	B10DL4
Fuel Capsule	12 (212 watts, thermal)	11 (207 watts, thermal)

S10P1 is the first fueled system. All assembly and performance testing was done at ORNL. The system will be shipped from there to Sandia for dynamic testing the early part of next quarter. Tables 2-10 through 2-12 show performance data for system S10P1. From the data, it appears that the system performance is satisfactory.

System S10P1 was removed from the water tank, and its cooling fins were attached prior to installation of the system into its container for shipment to Sandia Corporation for shock and vibration testing. A set of stable reference points was established for the system (fins in place) within the shipping container. System S10P2 will likewise be readied, and the two systems will be shipped together to Sandia.

Table 2-10. Performance Data for System S10P1

Thermocouple Location*	Identification	Reading
1	Segmented Retaining Ring at Pressure Vessel Wall	43
2	Segmented Retaining Ring Inner	55
3	TEG Cold Frame Center (External)	64
4	TEG Hot Frame Center (External)	1048
5	TEG Hot Frame Edge (External)	1064
6	Emitter Center	1248
7	Reference	40
8	Water Top	39
9	Water Center	39
10	Water Bottom	39
	Average Cold Junction (Estimated)	92
	Average Hot Junction (Estimated)	998

*See Figure 2-14.

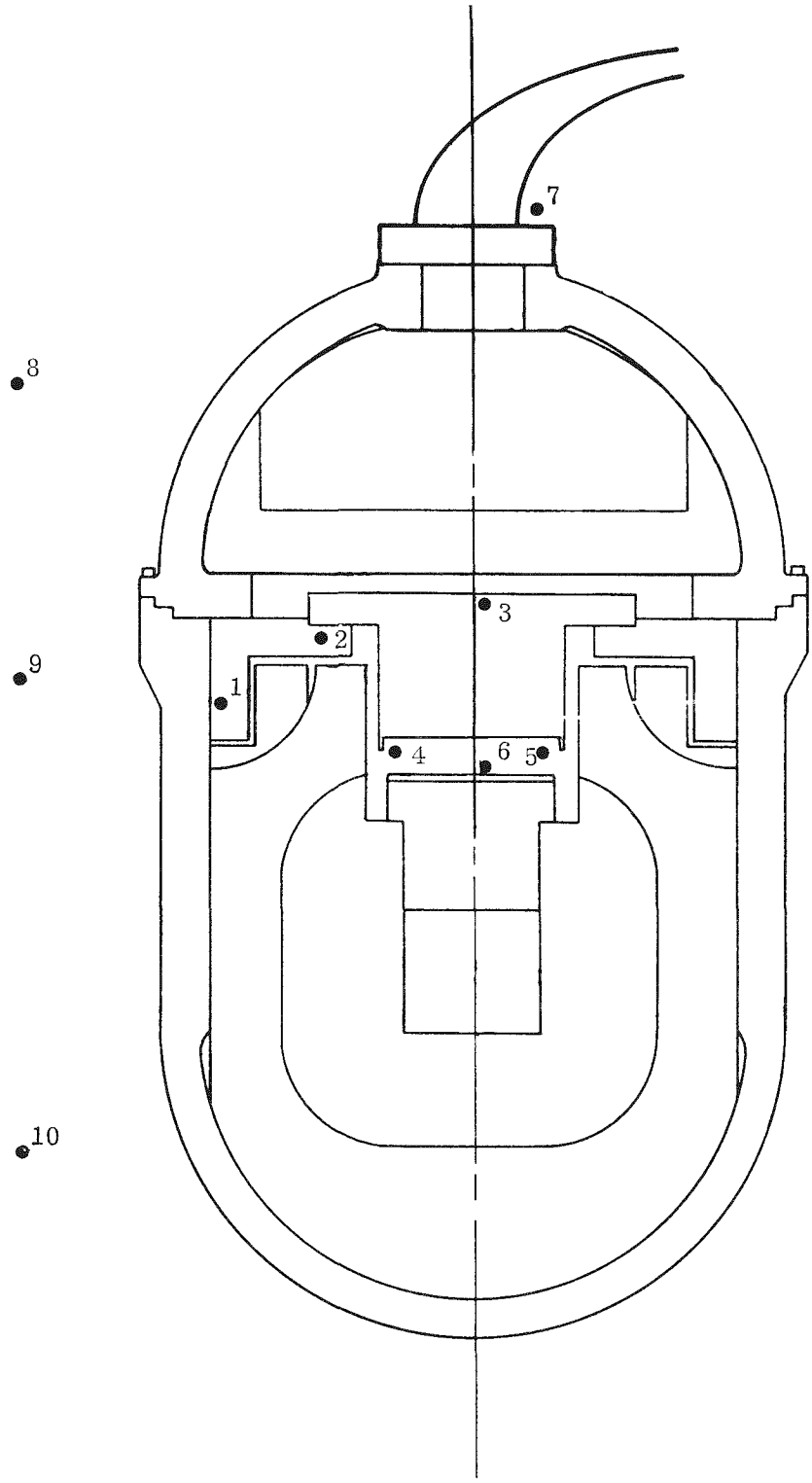

Figure 2-14. System S10P1 Instrumentation

Table 2-11. Performance Data for System S10P1

Item	Reading
System Fuel Input (watts)	211.8
Generator Primary Load Voltage (vdc)	4.98
Generator Bias Load Voltage (vdc)	0.695
Generator Primary Load Current (amperes)	2.82
Generator Bias Load Current (amperes)	0.114
Generator Primary Power Output (watts)	14.07
Generator Bias Power Output (watts)	0.079
Generator Total Power Output (watts)	14.15
Conditioner Primary Voltage Input (vdc)	4.94
Conditioner Bias Voltage Input (vdc)	0.650
Conditioner Primary Current Input (amperes)	2.82
Conditioner Bias Current Input (amperes)	0.695
Conditioner Primary Power Input (watts)	13.95
Conditioner Bias Power Input (watts)	0.074
Conditioner Total Power Input (watts)	14.024
System Load Voltage (vdc)	24.6
System Load Current (amperes)	0.427
System Load (ohms)	57.6
System Power Output (watts)	10.5
Test Hours	139

Table 2-12. Thermoelectric Performance in System S10P1 of Generator A10P3

Parameter	Reading
Primary Open Circuit	9.53
Primary Load Voltage	4.94
Primary Load Current	2.82
Bias Open Circuit	1.39
Bias Load Current	0.114
Internal Resistance	1.60
Total Power Output	14.15

2.2 FUEL CAPSULE

Representative photographs of the graphical output of the ultrasonic inspection of the fuel capsule closure welds are reproduced in Figures 2-15 and 2-16. Each end of a capsule is sealed with a weldment; hence, there are two photos. The detection of standard hole sizes is shown in Figure 2-17. The data reveals that all capsules are of sound construction.

The quantity of fuel present in each capsule on July 15, 1968, was as follows:

Capsule Number	Curies	Watts, Thermal
11	30,735	209
12	31,470	214
15	31,765	216
16	31,588	215

The gage for acceptance of the fuel capsules at Oak Ridge was fabricated by 3M, inspected, and forwarded to ORNL. The gage has been used for acceptance of fuel capsules in Systems S10P1 and S10P2.

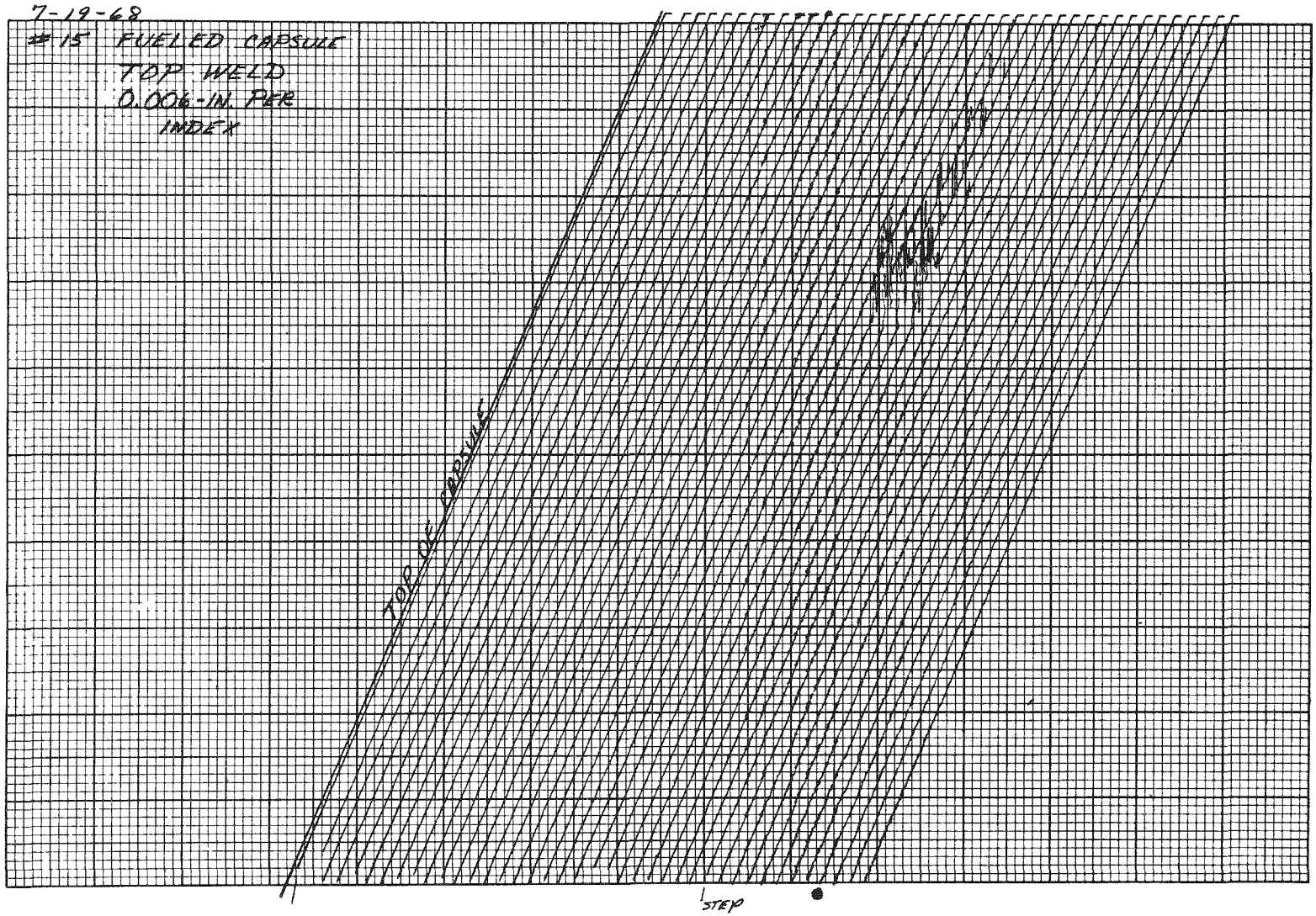

Figure 2-15. Ultrasonic Inspection of Fuel Capsule Top Weld

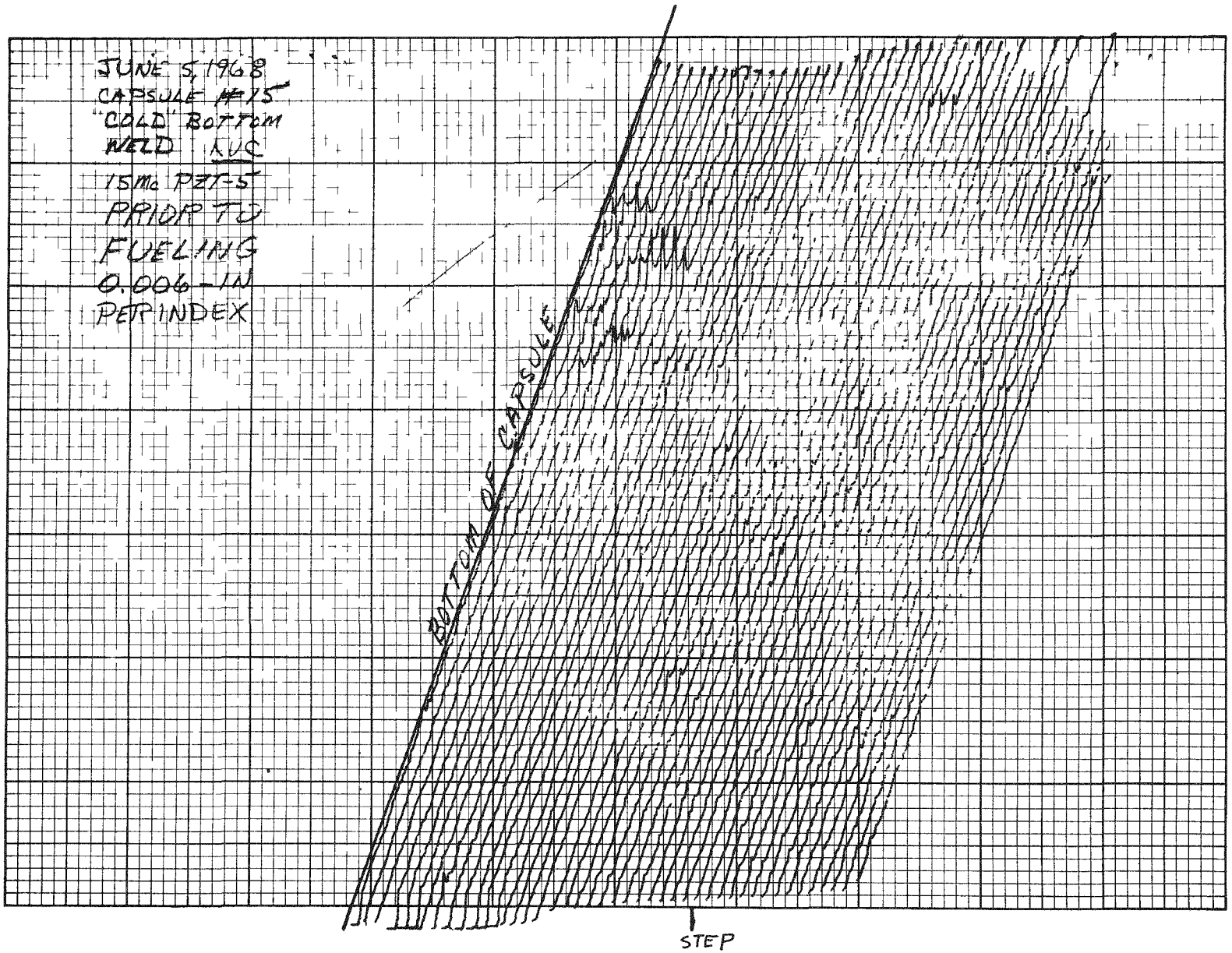

Figure 2-16. Ultrasonic Inspection of Fuel Capsule Bottom Weld

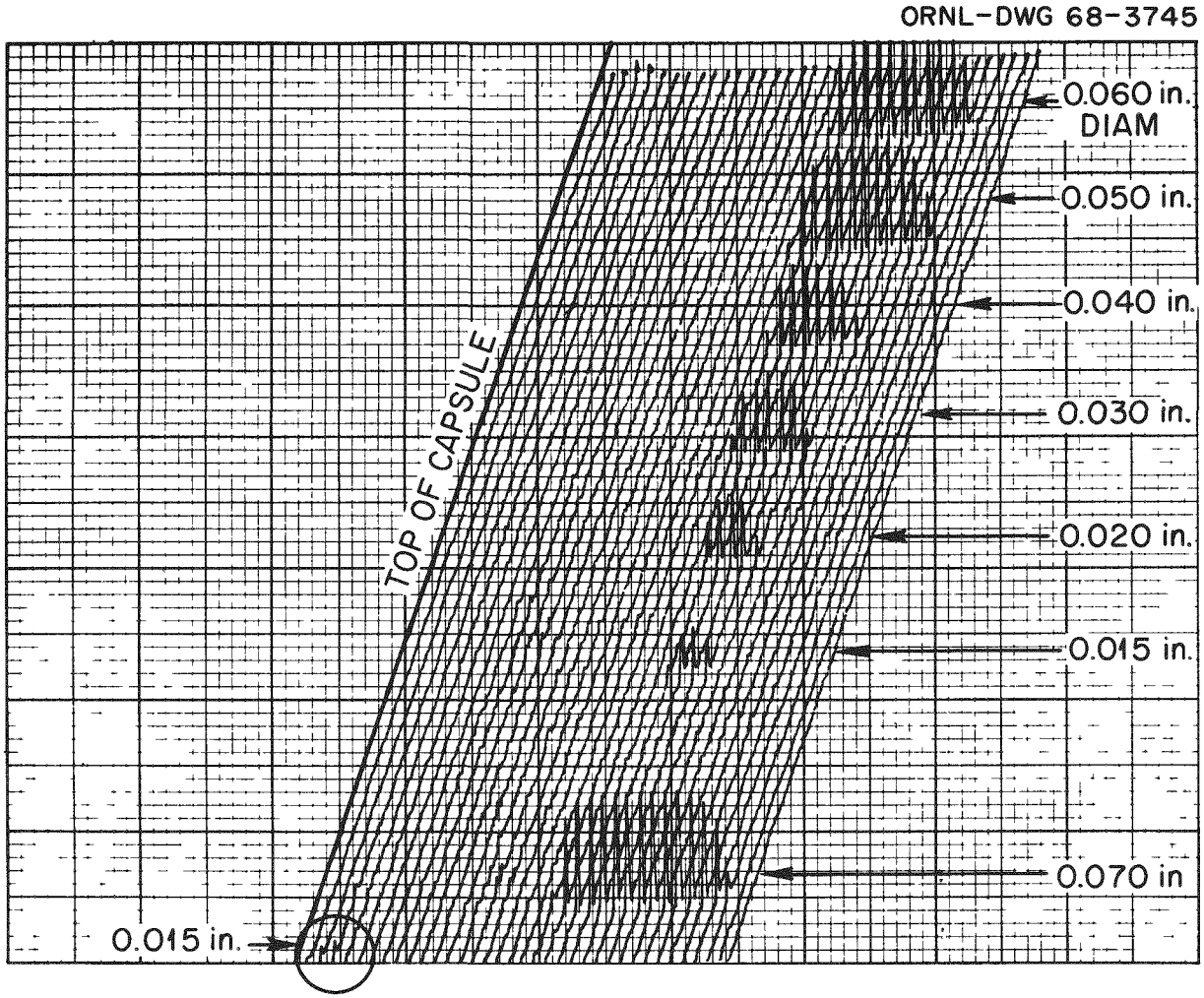

Figure 2-17. Recording of Ultrasonic Response from SNAP-21 Capsule Calibration Standard with Various Hole Sizes

2.3 BIOLOGICAL SHIELD

Biological Shields serial numbers 10 and 11 were received and inspected at 3M during the reporting period. Both Biological Shields were shipped to Linde.

X-ray films for all biological shields were requested from the National Lead Company. Films for biological shields were received and filed at 3M in component traceability files.

Shield Plug Assembly

Four radiation plugs were sent to National Lead for heat treatment. Upon return to 3M, it was noted that the aluminum oxide compatibility coating was separated from the base material.

The radiation plug is a solid right circular cylinder of U-8 w/o Mo alloy which completes the shielding of the fuel when it is inserted above the fuel capsule. (See Figure 2-18.)

The radiation plug is encapsulated in stainless steel to prevent oxidation. A compatibility barrier must be maintained between the U-8 w/o Mo and the stainless steel encapsulant to prevent the formation of a eutectic alloy at operating temperature.

The four radiation plugs had been coated with aluminum oxide to provide this compatibility barrier. The aluminum oxide was applied in accordance with the following procedure:

a) The plugs were grit-blasted to roughen the surface.

b) A molybdenum substrate (less than 0.001 inch thick) was plasma sprayed on all surfaces.

c) Aluminum oxide was plasma sprayed 0.016 to 0.018 inch thick on all surfaces.

d) The aluminum oxide coating was ground to final dimensions. Final coating thickness was from 0.012 to 0.014 inch.

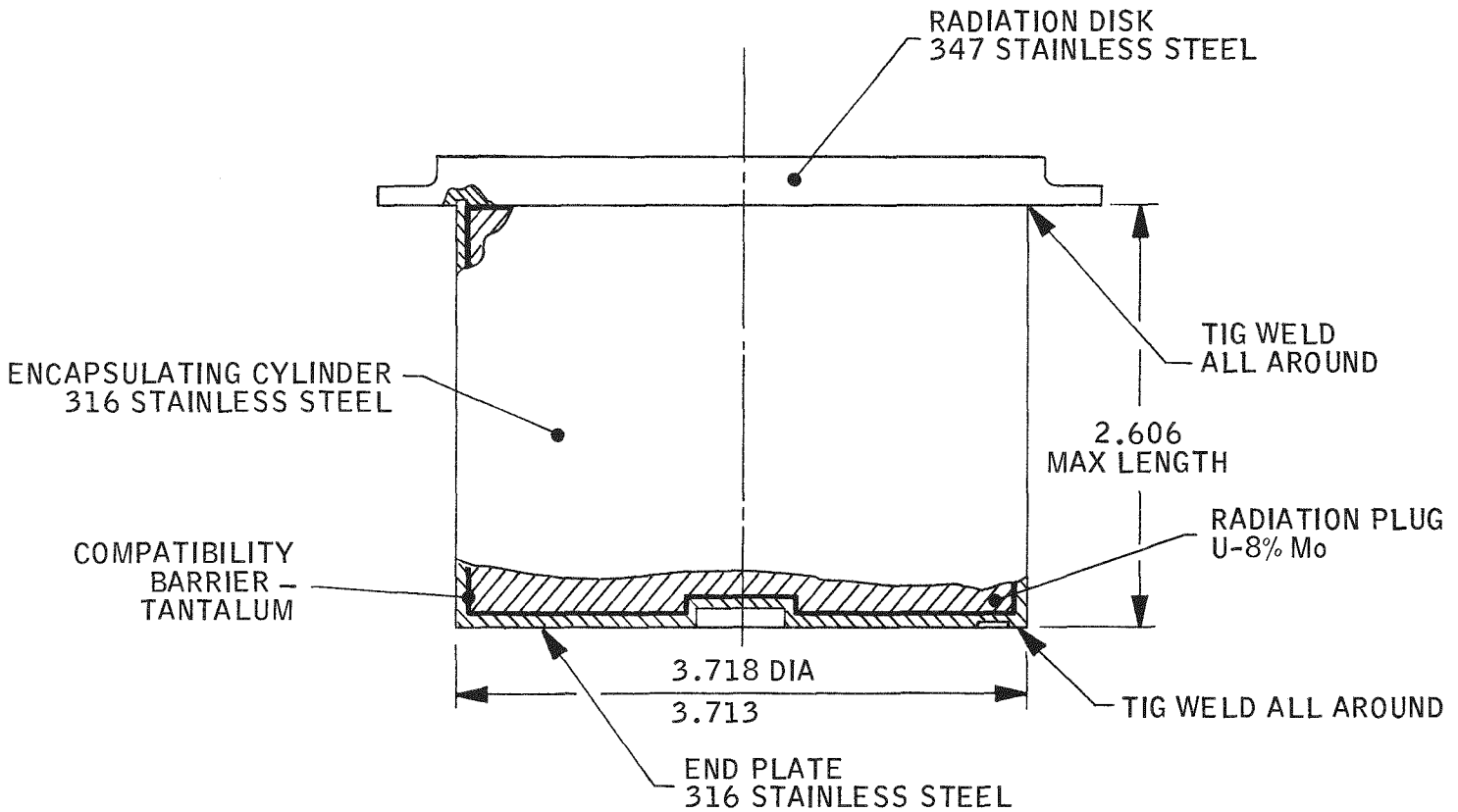

Figure 2-18. Shield Plug Assembly

This is the same coating and procedure used for coating the inner liner and support spider. Note that the shield plug coating was applied to U-8 w/o Mo rather than the Hastelloy-X side interface.

During the engineering analysis of HTVIS B10D4, it was found that the normal casting cool-down of U-8 w/o Mo could result in the formation of some alpha phase material. In view of this, some question existed as to the actual condition of the U-8 w/o Mo radiation plug. It is important that the radiation plug be in the all-gamma condition when it is machined so that the dimensions at operating temperature can be accurately predicted. If there is any alpha phase present in the material at room temperature, the final dimensions at operating temperature (which is above the phase transformation temperature) will be greater than that calculated. This is because the calculations are based on the assumption that the material is in the gamma stabilized condition at room temperature.

To ensure that the coated plugs were in the gamma stabilized condition prior to grinding to final dimensions, they were sent to National Lead for heat treatment. The heat treat cycle consisted of a slow heat-up to 1500°F and then a rapid quench in an inert atmosphere to a temperature below 600°F.

Following heat treatment, the plugs were returned to 3M where the loss of compatibility coating was noted. The aluminum oxide had cracked, or spalled off most of the surface, but the molybdenum substrate had not spalled off in all areas. The base material (U-8 w/o Mo) did not appear to be as rough as desired for good adhesion of a plasma sprayed coating. Photographs of the plugs are shown in Figure 2-19. The aluminum oxide coating was dark grey to black in color in contrast to its initial white color prior to treating.

In view of this problem with the compatibility coating, it was decided to remove the stainless steel jacket from the plug that was used in the early fueled system, S10D1A.

This plug had also been coated with Al_2O_3 (aluminum oxide) using the same process as described previously. The Al_2O_3 coating on this plug was also found to be spalled in the same way as the four heat treated plugs. There was no possibility of eutectic formation, however, since the close fit between the plug

Figure 2-19. Two Views of Radiation Plug Showing Spalled Areas

and the stainless steel jacket prevented any relative movement of the Al_2O_3 even though some of it had spalled off.

The probable cause of failure of the aluminum oxide coating was one or a combination of the following:

a) The surface of the plug was not rough enough for good adhesion of the molybdenum substrate. If is felt that the grit-blasting process used was not adequate for cutting the extremely hard, dense, U-8 w/o Mo.

b) The difference in coefficient of thermal expansion between U-8 w/o Mo and aluminum oxide is:

8.0×10^{-6} in/in °F at 1000°F for U-8 without Mo vs

3.9×10^{-6} in/in °F for Al_2O_3.

This difference in expansion, coupled with the low ductility of aluminum oxide, can cause cracking during temperature cycling.

c) Since the compatibility coating is rather thick, some tensile stresses are generated due to normal shrinkage during application. The relatively poor bond between the molybdenum substrate and the base material could not withstand these stresses.

In view of the apparent adhesion problem between aluminum oxide and U-8 w/o Mo, it was decided to use tantalum as the compatibility barrier. Tantalum has been shown to be as effective as aluminum oxide as a compatibility barrier (Ref. SNAP-21 Quarterly Report No. 8, MMM 3691-35), and has good ductility and bonding properties.

Two methods of providing the tantalum compatibility barrier were considered: 1) by plasma spraying the plug and, 2) by inserting thin tantalum sheets between the plug and the stainless steel cover. The preferred method, from an assembly standpoint, was the plasma-sprayed process because it minimized the number of components.

To evaluate the feasibility of plasma spraying tantalum on the U-8 w/o Mo, two plugs were sprayed with tantalum powder and then thermally tested.

The two plugs were prepared for spraying by first removing the remainder of the aluminum oxide on a lathe. A series of grooves were then turned on the O. D. and on the ends of the plug simulating a very fine thread to increase the roughness of the surface to be sprayed. In addition to the grooving, the parts were grit blasted using an improved technique. The plugs were not plasma sprayed in a controlled atmosphere since this type of facility was not available. A coating build-up of 0. 009 to 0. 011 inch of tantalum per side was applied.

The thermal test of the coated plugs consisted of heating them at a rate representative of a normal system heat-up and then cooling rapidly to retain the gamma stabilized condition. The rapid cool-down approximates the cooling rate of a hot plug removed from a system and placed on a flat surface that would serve as a heat sink.

The two plugs were heated in a circular furnace, 3 feet in diameter and 5 feet deep. The plugs were stacked one on top of the other with a thermocouple between them. The plugs were placed on an alumina block and shielded from direct thermal radiation by other alumina blocks placed around them. The furnace was evacuated to an absolute pressure of approximately 50 microns of argon.

Plots of the furnace temperature, of the thermocouple between the plugs and of a typical emitter plate heat-up curve are shown in Figure 2-20. The plug heat-up was slightly slower than a typical system heat-up.

Post-test examination of the two plugs revealed that approximately 50 percent of the tantalum coating was loose on each plug. The U-8 w/o Mo surface under the loose coating did not appear to be as rough as it was prior to coating. A possible explanation for this apparent "smoothing" of the surface is oxidation either during the plasma spraying operation or during the thermal cycling tests due to loss of furnace atmosphere control.

In view of the problems involved in obtaining good adherence of plasma sprayed coatings on U-8 w/o Mo, it was decided to abandon this method and use the

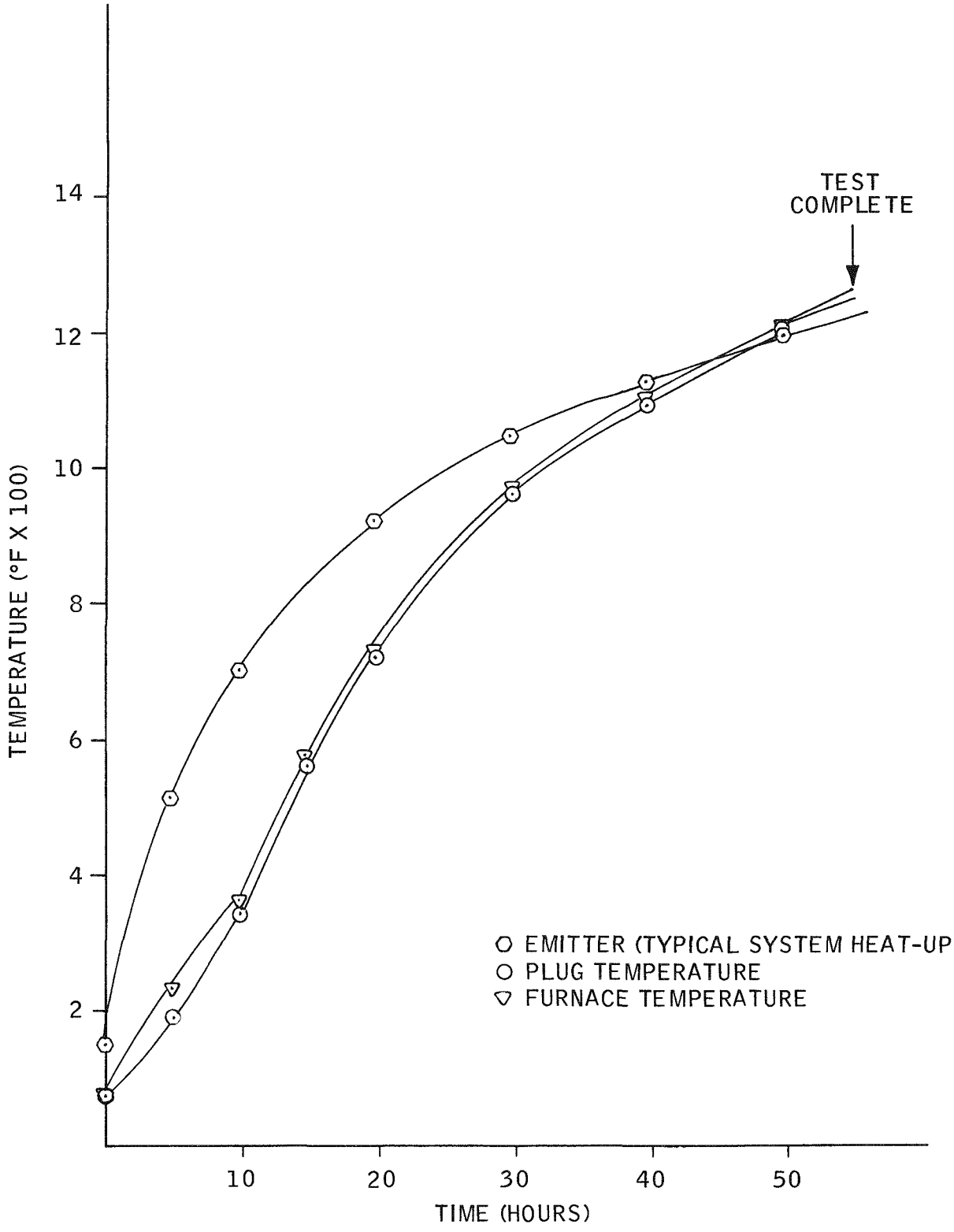

Figure 2-20. Thermal Cycle of U-8 w/o Mo Plugs Plasma Sprayed with Tantalum

alternate method of installing tantalum sheet between the plug and jacket. Sheet stock was cut and formed to completely cover the plug prior to encapsulation into the stainless steel capsule. The close fit between the plug and stainless steel jacket prevents any movement of the tantalum sheets.

Two plugs were encapsulated using this method with no difficulty.

2.4 INSULATION SYSTEM

Work performed on the insulation system during this report period includes completion of the engineering analysis of B10D4, assembly and testing of B10DL1, B10DL2, B10DL3, assembly of B10DL4 and partial assembly of B10DL5.

2.4 1 Engineering Analysis of B10D4

This section covers the third and fourth thermal force cycles performed on insulation system B10Q1, completion of the engineering analysis report and a re-evaluation of the cause of the unit failure.

2.4.1.1 Third Thermal-Force Cycle

Since the details of the third thermal-force cycle were not included in Quarterly Report No. 9 (MMM 3691-39) the entire test procedure and results will be repeated here to maintain continuity.

The results of the first two thermal-force cycles clearly indicated the need for design and processing procedure changes. Accordingly, these changes were made and evaluated during the third thermal-force cycle. The changes incorporated were as follows:

- Tie Rod Angle – A new tie rod angle was calculated using the experimentally determined temperature difference between the emitter plate and the spider. The new tie rod angle was calculated to be 27 degrees 11'. The system was assembled with a tie rod angle as close to 27° 11' as possible by measuring the actual dimensions of each component and adjusting the tie rod accordingly.

The previous systems were assembled by using nominal dimensions and then adding a tolerance to the tie rod angle to allow for component dimensional tolerances. This resulted in a tie rod angle of $27° 49' \begin{smallmatrix}+30' \\ -0\end{smallmatrix}$.

- The system conditioning temperature was reduced 200°F, from 1550°F to 1350°F, to reduce the amount of primary creep in the male portion of the tie rods during conditioning.

- A new method of cooling the unit was devised to eliminate the argon backfill and therefore eliminate the possibility of oxygen contamination. This new cooling method consists of removing the heater block and inserting in its place a water cooled chill block during the cool-down transient.

A summary of the third thermal-force cycle is given in the following paragraphs.

a) Objectives

The objectives of the third thermal-force cycle were to:

- Determine the effect of a new tie-rod angle on the tie rod load profile when heating the system at the same rate as B10D4 and the first thermal-force cycle of B10Q1.

- Determine the effect of a lower processing temperature (1350°F rather than 1550°F) on tie rod loads and creep.

- Determine the effectiveness of a water cooled chill block technique to avoid shield phase change. Using this technique the argon backfill, with its potential oxygen contamination problem, could be eliminated.

- Demonstrate that the tie rods retain some pre-load at ambient temperature following cool-down.

b) Test Set-Up

The following repairs and changes were incorporated in HTVIS B10Q1 in preparation for the third cycle:

- New strain gauges were installed on the female rods because the old gauges were damaged during disassembly. The new gauges were calibrated for temperature and load, as they were for the previous cycles.
- New male tie rods were installed to replace the elongated ones. They were lapped to fit the spider socket and lubricated by burnishing with molybdenum disulfide.
- The super insulation foils were reinstalled over the spider.
- A new heater block was installed and the neck tube was insulated in the same manner as for the first cycle (copper disk and stainless steel ring). The system was then closed and attached to the instrumentation equipment in the same manner as for the previous cycles.
- The tension tie rods were torqued in 5 inch-pounds increments to 23 inch-pounds to provide the required pre-load.

c) Test Procedure and Observations

The cycle required a total of 216 hours to complete. It consisted of a heat-up to 1285°F at a rate that reproduced the heat-up of B10D4 and the first thermal-force cycle on B10Q1. The system was held at operating temperature for 36 hours to determine the tie rod load stability at operating temperature. The system was then heated to 1350°F and held for 24 hours to determine the effects of this conditioning temperature on the tension rod loads. After this simulated conditioning, the system was cooled to, and held at, operating temperature (1285°F) for 15.5 hours to obtain a stable reading on the tie rod loads. The copper rod was then installed in the neck tube area of the system and the heat input increased to simulate a thermoelectric generator. The power was increased to 215 watts and the system was held at operating temperature for 25 hours. It was then quick cooled to ambient temperature using the water cooled copper chill block.

Figure 2-21 shows the temperature and power input vs cycle time. Plotted on this figure are the average emitter plate temperature, average spider temperature and temperature at the bottom of the heater block. Figure 2-22 is an expanded scale plot of the spider temperature during the cool-down transient. As shown, there was no evidence of a phase change during this cool-down.

The temperature difference between the emitter plate and the spider versus the cycle time is shown in Figure 2-23. As shown, the temperature difference at operating temperature and with 215 watts input is about 45°F.

The average load in each tension rod versus the cycle test time is shown in Figure 2-24. Prior to applying power to the system, the average rod pre-loads were: rod No. 1, 400 pounds; rod No. 2, 320 pounds; rod No. 3, 255 pounds. During the first 4 hours of the test, the rod loads increased. This initial increase was caused by the emitter plate, and therefore the neck tube, being higher in temperature than the spider. From 4 hours total accumulated time (TAT) until 19 hours TAT, the rod loads decreased slightly. At 19 hours, when the power was increased, the load in the tension rods increased. This increase was also caused by the emitter plate becoming higher in temperature than the spider. At 40 hours TAT, the tension rod average loads were relatively stable and were: rod No. 1, 425 pounds, rod No. 2, 325 pounds; rod No. 3, 225 pounds. At 46 hours TAT (850°F emitter temperature) the loads in the tension rods began to decrease and finally reached a minimum load condition at 53.5 hours TAT (emitter plate temperature 1060°F). The average loads in the tension rods at this time were: rod No. 1, 212 pounds; rod No. 2, 137 pounds; rod No. 3, 34 pounds. This decrease in rod loading was caused by transformation of some of the initial gamma phase of the radiation shield material to alpha phase, with a corresponding dimensional decrease. From 53.5 hours TAT until 66 hours TAT, the average load in the tension rods increased to: rod No. 1, 538 pounds; rod No. 2, 462 pounds; rod No. 3, 368 pounds. At 67 hours the system was at operating temperature (1285°F) and the power was reduced. The rod loads slowly decreased while holding the system at operating temperature until, at 99 hours TAT, the rod loads were: rod No. 1, 436 pounds; rod No. 2, 380 pounds; rod No. 3, 290 pounds.

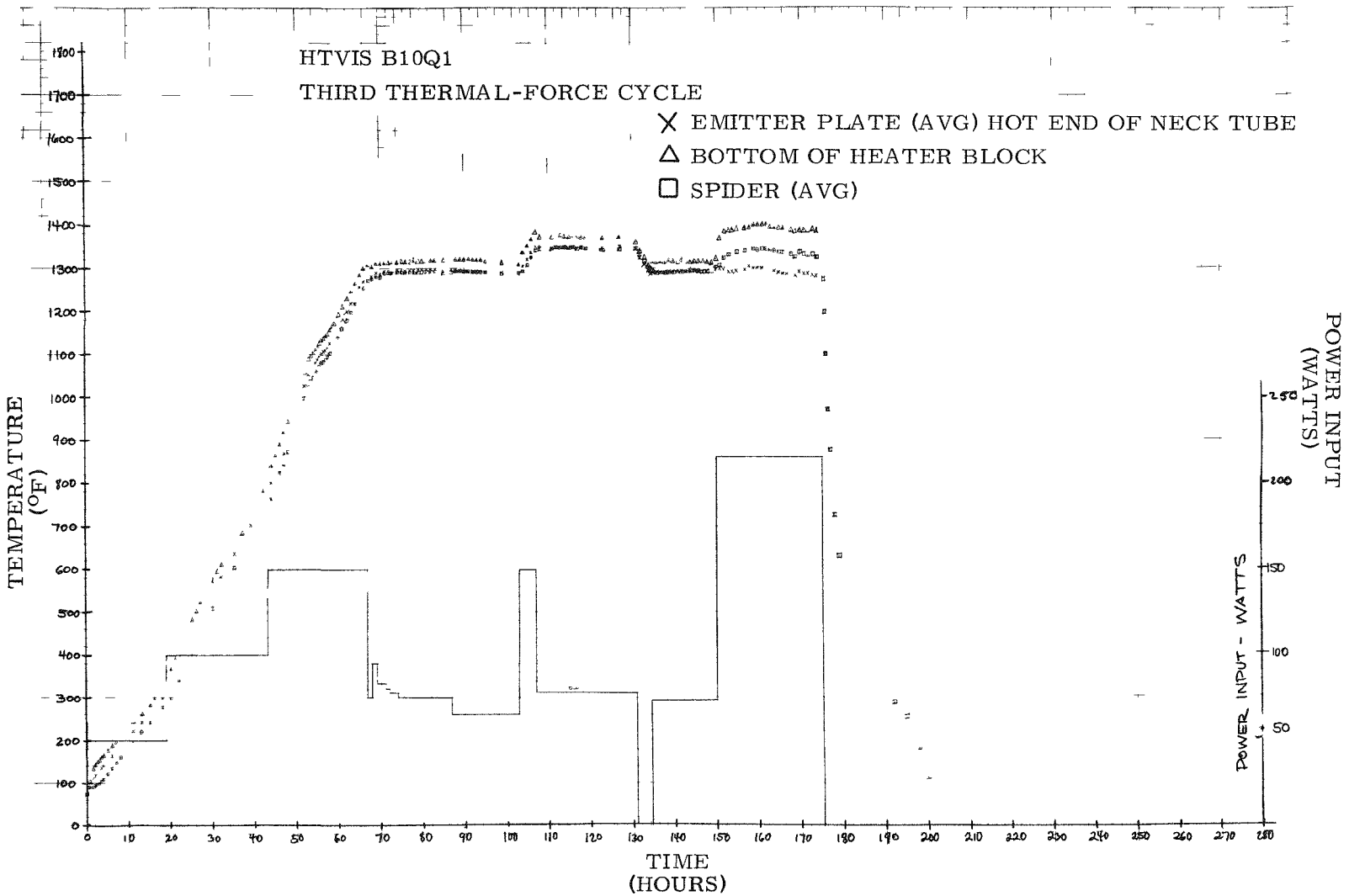

Figure 2-21. HTVIS B10Q1 – Third Thermal-Force Cycle, Time vs Temperature and Power Input

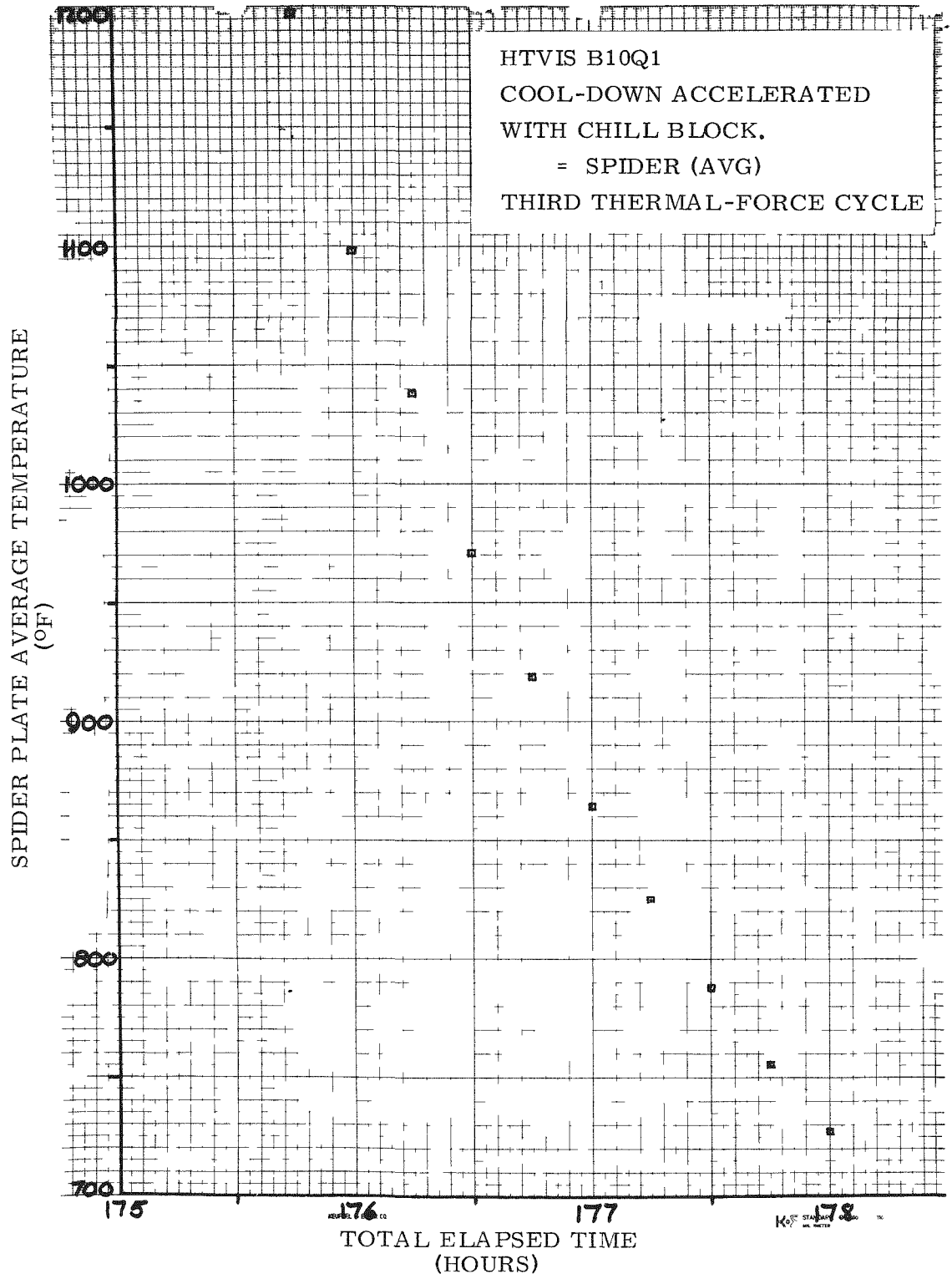

Figure 2-22. HTVIS B10Q1 – Third Thermal-Force Cycle, Time vs Spider Temperature

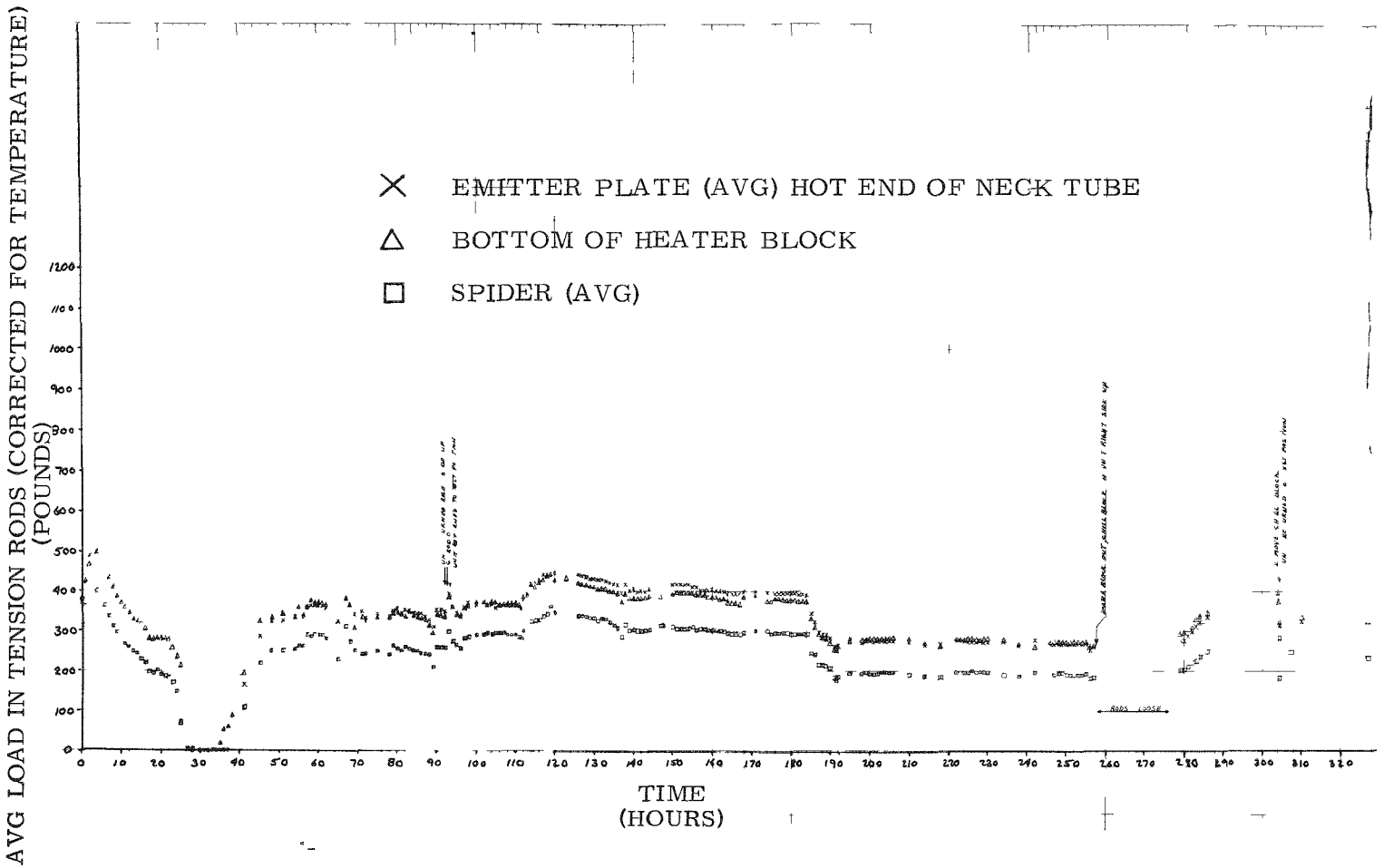

Figure 2-23. HTVIS B10Q1 – Third Thermal-Force Cycle, Time vs Tension Rod Load

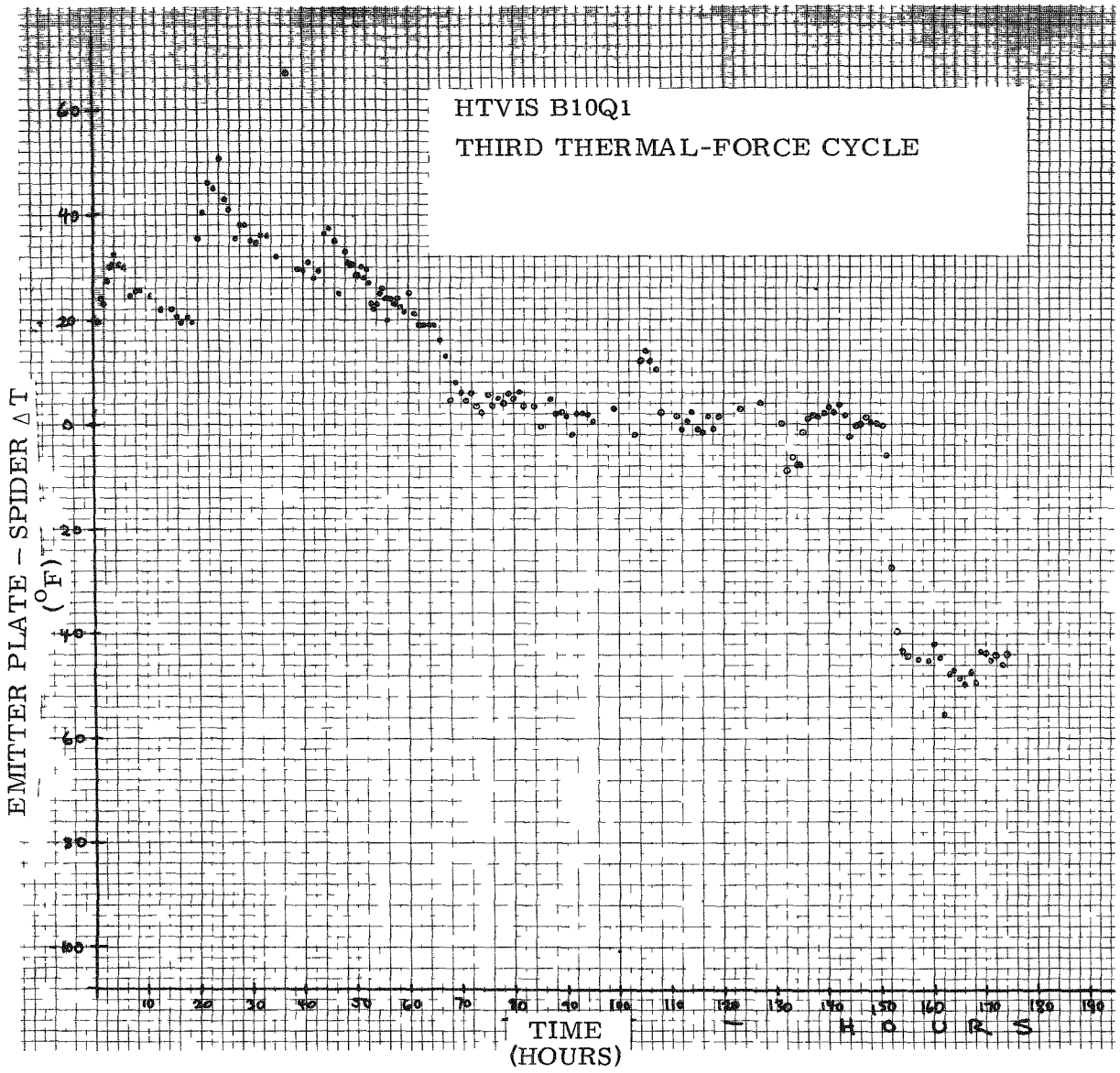

Figure 2-24. HTVIS B10Q1 – Third Thermal-Force Cycle, Time vs Temperature (Emitter Plate and Spider Plate Temperature Differential)

When the power was increased to bring the unit to the new conditioning temperature of 1350°F, the rod loads increased so that initially each rod was approximately 40 pounds higher than the load at operating temperature. After the system was cooled from 1350°F, the average loads in the tension rods at operating temperature were: rod No. 1, 400 pounds; rod No. 2, 360 pounds; rod No. 3, 284 pounds. It appears that 24 hours of conditioning at 1350°F caused the following approximate loss of load in each tension rod, when comparing the loads at operating temperature before and after conditioning: rod No. 1, 36 pounds; rod No. 2, 20 pounds; rod No. 3, 6 pounds.

After the copper rod was installed and the thermal input was increased to 215 watts, the tension rod loads remained relatively unchanged from the loads measured without the copper rod, although the temperature difference between the emitter plate and the spider increased by approximately 50°F upon installation of the copper rod. Calculations show that if the spider-emitter plate temperature relationship is increased with the emitter temperature held constant, the tension rod loads should decrease. Apparently factors which are not well understood are causing the rod loads to remain relatively stable. These factors could include the influence of the copper rod on the neck tube temperature profile and the influence of the copper rod on the mean temperature of the biological shield.

Following the fast cool-down with the water cooled chill block, the average rod loads were: rod No. 1, 370 pounds; rod No. 2, 385 pounds; and rod No. 3, 312 pounds. Comparing these loads with the starting rod loads, it appears that only rod No. 1 lost any load (30 pounds), while rod No. 2 and rod No. 3 increased in load by 65 pounds and 43 pounds, respectively. This increase in rod loading is probably due to the shield retaining a small amount of alpha phase following the cool-down after the second thermal-force cycle. The extremely fast cool-down achieved during this thermal-force cycle undoubtedly left the shields in the all-gamma condition which is larger in volume; therefore, this could result in a small amount of increased rod load.

d) Post-Test Disassembly

The system was not disassembled following this cycle.

e) Summary of Findings

This cycle was very successful and informative. The findings can be summarized as follows:

(1) The new tension tie rod angle reduced the tie rod loads at operating temperature to acceptable levels.

(2) The tie rods remained under load throughout the cycle and retained their pre-load after the cool-down.

(3) The amount of primary creep experienced during 1350° F conditioning temperature is well within acceptable limits.

(4) The temperature difference between the emitter plate and the spider at 215 watts input was approximately one-half of what it was under similar conditions during the first cycle. This could be due to instrumentation accuracy, since new thermocouples were installed on both the spider and the emitter plate for this cycle. A difference was also noted for the heater block temperature which would tend to bear out this possibility.

(5) The water cooled chill block was very successful in preventing alpha formation in the shield during cool-down.

2.4.1.2 Fourth Thermal-Force Cycle

The fourth thermal-force cycle was conducted with the same components as the third thermal-force cycle.

a) Objectives

The objectives of the fourth thermal-force cycle were to:

- Determine the tie rod load profile (at the new 27° 11' tie rod angle) during heat-up at a rate similar to a fueled system.
- Determine the feasibility of processing at 1400° F.

- Verify the reproducibility of the cool-down technique used during the third thermal-force cycle.
- Demonstrate that the tie rods retain some pre-load following a thermal cycle.

b) Test Set-Up

The only change in hardware between cycle three and this cycle was the installation of a new heater block. The neck tube was insulated the same as it was for cycle three.

c) Test Procedure and Observations

The fourth thermal-force cycle required a total of 310 hours to complete. The cycle consisted of a heat-up to 1285°F at a rate simulating the heat-up of a fueled system. The system was held at operating temperature for 25 hours before reducing power input and removing the copper rod which simulates the thermoelectric generator. With the copper rod removed, the system was held at operating temperature for an additional 19.5 hours. Following this hold, the system was heated to 1400° F emitter plate temperature and held for 65 hours to determine the effects of this conditioning temperature on the tension rod loads. After the simulated conditioning cycle, the system was cooled to, and held at, operating temperature (1285° F) for 66.5 hours. This was followed by a fast cool to ambient temperature using the water cooled chill block. Figure 2-25 shows the temperature and power input versus the cycle time. Plotted on this figure is the average emitter plate temperature, average spider temperature, and the temperature at the bottom of the heat block.

An expanded plot of spider temperature versus time is shown in Figure 2-26. As shown, there is no evidence of phase change. The temperature difference between the emitter plate and the spider versus the cycle time is shown in Figure 2-27. The emitter reached a maximum of 104° F higher than the spider at 6 hours TAT. After the maximum was reached, the temperature difference decreased until both the spider and emitter were at the same temperature, at approximately 22 hours TAT. After this time, the spider was higher in temperature than the emitter

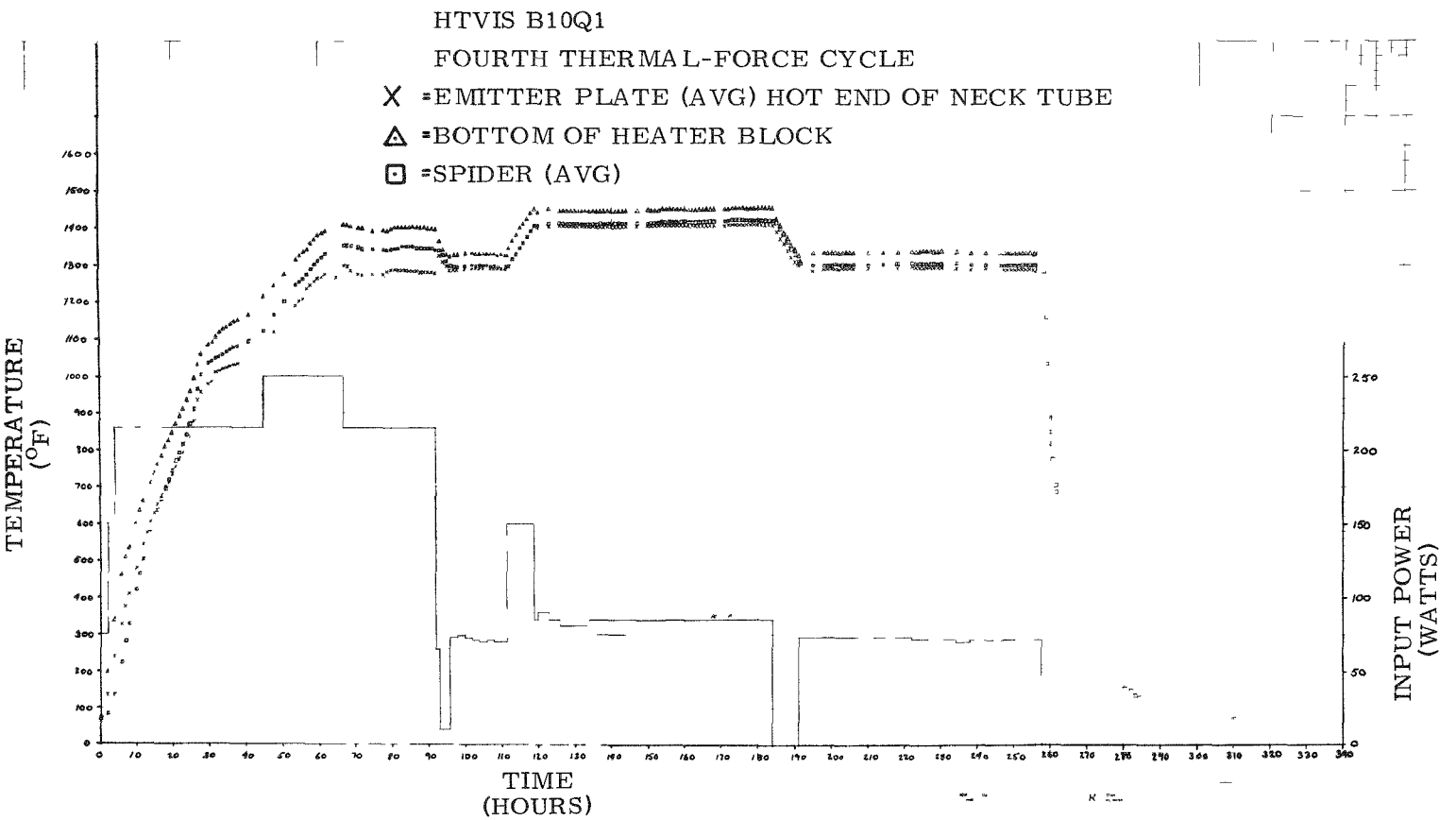

Figure 2-25. HTVIS B10Q1 – Fourth Thermal-Force Cycle, Time vs Temperature and Power Input

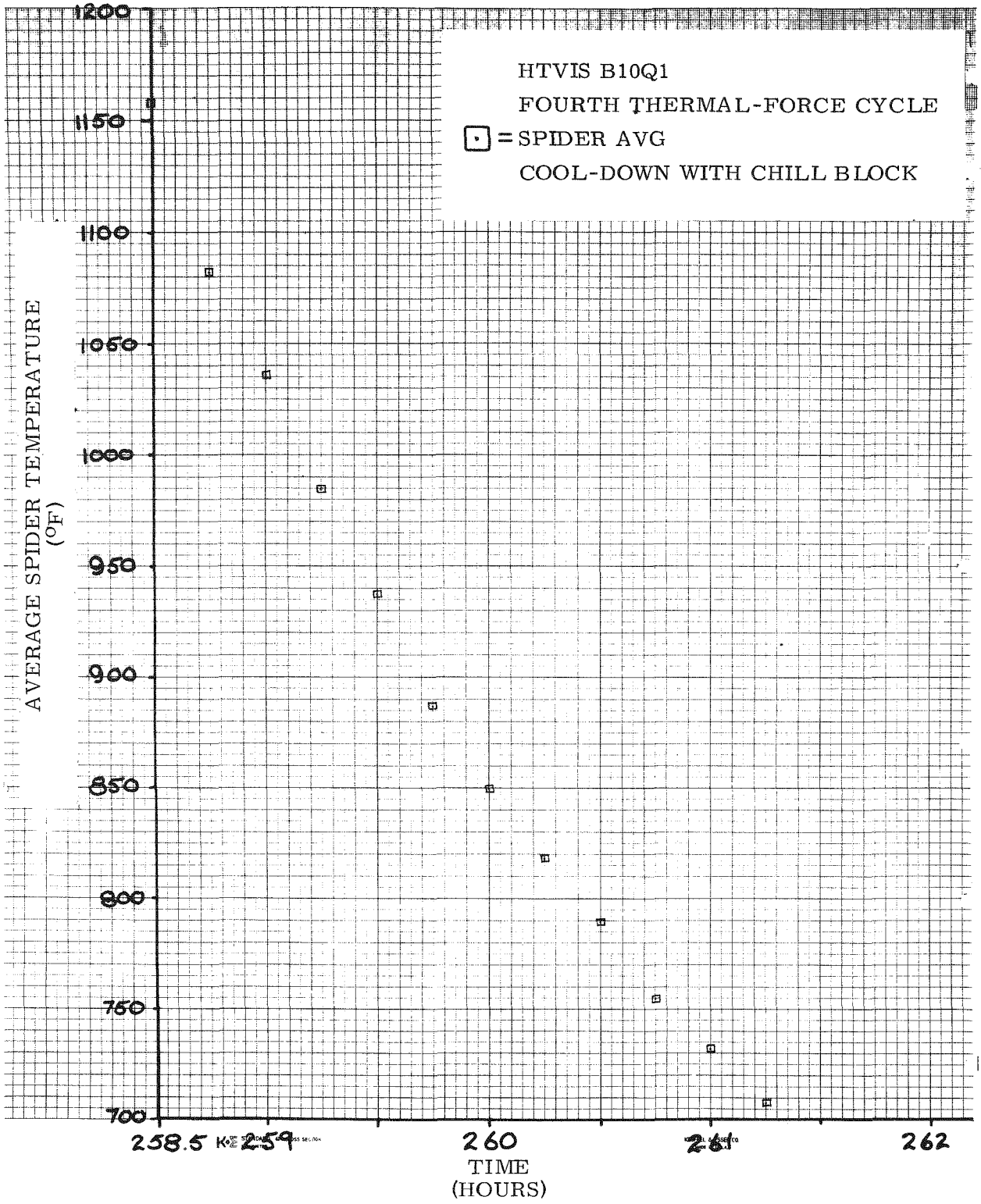

Figure 2-26. HTVIS B10Q1 – Fourth Thermal-Force Cycle, Time vs Average Spider Temperature

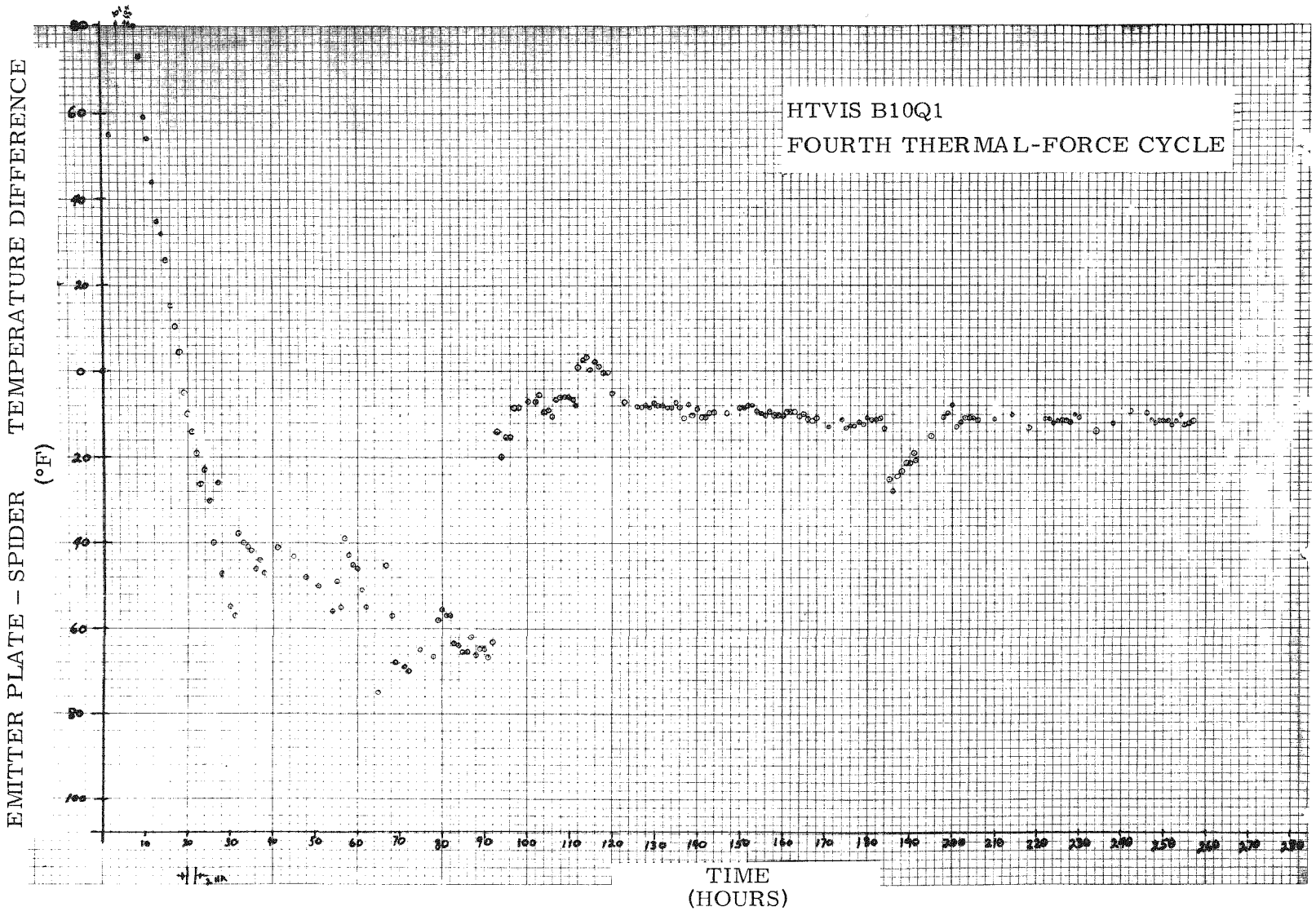

Figure 2-27. HTVIS B10Q1 – Fourth Thermal-Force Cycle, Time vs Temperature Between Emitter Plate and Spider

plate, finally achieving a difference of approximately 65° F just before the copper rod was removed at 92 hours TAT. On the second thermal-force cycle, the temperature differential was approximately 100° F while exposing the system to the same heat-up cycle. The reason for the difference between the spider-emitter plate relationship on this run and on the second thermal-force cycle is not completely understood. Possible explanations include the relative tightness of the heater block in the inner liner for each test, the tightness of the fits between the spider-shield and inner liner, and cumulative instrumentation error, since different thermocouples were used for each test. With the copper rod removed, the spider was 8° F to 12° F higher in temperature than the emitter plate for the remainder of the run except when heating to, and cooling from, the conditioning temperature.

The average load in each tension rod versus the test cycle time is shown in Figure 2-28. Prior to applying power to the unit, the average residual rod pre-loads from the third cycle were: rod No. 1, 370 pounds; rod No. 2, 385 pounds; rod No. 3, 312 pounds. During the first four hours the rod loads increased and then they experienced a period of steady decrease until approximately 25 hours TAT when the tension rods became unloaded. The unloading of the rod was caused by the biological shield being transformed to the alpha condition with the subsequent dimensional decrease and because the spider was continuing to become higher in temperature than the emitter plate. This temperature relationship will normally cause looseness. At approximately 36 hours TAT the tension rods started to become loaded again. The emitter plate temperature at this time was 1026° F. The tension rod loads continued to increase until the unit reached operating temperature at 67 hours TAT. The average rod loads at operating temperature, with the copper rod in place to simulate the thermoelectric generator were approximately: rod No. 1, 350 pounds; rod No. 2, 340 pounds; rod No. 3, 260 pounds. The system was held at operating temperature for 25 hours with no appreciable change in the rod load. The copper rod that simulates a thermoelectric generator was then removed and power reduced to maintain 1285° F. This condition was held for 19.5 hours. The tie rod loads at the end of this time, 110 hours TAT, were: rod No. 1, 360 pounds; rod No. 2, 365 pounds; rod No. 3, 290 pounds.

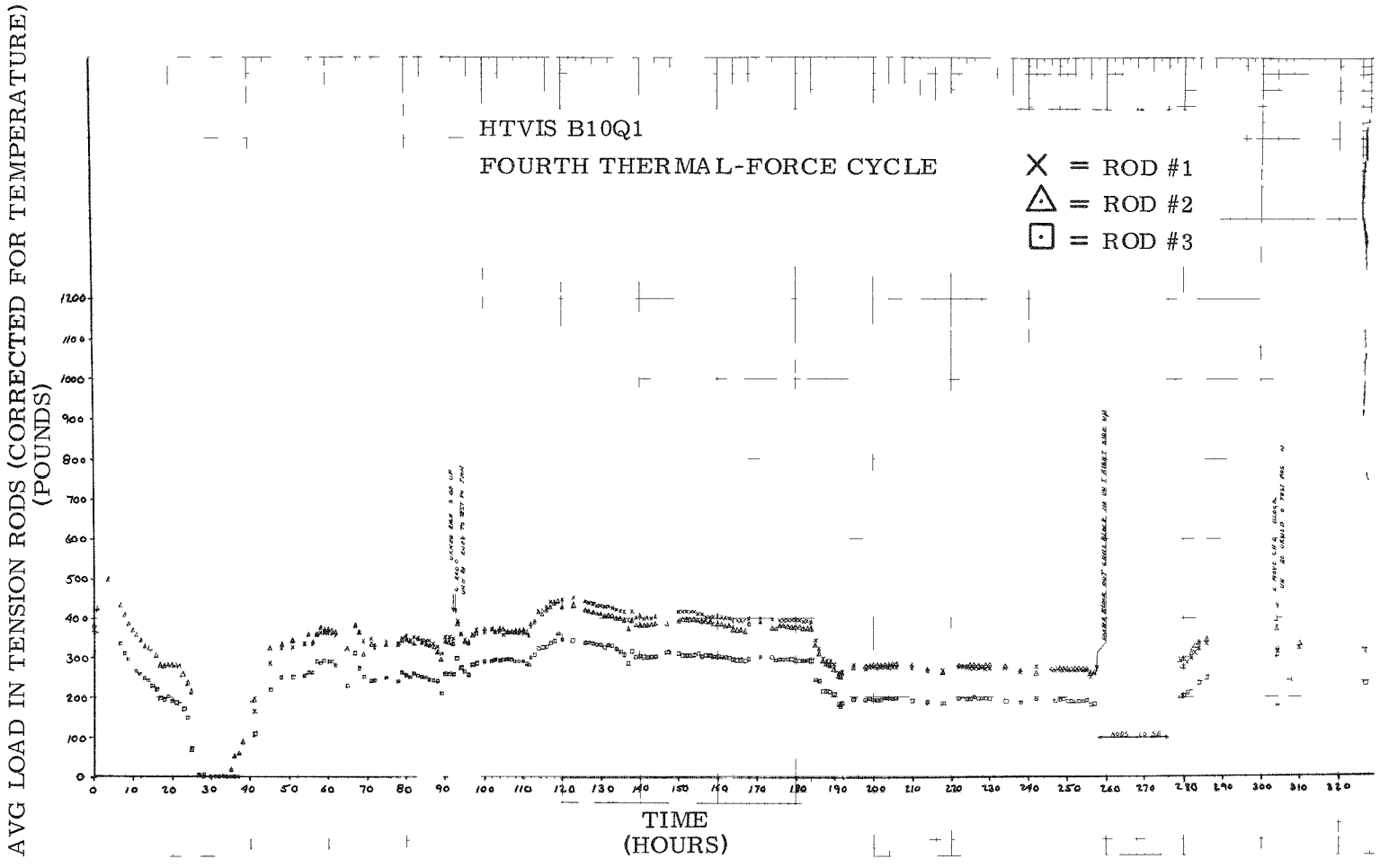

Figure 2-28. HTVIS B10Q1 – Fourth Thermal-Force Cycle, Time vs Tension Rod Load

The system was then heated to the 1400° F conditioning temperature and the rod loads were: rod No. 1, 450 pounds; rod No. 2, 430 pounds; rod No. 3, 345 pounds. After 65 hours of conditioning at 1400° F (184 hours TAT) the rod loads were: rod No. 1, 387 pounds; rod No. 2, 371 pounds; rod No. 3, 290 pounds. It appears, therefore, that the rods decreased in loading at the 1400°F conditioning temperature by approximately 60 pounds. Upon cooling the system to operating temperature, the average loads in the tension rods were: rod No. 1, 275 pounds; rod No. 2, 280 pounds; rod No. 3, 192 pounds. Comparison of the average loads in the tension rods before and after the conditioning show that approximately 85 pounds of load were lost during conditioning, most likely by primary creep of the male tension rod.

At 257.5 hours, the system was cooled quickly with a water cooled chill block which was bolted to the inner liner. As soon as the Min-K insulation was removed from the inner liner, the load on the tension rods decreased to essentially zero load and did not return until the system had cooled to approximately 300° F. This loss of rod load was caused by a sudden change in the inner liner temperature profile, resulting in a shorter inner liner and, therefore, loose tension rods. As previously discussed, the cool-down was fast enough to prevent the formation of alpha phase in the shield.

After the system was at ambient temperature, the average loads in the tension rods were: rod No. 1, 310 pounds; rod No. 2, 325 pounds; rod No. 3, 235 pounds. Comparison of these end-of-run loads with the starting loads reveals that each tension rod lost the following amount of load:

Rod No. 1 – 60 pounds

Rod No. 2 – 60 pounds

Rod No. 3 – 77 pounds

d) Post-Test Disassembly

The system was not disassembled.

e) Summary of Findings

(1) The tension tie rods at the new tie rod angle retain load at operating temperature following a heat-up cycle simulating a fueled system.

(2) The tie rods retain pre-load following a rapid cool-down.

(3) Conditioning at 1400° F emitter plate temperature for 65 hours resulted in an average tension rod load loss of 85 pounds due to primary creep. There is adequate pre-load so that the loss of 85 pounds load during conditioning is not critical and will not affect the performance of the system.

(4) Rapid cooling of the system, using the water cooled chill block, is a reproducible procedure and is effective in preventing shield phase change.

2.4.1.3 Completion Engineering Analysis of B10D4 Topical Report

The report on the Engineering Analysis of High Temperature Vacuum Insulation System B10D4, Report Number MMM 3691-40, was completed and submitted to the AEC.

2.4.1.4 Re-evaluation of Cause of Failure of B10D4

After it was observed that units B10DL1 and B10DL3 were damaged during dynamic vibration testing by a malfunctioning test machine (see Sections 2.5.2 and 2.5.4), the oscillograph trace which recorded the accelerations during the vibration test of unit B10D4 was reviewed. A review of the oscillograph recording of the vibration test for unit B10D4, revealed that the vibration machine experienced a shut-down "dump" at 9 Hz which was the same as experienced by unit B10DL1 at 7-1/2 Hz. This machine shut down induced loads similar to those which caused the neck tube of unit B10DL1 to buckle. It is believed that the B10D4 neck tube was buckled by the machine shut down. Continuation of the test cycle caused the neck tube to completely fail, resulting in the high amplification observed on the oscillograph trace above 15 Hz which occurred approximately 1-1/2 minutes after the machine was restarted. Figure 2-29 shows that portion of the oscillograph trace where the test machine malfunctioned resulting in a machine shut down.

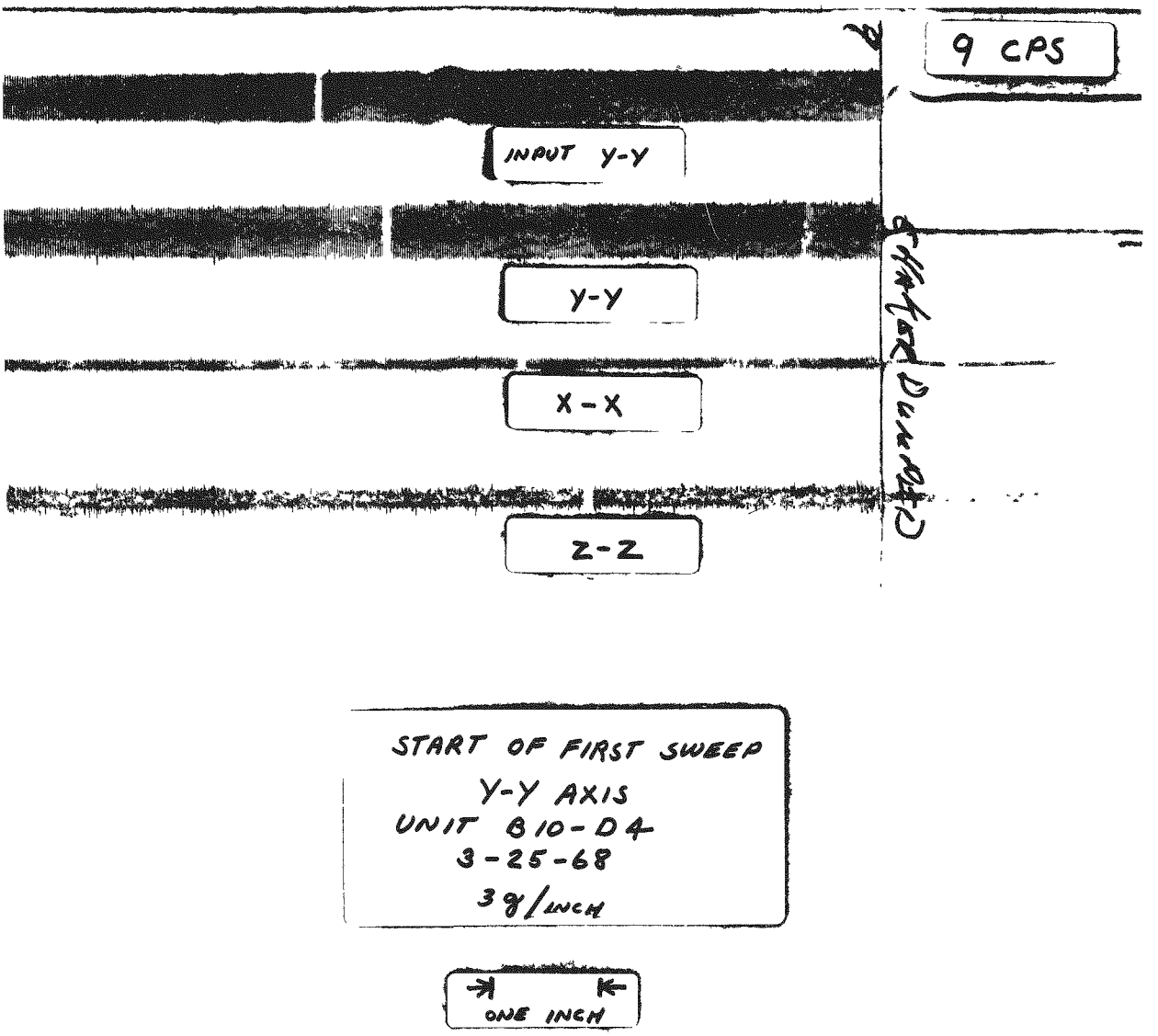

Figure 2-29. Oscillograph Trace

2.4.2 Assembly and Test of B10DL1

2.4.2.1 Unit Assembly

The lower enclosure head was welded to the upper enclosure head and the tension rods were installed. Thermal processing at 1400° F was then performed and the thermal test showed that the heat loss of this unit was 48.1 watts at operating temperature under test conditions. This is equivalent to 50.5 watts under operating conditions or 5.5 watts above the technical specification. The getter was installed and the seal off was made. The system was then cooled down, placed in the shipping container and shipped by common carrier to the dynamic test facility.

2.4.2.2 Unit Dynamic Test

The dynamic test of HTVIS unit B10DL1 was conducted on November 6, at Ogden Technology Laboratory, Deer Park, Long Island, New York. The first test was on the Y-Y axis and was initiated at 12:08 p.m. with a 0.5 g survey followed by 3-15 minute 5-50-5 Hz sweeps. Y-Y axis testing was complete at 1504 hours. Examination of the traces from the accelerometers indicated no malfunction. All temperatures were stable and within tolerances.

The fixture and emitter were rotated on the exciter head, and testing in the Z-Z axis was initiated at 1638 hours with a 0.5 g survey sweep. Following this sweep, which was "clean", a 5-50 Hz 7-1/2 minute up-sweep was run with the recorder running at "high" speed (4 inches per second chart speed). This trace was clean and the down-sweep was run ending at 1717 hours. The second sweep (5-50-5 Hz) was initiated at 1734 hours. During the down-sweep (50-5 Hz) at 7.6 Hz, the vibration exciter head shut down suddenly without warning. The power to the exciter was turned off and after the amplifier came back on, it shut itself down once more. The accelerometer traces, at shutdown, went off the paper and ran together indicating that the unit had seen a high "g" shock. The HTVIS outer shell temperature rose rapidly (within 15-30 minutes) to approximately 150° F indicating that the unit had lost vacuum integrity.

At this time, the test was terminated and the HTVIS and fixture were removed from the exciter head. An investigation was then undertaken to determine the cause of the exciter shutdown. The exciter was cycled from 5 to 17 Hz at 0.4 inch double amplitude displacement which was the level at which shutdown occurred. The unit operated satisfactorily. Since the spring rate of the shaker armature mounts is 7,000 lbs/inch and the HTVIS fixture weighs approximately 700 lbs., it was decided to try 0.6 inch double amplitude displacement which would give the same armature down-stroke as at shutdown. At this setting the shaker shut down by itself. The cause of this malfunction was traced to one of 18-9 kv 20-ampere rectifiers in the exciter amplifier "arcing" or "flashing" over.

On November 6, in order to determine the magnitude of the shock seen by the unit, the exciter head was instrumented with accelerometers and the unit caused to shut down automatically. At 0.9 inch double amplitude displacement and 7.6 Hz, a 3.3 ms 60 g shock was recorded. Attempts at 0.4 inch double amplitude displacement, 7.6 Hz shutdown, were unsuccessful due to another amplifier malfunction caused by the overloads at 0.9 inch double amplitude displacement shutdowns. However, at 0.2 inch double amplitude displacement and 7.6 Hz, a shock with approximately a 30 g peak was recorded.

An electrodynamic vibration exciter has built into it an automatic shutdown feature to prevent the machine from being destroyed during testing if a malfunction in the test item or exciter network occurs which would cause the exciter to operate unstably. The shutdown network causes the field and armature to be short circuited such that the collapsing fields act as a "dynamic" brake on the armature. The dynamic braking force then becomes a function of the place where the failure occurs in the sinusoidal cycle, being maximum at the peak of the cycle where maximum driving force is required to reverse the cycle and minimum through the zero axis where minimum driving force is required. The rectifier which failed was in the plate supply to the amplifier supplying power to the exciter armature or head. This failure was a "flashover" or "arcing" type and would only occur when the tube was conducting a given load. The load to cause failure is unknown; however, the load increases with frequency, for a given displacement, and is a maximum at the peak of the sine wave. Thus, the failure would probably occur at the peak of the sine wave at the frequency at which the tube would be required

to conduct beyond its weakened capacity. At this time, for the reason given above, the inherent dynamic braking would also be maximized, the most severe condition for an HTVIS.

Based on this, and the bare head tests conducted, it is believed that HTVIS B10DL1 experienced a shock pulse in excess of 20 g during the exciter shutdown. The subsequent buckling of the neck tube and loss of vacuum integrity were the result of dynamic loads well beyond the design capability of the system.

This system was placed in its shipping container and is at Ogden Laboratory on hold awaiting further disposition.

2.4.3 Assembly and Test of B10DL2

After the upper and lower enclosure shells were welded onto the unit, a leak check was performed. The leak rate was found to be 6.0×10^{-8} std. cc per second of helium which was within the specified requirements but greater than previous units by two orders of magnitude. A slight leak was discovered near the neck tube weld, so a second and third weld pass was made with intermediate leak checks. This rewelding did not seal the leak but made it larger to the point where it could now be pinpointed to an area approximately 5/16 of an inch below the weld zone. The leak rate at this point was 2.4×10^{-7} std. cc per second helium. The unit was submitted to Material Review, and a disposition was made to rework the affected area using a brush-on type plating process. It was decided that plating the neck tube with nickel would be the least hazardous and provide a reliable repair. An examination of the neck tube with a stereo-microscope indicated a spot which, from all points of view, appeared to be a valley-shaped area about 0.001" to 0.002" wide and 0.006" to 0.008" long, the depth which could not be determined. When using the helium probe with a very fine point and placing it over this spot, it would register immediately on the mass spectrometer. All other spots in this area were checked this way also, and none caused the mass spectrometer to indicate a leak.

A search of the Buffalo area was made to find a plating facility which had a portable plating unit.

The Keystone Corporation of Buffalo was located who had equipment called "Rapid Electro-Plating Process." This unit was capable of spot or so-called brush-plating.

The selection of the plating material was based on the coefficient of thermal expansion of Hastelloy-X versus the plating material. Nickel was chosen due to its close resemblance in thermal expansion compared to other alloys available.

Arrangements were made to have some samples of Hastelloy-X stock plated with nickel at their shop. These samples were then brought back to 3M for evaluation of the plating interface on the Hastelloy surface. The samples were sectioned, mounted, polished, and evaluated under the microscope for plating interface bond. Two samples were evaluated. One sample had a copper flash with 0.001" to 0.0015" nickel plate on Hastelloy-X. The second sample was plated with the 0.001" to 0.0015" nickel on the Hastelloy-X stock. Stock material used was 0.012" thick Hastelloy-X sheet. Of the two samples, the sample with the copper flash and nickel plate exhibited a more uniform interface bond. A decision was made to use this plating process. A representative of Keystone Corporation went to Linde to do the plating.

The unit was prepared for plating in the following manner:

> The system was allowed to remain at atmospheric pressure. The identified suspect area was wiped with acetone. Then a liquid electroplate cleaner (rapid activator #7) was applied to the plating area. After drying, a copper flash plating was applied (copper Coatalyte #314). The area was dried and rapid metal Coatalyte #21 was applied. The Keystone representative said that this was nickel.

The application of the solution is applied with a tool similar to a spatula with cloth sleeve covering the metal blade. The blade is about 5/8-inch wide and four inches long.

After the final application of the solution, the area was viewed under the stereomicroscope, and it was decided to make a second application due to thin spots in the first coating. The applicator blade was formed to fit the curvature of the inner liner for the second application. This second plating was applied, and

subsequently, viewed with the stereomicroscope and accepted as a proper plating. The plating area was then washed with de-ionized water, rinsed with isopropyl alcohol, and dried.

The system was leak checked and found to be 7.5×10^{-10} cc/sec helium. The leak rate was acceptable, and the unit was prepared for thermal performance testing. The thermal processing was completed and the thermal performance of the unit was found to be 49.1 watts under test conditions. After translating this into operating conditions, the heat loss would be 51.5 watts or 6.5 watts above the 45-watt specification. The weight of the unit is 63.1 pounds (or 3.1 pounds above the specification). After the thermal test, the heater block was removed and the unit was shipped to Ogden Technology Laboratory for dynamic test. The neck tube was reinspected in the area of the plating and it was noticed that the plating material appeared to have puddled while it was hot. A microprobe of the samples plated by Keystone Corporation shows that the plated material from Coatalyte #21 is a tin-indium and cadmium-eutectic alloy. Because of the possible undesirable metallurgical effects of this molten alloy on Hastelloy-X, the unit was submitted to Material Review, and a rework disposition was made both to remove the original repair material by "reverse" process and to replate with nickel only. The portable electroplating equipment was purchased and samples of Hastelloy-X were plated with (1) bright nickel on Hastelloy-X and (2) copper flash on Hastelloy-X with bright nickel on the copper flash. These samples were taken to the New York Testing Laboratories Incorporated of Westbury, Long Island, New York. Metallographic analysis shows that the bond between the nickel and the Hastelloy-X is superior to the bond using copper flash and nickel plate and Hastelloy-X. When the sample with copper was slightly bent, the plating flaked off. The nickel sample was bent 180° without any evidence of flaking. At this point the neck tube was plated with bright nickel directly onto the Hastelloy-X after removal of the original plating. The material used for plating was certified by the vendor to be nickel.

To remove the original plating, the power supply from the plating unit was used with the current reversed. A special deplating solution was also used. As the plating was being removed, the area was visually inspected with the stereomicroscope. Then the area was cleaned to remove any hydrocarbons. The area was replated with bright nickel in approximately 30 minutes.

The unit was then instrumented for heat-up and placed in its dynamic test holding fixture. Because the testing machine at Ogden was not operating properly, the unit was transported to Fairchild Camera and Instrument Company on Long Island for the vibration test. This vibration test was completed without incident. The shock test could not be done at Fairchild and since Ogden's machine was not operating properly, the shock test was waived. This unit will be dynamically tested with system S10P1 at Sandia. The unit was placed in its shipping container and shipped by air to Oak Ridge National Laboratory where it was integrated into system S10P1.

2.4.4 Assembly and Test of B10DL3

After assembling the biological shield, the inner liner and spider and installing the male tie rods, the insulation was attached to the assembly. The upper head was welded to the inner liner and the lower head was welded to the upper head. The tension tie rods were then installed. Closure of this unit was completed and thermal processing was accomplished. The thermal performance of this unit was found to be 50.6 watts under test conditions. By translating this into operating conditions, the heat loss would be 53.0 or 8 watts above the 45-watt specification. The unit was shipped by common carrier to Ogden for dynamic test.

When the unit arrived by common carrier truck at Ogden Laboratories, the cover of the shipping container was removed and the unit neck tube was visually inspected and found to be in good condition. Because the Ogden Laboratory test machine has been subject to malfunction resulting in "burps" and "dumps", it was arranged by Ogden for the unit vibration test to be performed at Fairchild Camera and Instrument Company, Long Island, New York.

The unit was transported to Fairchild Camera in the shipping container. Upon arrival the unit was removed from the shipping container and placed in the dynamic test fixture. The contact between the unit and the fixture was checked and the fixture bolts were tightened to 85 ft-lbs. torque.

Before the unit was put on the vibration machine, the machine was run empty to calibrate the accelerometers and to determine if the machine was in good working order. Following the calibration of the accelerometers the machine was run from 5-15-5 Hz at 0.7 inch double amplitude, from 5-8-5 Hz at 0.8 inch double amplitude,

and from 5-50 Hz at specification "g" level (3 g maximum). The machine operated perfectly during these test runs. Particularly, it was observed that the machine did not "burp" or "dump".

Following the test machine checkout, the unit was mounted on the machine for the ambient temperature vibration test according to the acceptance test plan. With the unit oriented for test in the Y-Y direction, the 1/2-g sweep was performed from 5-50-5Hz. During this sweep no amplification was recorded by the accelerometer mounted inside the neck tube (indicating that the tension rods were tight). The test to specification was then started, with the crossovers (changes from constant displacement to constant acceleration or vice versa) made normally by temporarily stopping the machine. At 40. 5 cps the machine was stopped for a crossover. The test personnel were looking at the oscillograph trace of recorded accelerations when suddenly the test machine "burped" and "dumped". This machine malfunction caused a shock load which buckled the unit neck tube. The oscillograph was not running when the machine burped so consequently the accelerations received during the machine malfunction were not recorded in a manner which could be accurately interpreted. Investigation directly after the unit neck was buckled showed that the machine was on standby, meaning that the amplitude was turned to zero while the amplifier remained turned on. The machine operator was in the control room during the malfunction. The unit was removed from the machine to allow the empty machine to be checked out. The following morning the cause of the test maching "dumping" was discussed with Fairchild's Environmental Laboratory Supervisor. It was Fairchild's opinion that the machine "dumping" was caused by a surge in the power line, which went through the amplifier causing the machine head to move. The sudden and large movement of the machine head caused the amplitude protection device to trip, shutting down the amplifier and causing the machine to "dump".

Following the discussion with Fairchild's Environmental Laboratory Supervisor, the test machine was run in an attempt to determine its condition. It was found that the machine "dumped" five times at 0. 7 inch double amplitude – twice at 13 Hz and three times at 5 Hz. These "dumps" occurred while the machine was moving in contrast to the "dump" which caused the unit neck tube to buckle which occurred while the machine was not moving. The cause of the machine dumping while moving was attributed to the overheating of the amplifier and high humidity conditions by Fairchild personnel. A vent to the amplifier was opened to permit better

cooling. The machine was started again and run at 0.6 inch double amplitude, 0.65 inch double amplitude, and 0.7 inch double amplitude between 5-15-5 Hz without any further machine "dumping".

The unit was removed from the test fixture and installed in the shipping container and transported to Ogden Laboratories for storage pending a decision on the disposition of the unit.

2.4.5 Assembly of Unit B10DL4

The biological shield inner liner and spider were assembled. The male end of the tie rods, which has previously been lapped into the spider, were then installed. Wrapping of this unit was completed. The upper and lower enclosure heads were installed and welded, and the neck tube and girth welds were completed. The tension rods were installed at an angle of 27°30'. The tension rod spherical washers were pinned to the receptacles, the anti-rotation pins were installed, and the receptacle seal-off plugs were welded into place. The unit was evacuated and helium leak tested. The leak rate was found to be acceptable.

The unit was instrumented for conditioning. The unit was evacuated and heated to 1400°F and held at this temperature for 48 hours to provide the required processing. Following the conditioning the unit was cooled to operating temperature and the pressure rise rate was determined to be 2.0 microns per hour. The maximum allowable pressure rise rate is 2.42 microns per hour.

Following the pressure rise test, 15 grams of getter were installed in the unit; the unit was sealed off.

After the unit was sealed off, the thermal performance test was conducted. It was found that a corrected power input of 68.0 watts was required to maintain the unit at a nominal 1285°F operating temperature. The subtractable heat loss due to the Min-K insulation, heater and thermocouple wires, and power lead loss is 14.1 watts. This yields a total heat loss of the unit of 53.9 watts. The required heat loss at test conditions (equivalent to the specification heat loss of 45 watts) is 42.6 watts. This unit, therefore, has a heat loss in excess of specification of 11.3 watts.

Following the thermal performance test, the unit was fast cooled. After cooldown the unit was installed in a HTVIS shipping container. An impactograph was mounted on the unit holding fixture to record the shocks transmitted to the unit during transit. The unit was then shipped to Oak Ridge National Laboratory where it was integrated with system S10P2. No abnormal shocks were noted on the impactograph trace.

2.4.6 Assembly of Unit B10DL5

The inner liner and spider were assembled onto the biological shield. A gap was noted between the shield and the spider at the outside edge of the spider. The spider was removed and it was found that the aluminum surface was tapered from the outside to about one-third of the way in toward the center. Only two-thirds of the surface of the spider was contacting the shield. The spider was reground and then reassembled. Approximately 15 percent of the required insulation on the biological shield was installed. In addition, the bottom enclosure head subassembly was fabricated and leak checked.

2.4.7 Quality Assurance

The 3M Quality Assurance has received a certified analysis of the nickel plate solution used to re-plate the inner liner neck tube of unit B10DL2.

The vendor used for re-grinding the spider for unit B10DL5 was surveyed and approved. The re-grinding operation was also observed by 3M quality personnel. A drawing change will be made to clarify the requirements so that a tapered condition will be unacceptable.

A step-plug gage has been furnished to Linde Corporation by 3M Company for use in assuring minimum inner liner cavity dimensions after the unit has been thermally cycled. Figure 2-30 shows an example of the gage and its application.

A Certificate of Conformance for the Insulation Systems has been prepared by 3M and submitted to Linde for concurrence. This Certificate, in addition to the documentation required by contract for each unit (interface dimensions, MRB data, and exceptions) will be forwarded to 3M for historical data files. Any "exceptions" (specifically, dimensions) that could cause interface problems will be brought to the attention of 3M prior to shipment of the HTVIS from Linde.

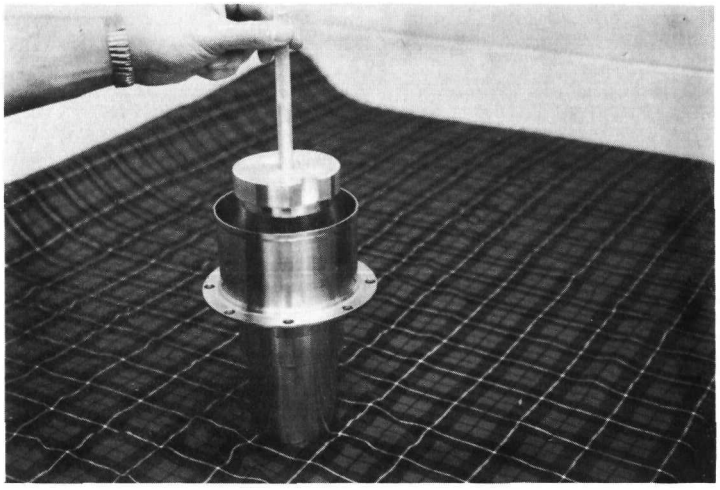

Figure 2-30. Inner Liner Cavity Dimension Gage

2.5 THERMOELECTRIC GENERATORS

2.5.1 Phase I

Data collection and analysis of the Phase I 6-couple modules and prototype generators continued during this part of the quarter. Performance data for 6-couple modules A1, A3, and A4 is given in Table 2-13 and Figures 2-31 through 2-33. Data from prototypes P5, P6, and P7 is given in Tables 2-14 through 2-16 and Figures 2-34 through 2-36. This data indicates no significant change in 6-couple or prototype generator performance.

The input power to modules A1, A3, and A4 was reduced on December 9, 1968. The new hot button operating temperature is 1020°F.

2.5.2 Phase II Generator Testing

A10D1

Generator A10D1 continued to leak throughout the first half of this report period. On October 9, 1968, two of the heater elements burned out. Voltage was increased to the remaining heater elements to maintain the required input power.

The generator Conax fittings were torqued to 75 inch-pounds on October 18, 1968 in an attempt to stop the leak. Since torquing did not seem to affect the leaking,

Table 2-13. Performance Data of SNAP-21 6-Couple Modules

Module	Date	T_h (°F, est)	T_c (°F)	E_o (volts)	E_L (volts)	I_L (amps)	P_o (watts)	R (milliohms)	P_I (watts)	Hours
A1	8-13-68	1040	115	1 29	0 64	1 75	1 12	371	32 0	35,543
	8-27-68	1040	114	1 28	0 63	1 73	1 10	373	32 0	35,879
	9-6-68	1040	115	1 28	0 63	1 73	1 10	373	32 0	36,119
	9-16-68	1040	116	1 27	0 63	1 73	1 09	369	32 0	36,359
	10-9-68	1040	115	1 27	0 63	1 72	1 08	373	32 0	36,911
	10-21-68	1040	114	1 27	0 63	1 73	1 09	369	32 0	37,199
	11-7-68	1040	114	1 27	0 63	1 72	1 09	371	32 0	37,607
	11-25-68	1040	115	1 27	0 63	1 72	1 09	370	32 0	38,039
	12-9-68	1040	115	1 27	0 63	1 71	1 08	374	32 0	38,375
	12-9-68			Power Input Reduced						
	12-11-68	1030	116	1 24	0 62	1 67	1 03	374	30 0	38,423
	12-16-68	1030	115	1 24	0 61	1 67	1 03	375	30 0	38,543
A3	8-13-68	1040	117	1 30	0 65	1 76	1 14	372	46 5	34,211
	8-27-68	1040	119	1 30	0 64	1 77	1 14	371	46 5	34,547
	9-6-68	1040	119	1 30	0 64	1 76	1 13	374	46 5	34,787
	9-16-68	1040	119	1 29	0 64	1 76	1 13	367	46 5	35,027
	10-9-68	1040	118	1 30	0 64	1 76	1 13	373	46 5	35,579
	10-21-68	1040	119	1 31	0 64	1 77	1 14	376	46 5	35,867
	11-7-68	1040	118	1 31	0 65	1 77	1 14	375	47 0	36,275
	11-25-68	1040	119	1 31	0 65	1 76	1 14	378	47 0	36,707
	12-9-68	1040	120	1 30	0 65	1 77	1 14	370	47 0	37,043
	12-9-68			Power Input Reduced						
	12-11-68	1020	117	1 28	0 63	1 74	1 10	371	45 5	37,091
	12-16-68	1020	117	1 28	0 63	1 74	1 10	372	45 5	37,211
A4	8-13-68	1040	117	1 24	0 62	2 28	1 42	271	39 5	33,571
	8-27-68	1040	118	1 23	0 61	2 28	1 39	272	39 5	33,707
	9-6-68	1040	119	1 24	0 61	2 28	1 39	276	39 5	33,947
	9-16-68	1040	118	1 24	0 61	2 28	1 40	275	39 5	34,187
	10-9-68	1040	119	1 24	0 61	2 20	1 33	288	39 5	34,739
	10-21-68	1040	119	1 24	0 61	2 20	1 33	288	39 5	35,027
	11-7-68	1040	119	1 23	0 60	2 20	1 32	296	39 5	35,435
	11-25-68	1040	118	1 25	0 59	2 20	1 31	298	39 5	35,867
	12-9-68	1040	117	1 24	0 56	2 04	1 15	332	39 5	36 203
	12-9-68			Power Input Reduced						
	12-11-68	1020	112	1 22	0 56	2 03	1 13	327	38 8	36,251
	12-16-68	1020	112	1 23	0 55	2 00	1 10	341	38 5	36,371

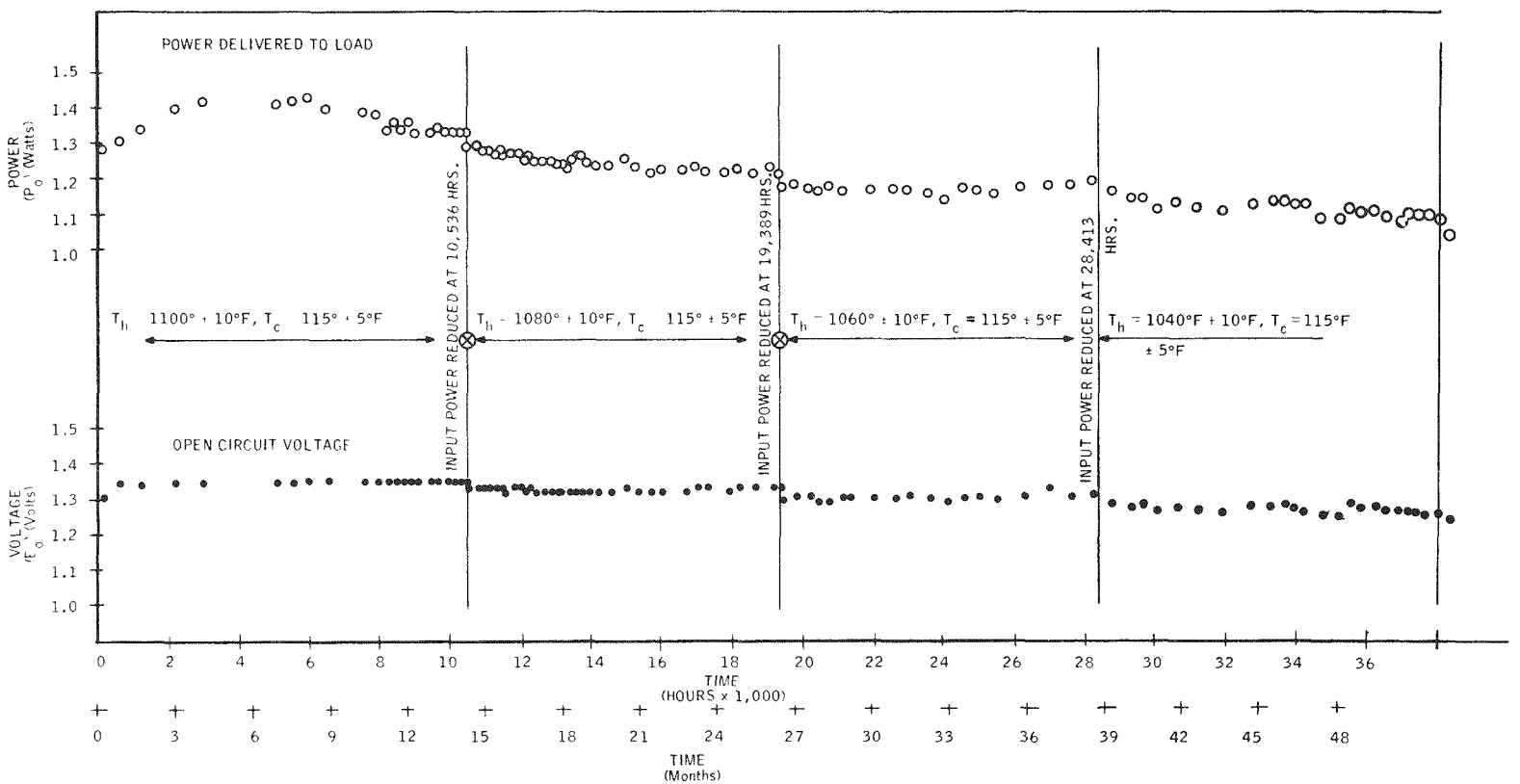

Figure 2-31. Performance of SNAP-21B 6-Couple Module A1

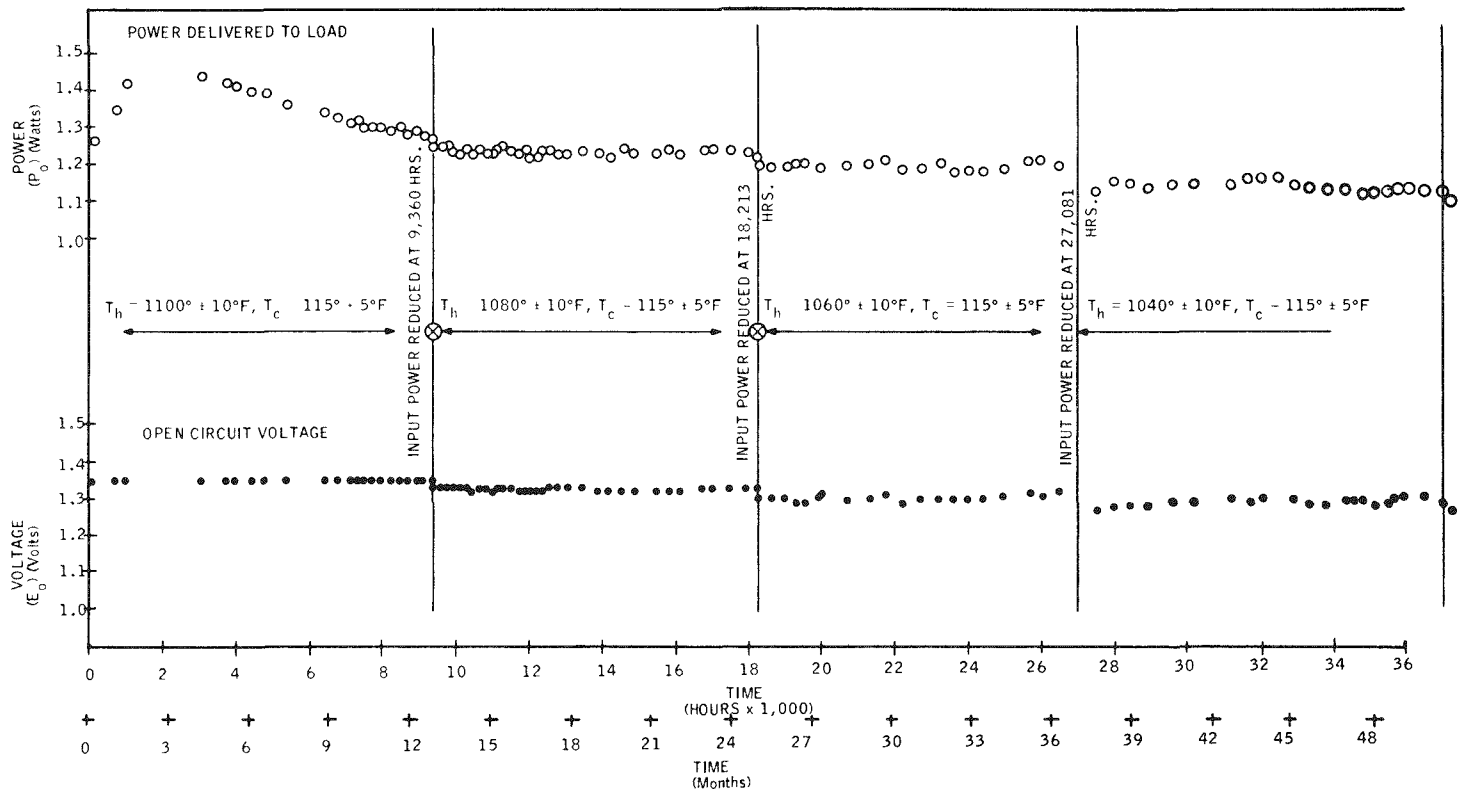

Figure 2-32. Performance of SNAP-21B 6-Couple Module A3

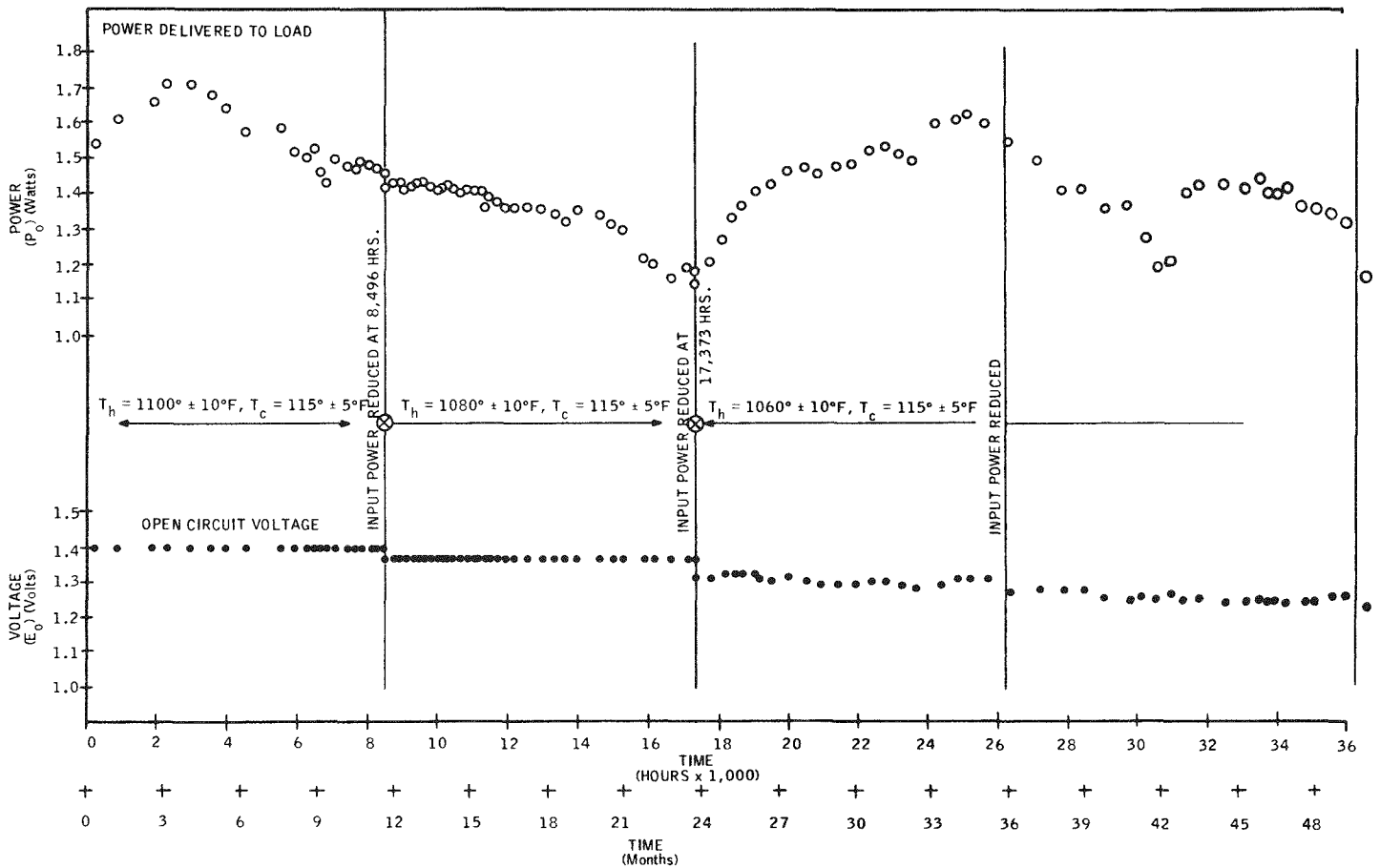

Figure 2-33. Performance of SNAP-21B 6-Couple Module A4

Table 2-14. Typical Performance Data SNAP-21B Prototype P5*

Date	T_h [1] (°F)	T_c [2] (°F)	E_o (volts)	E_L (volts)	I_L (amp)	P_o (watts)	R (ohms)	P_I (watts)	E_x/E_c	R_x/R_c	P_x/P_c	Hours on Test
4-19-65	1112	117	11.20	5.60	2.04	11.42	2.74	-	0.99	1.26	0.78	24
5-12-65	1115	127	10.92	5.46	2.00	10.92	2.73	--	0.97	1.24	0.77	576
6-30-65	1097	135	10.65	5.32	2.02	10.74	2.64	176	0.97	1.20	0.78	1,320
7-26-65	1097	142	10.68	5.34	2.01	10.72	2.66	176	0.98	1.21	0.79	1,944
9-10-65	1095	144	10.60	5.30	2.06	10.92	2.57	--	0.97	1.17	0.81	3,048
10-26-65	1097	147	10.56	5.28	2.05	10.81	2.58	180	0.97	1.16	0.82	4,152
12- 1-65	1102	151	10.58	5.29	2.10	11.11	2.52	--	0.98	1.13	0.84	5,016
1-28-66	1094	149	10.56	5.28	2.14	11.30	2.47	180	0.98	1.11	0.86	6,408
3-28-66	1094	152	10.54	5.27	2.16	11.38	2.44	180	0.98	1.10	0.87	7,821
4-28-66	1074	151	10.20	5.10	2.19	11.17	2.33	176	0.97	1.07	0.87	8,565
6-21-66	1073	151	10.24	5.00	2.18	10.90	2.40	174	0.97	1.10	0.86	9,834
8-12-66	1078	161	10.15	5.07	2.20	11.15	2.30	178	0.97	1.04	0.89	11,081
9-14-66	1075	161	10.16	5.07	2.19	11.10	2.32	175	0.97	1.06	0.89	11,873
12-27-66	1077	153	10.22	5.11	2.19	11.19	2.33	184	0.97	1.07	0.87	14,369
1-31-67	1073	159	10.12	5.06	2.20	11.13	2.30	179	0.96	1.05	0.90	15,209
4- 1-67	1074	148	10.20	5.10	2.24	11.42	2.28	175	0.97	1.05	0.89	16,649
5-24-67	1076	150	10.28	5.14	2.20	11.31	2.34	179	0.97	1.08	0.88	17,921
6-30-67	Power Failure, Emergency Power Came On at 8:28 PM to 10:30 PM											
7- 1-67	1067	159	10.00	5.00	2.19	10.95	2.28	175	0.95	1.00	0.88	18,833
8- 5-67	1069	164	10.01	5.00	2.22	11.10	2.26	170	0.95	1.01	0.90	19,673
9-26-67	1068	160	10.04	5.02	2.17	10.89	2.31	172	0.96	1.05	0.88	20,921
11- 6-67	1067	158	10.08	5.04	2.19	11.04	2.30	174	0.96	1.00	0.89	21,953
12-29-67	1066	150	10.20	5.10	2.22	11.32	2.30	175	0.97	1.06	0.90	23,225
1-15-68	Power Failure, Emergency Power Came On for One Hour											
1-30-68	1070	151	9.90	4.95	2.21	10.94	2.26	175	0.94	1.01	0.87	23,993
2-17-68	Power Failure, Emergency Power Came On for Five Hours											
2-19-68	1068	149	10.10	5.05	2.17	10.96	2.33	177	0.96	1.00	0.87	24,473
3-14-68	1052	156	9.96	4.98	2.19	10.91	2.27	177	0.98	1.03	0.90	25,049
5-22-68	1077	154	10.02	5.02	2.22	11.14	2.25	176	0.95	1.04	0.87	26,705
6-17-68	1042	157	9.92	4.96	2.14	10.61	2.32	171	0.98	1.06	0.90	27,329
6-17-68	Reduced Input Power											
8-13-68	1044	166	9.80	4.90	2.09	10.24	2.34	169	0.98	1.14	0.87	28,697
9-16-68	1050	164	9 82	4 90	2 09	10 24	2 35	169	0 97	1 14	0 86	29,513
11-6-68	1052	162	9 76	4 88	2 10	10 25	2 32	170	0 97	1 13	0 87	30,737
12-16-68	1052	152	9 86	4 93	2 15	10 60	2 29	170	0 97	1 13	0 86	31,697

*Begin test on 4-19-65
Turned off from 5-20-65 to 6-7-65

1 Based on average of two N leg Seebeck voltages
2 Based on average of four cold electrode thermocouples

Table 2-15. Typical Performance Data SNAP-21B Prototype P6*

Date	T_h[1] (°F)	T_c[2] (°F)	E_o (volts)	E_L (volts)	I_L (amp)	P_o (watts)	R (ohms)	P_I (watts)	$\frac{E_x}{E_c}$	$\frac{R_x}{R_c}$	$\frac{P_x}{P_c}$	Hours on Test
6- 2-65	1095[1]	132	10.88	5.44	2.58	14.03	2.10	204	1.03	1.02	1.02	24
6-30-65	1095[2]	145	10.88	5.44	2.34	12.73	2.32	206	1.04	1.11	0.96	720
7-29-65	1095[2]	157	10.88	5.44	2.28	12.40	2.38	--	1.04	1.13	0.96	1,416
9- 1-65	1095[2]	162	10.80	5.40	2.20	11.88	2.45	201	1.04	1.16	0.93	2,184
9-30-65	1095[2]	166	10.72	5.36	2.19	11.74	2.45	198	1.04	1.15	0.93	2,880
11-17-65	1095[2]	169	10.80	5.40	2.16	11.66	2.50	201	1.05	1.16	0.94	4,032
12-28-65	1095[2]	171	10.78	5.39	2.18	11.75	2.47	200	1.05	1.15	0.95	5,016
2- 5-66	1095[2]	171	10.74	5.37	2.14	11.49	2.51	197	1.04	1.17	0.93	5,952
3-28-66	1095[2]	171	10.74	5.39	2.13	11.44	2.52	197	1.04	1.17	0.92	7,173
4-28-66	1095[2]	172	10.76	5.38	2.11	11.35	2.55	201	1.04	1.19	0.92	7,941
8-12-66	1075[2]	181	10.52	5.23	2.05	10.72	2.58	191	1.05	1.20	0.92	10,452
9-14-66	1075[2]	182	10.53	5.24	2.06	10.79	2.57	190	1.05	1.20	0.93	11,244
12-27-66	1075[2]	176	10.82	5.41	2.09	11.28	2.59	192	1.07	1.22	0.95	13,740
1-27-67	1075[2]	176	10.84	5.42	2.10	11.38	2.58	199	1.08	1.22	0.96	14,484
3-13-67	1075[2]	173	10.86	5.43	2.09	11.35	2.60	198	1.08	1.23	0.95	15,564
4-27-67	1075[4]	168	10.38	5.19	2.07	10.72	2.51	194	1.03	1.20	0.89	16,524
6-16 67	1075[4]	176	10.58	5.29	2.05	10.84	2.58	194	1.05	1.23	0.90	17,844
6-22-67	Power Input Reduced							186				17,988
6-30-67	1055[4] Bldg Power Failure, Emergency Power for Approx. 2 Hours											
7- 1-67	1055[4]	172	10.10	5.05	2.04	10.28	2.48	184	1.03	1.20	0.88	18,204
8- 4-67	1055[4]	178	9.95	4.98	2.03	10.11	2.45	185	1.02	1.18	0.90	19,020
9-26-67	1055[4]	175	10.08	5.04	2.02	10.18	2.50	186	1.03	1.21	0.88	20,292
11- 6-67	1055[4]	172	10.08	5.04	2.02	10.18	2.50	185	1.03	1.21	0.87	21,324
11-30-67	1055[4]	166	10.00	5.00	2.04	10.20	2.45	190	1.02	1.20	0.86	21,900
1-15-68	Bldg. Power Was Off—Emergency Power Came On for One Hour											
1-17-68	1055[4]	166	10.04	5.02	2.03	10.19	2.47	192	1.02	1.20	0.86	23,052
2-17-68	Bldg. Power Was Off—Emergency Power Came On for 5 Hours											
3-14-68	1055[4]	171	10.02	5.01	2.04	10.22	2.46	192	1.02	1.19	0.88	24,420
5- 9-68	1055[4]	169	10.00	5.00	2.04	10.20	2.45	192	1.01	1.19	0.87	25,764
7-10-68	1035[4]	173	9.76	4.88	1.97	9.61	2.48	188	1.03	1.23	0.87	27,252
8-13-68	1035[4]	182	9.76	4.88	1.99	9.71	2.45	188	1.04	1.21	0.89	28,068
9-16-68	1035[4]	175	9.76	4.88	1.98	9.66	2.46	188	1.03	1.22	0.87	28,884
5-9-68	1055	169	10 00	5 00	2 04	10 20	2 45	192	1 01	1 19	0 87	25,764
6-17-68	Reduced Input Power											
7-10-68	1035[4]	173	9 76	4 88	1 97	9 61	2 48	188	1 03	1 23	0 87	27,252
8-13-68	1035[4]	182	9 76	4 88	1 99	9 71	2 45	188	1 04	1 21	0 89	28,068
9-16-68	1035[4]	175	9 76	4 88	1 98	9 66	2 46	188	1 03	1 22	0 87	28,884
11-6-68	1035[4]	174	9 80	4 89	1 99	9 73	2 47	188	1 04	1 22	0 88	30,108
12-16-68	1035[4]	165	9 80	4 89	2 00	9 78	2 46	188	1 03	1 23	0 87	31,068

Begin test 6-1-65

1 Based on average of two hot electrode thermocouples
2 Based on hot frame thermocouple referenced to 6-2-65
3 Based on average of two cold electrode thermocouples
4 Based on average input power from 6-5-66 to 12-27-66

Table 2-16. Typical Performance Data SNAP-21B Prototype P7*

Date	T_h[1] (°F)	T_c[2] (°F)	E_o (volts)	E_L (volts)	I_L (amp)	P_o (watts)	R (ohms)	P_1 (watts)	$\frac{E_x}{E_c}$	$\frac{R_x}{R_c}$	$\frac{R_x}{P_c}$	Hours on Test
6- 8-65	1099[1]	127	10.80	5.40	2.44	13.17	2.21	200	1.01	1.08	0.95	168
7-14-68	1098[1]	142	10.80	5.40	2.21	11.95	2.44	194	1.01	1.18	0.88	1,032
8-24-65	1100[3]	152	10.82	5.41	2.13	11.52	2.54	192	1.03	1.21	0.88	1,968
10-12-65	1100[3]	156	10.86	5.43	2.11	11.47	2.57	194	1.04	1.22	0.82	3,144
11-17-65	1095[3]	158	10.80	5.40	2.08	11.23	2.60	188	1.04	1.23	0.87	4,008
12-28-65	1095[3]	159	10.78	5.39	2.07	11.16	2.60	191	1.04	1.23	0.88	4,992
2-10-66	1095[3]	158	10.82	5.41	2.06	11.14	2.63	191	1.04	1.24	0.88	6,048
3-28-66	1095[3]	160	10.80	5.40	2.05	11.07	2.63	191	1.04	1.24	0.87	7,149
5-16-66	1095[3]	163	10.82	5.41	202	10.93	2.68	189	1.04	1.26	0.86	8,324
6- 4-66	Reduced Input Power											
6-21-66	1075[3]	158	10.72	5.40	1.99	10.75	2.67	186	1.06	1.28	0.87	9,181
6-28-66	Moved Test from T. C. A. to Space Center											
8-12-66	1075[3]	173	10.56	5.26	1.96	10.31	2.55	188	1.05	1.26	0.86	10,428
10- 3-66	1075[3]	178	10.62	5.31	1.95	10.35	2.72	185	1.05	1.27	0.89	11,676
12-28-66	1075[4]	165	10.70	5.35	1.94	10.37	2.76	186	1.05	1.31	0.84	13,760
1-31-67	1075[4]	171	10.70	5.35	1.96	10.49	2.73	186	1.06	1.30	0.86	14,576
3-13-67	1075[4]	173	10.60	5.30	1.94	10.26	2.74	186	1.06	1.29	0.86	15,560
5-13-67	1075[4]	175	10.61	5.30	1.91	10.11	2.78	186	1.06	1.31	0.85	17,024
6-22-67	Input Power was Reduced							180				
6-23-67	1055[4]	171	10.30	5.15	1.91	9.84	2.70	180	1.05	1.31	0.84	18,008
6-30-67	Bldg. Power Failure, Emergency Power was on for Approx. 2 Hours											
7- 1-67	1055[4]	165	10.30	5.15	1.86	9.58	2.77	180	1.05	1.35	0.81	18,192
8- 8-67	1055[4]	182	10.19	5.10	1.92	9.79	2.65	178	1.05	1.27	0.86	19,110
9-26-67	1055[4]	166	10.26	5.13	1.92	9.85	2.67	179	1.04	1.30	0.83	20,286
10-20-67	1055[4]	171	10.14	5.07	1.91	9.68	2.65	176	1.03	1.29	0.83	21,091
1-15-68	Bldg. Power was off - Emergency Power came on for One Hour											
1-17-68	1055[4]	169	10.40	5.20	1.92	9.98	2.71	177	1.06	1.32	0.85	23,203
2-17-68	Bldg. Power was off - Emergency Power came on for about 5 Hours											
2-19-68	1055[4]	164	10.20	5.10	1.92	9.79	2.66	180	1.04	1.30	0.83	23,997
3-20-68	1055[4]	169	10.28	5.14	1.92	9.87	2.68	181	1.05	1.30	0.85	24,717
4-18-68	1055[4]	177	10.20	5.10	1.93	9.84	2.64	189	1.04	1.28	0.85	25,384
5- 9-68	1055[4]	179	10.28	5.14	1.93	9.92	2.66	180	1.06	1.28	0.87	25,917
6-17-68	1055[4]	182	9.94	4.97	1.90	9.44	2.62	176	1.02	1.26	0.83	26,853
8-13-68	1035[4]	177	9.78	4.89	1.91	9.34	2.56	174	1.04	1.27	0.85	28,221
9-16-68	1035[4]	173	9.75	4.88	1.90	9.27	2.56	174	1.03	1.27	0.84	29,037
6-17-68	1055[4]	182	9 94	4 97	1 90	9 44	2 62	176	1 02	1 26	0 83	26,853
6-17-68	Reduced Power Input											
8-13-68	1035[4]	177	9 78	4 89	1 91	9 34	2 56	174	1 04	1 27	0 85	28,221
9-16-68	1035[4]	173	9 75	4 88	1 90	9 27	2 56	174	1 03	1 27	0 84	29,037
11-6-68	1035[4]	170	9 82	4 91	1 87	9 18	2 63	174	1 03	1 30	0 82	30,261
12-16-68	1035[4]	169	9 83	4 93	1 88	9 27	2 61	174	1 03	1 30	0 82	31,221

* Begin test 6-2-65.

1. Based on average of two hot electrode thermocouples.
2. Based on average of two cold electrode thermocouples.
3. Based on hot frame thermocouple referenced to 6-30-65.
4. Based on average input power from 7-13-66 to 11-12-66.

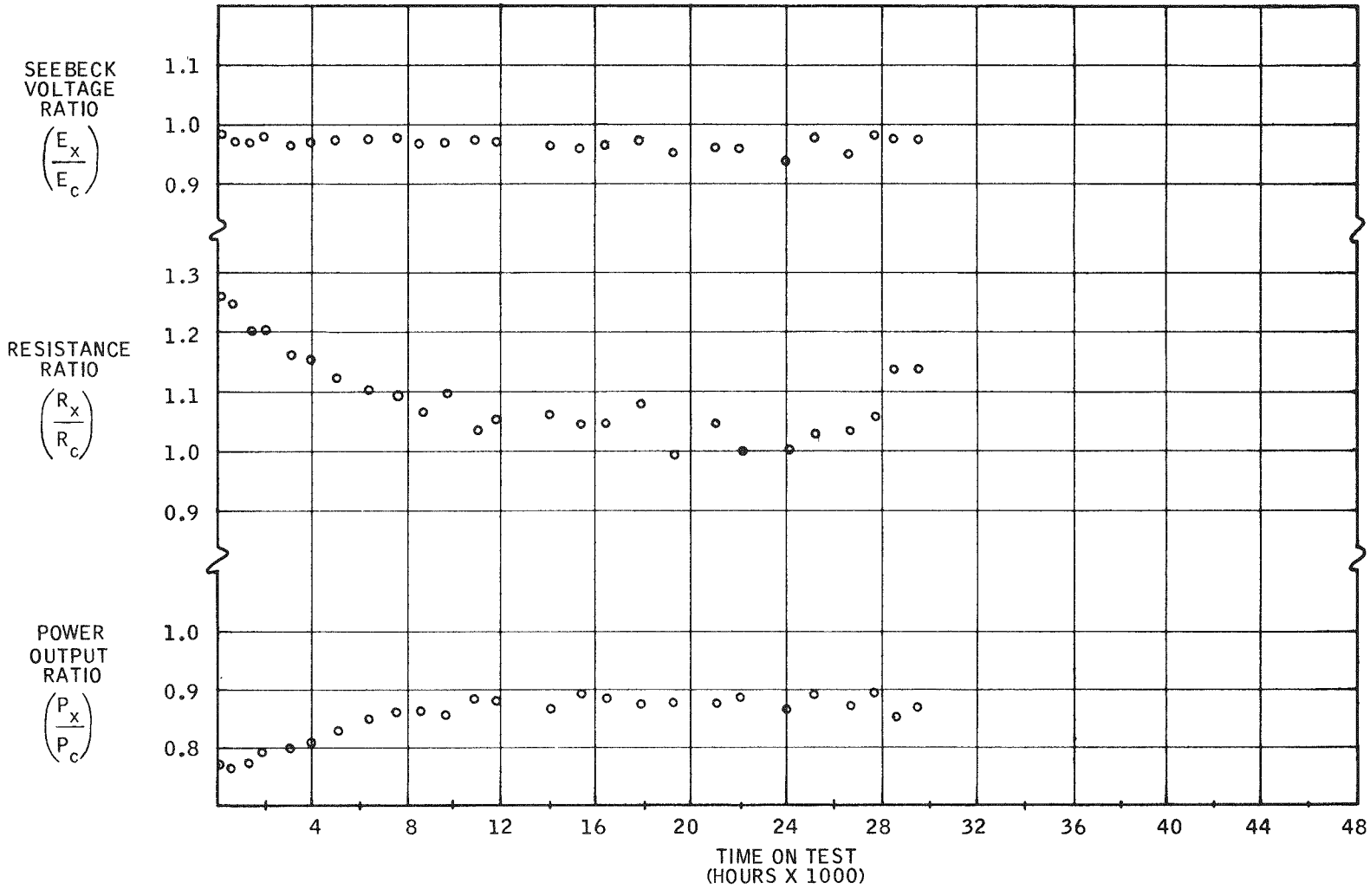

Figure 2-34. SNAP-21B 48-Couple Prototype Generator P5 Performance Ratios (Experimental/Calculated)

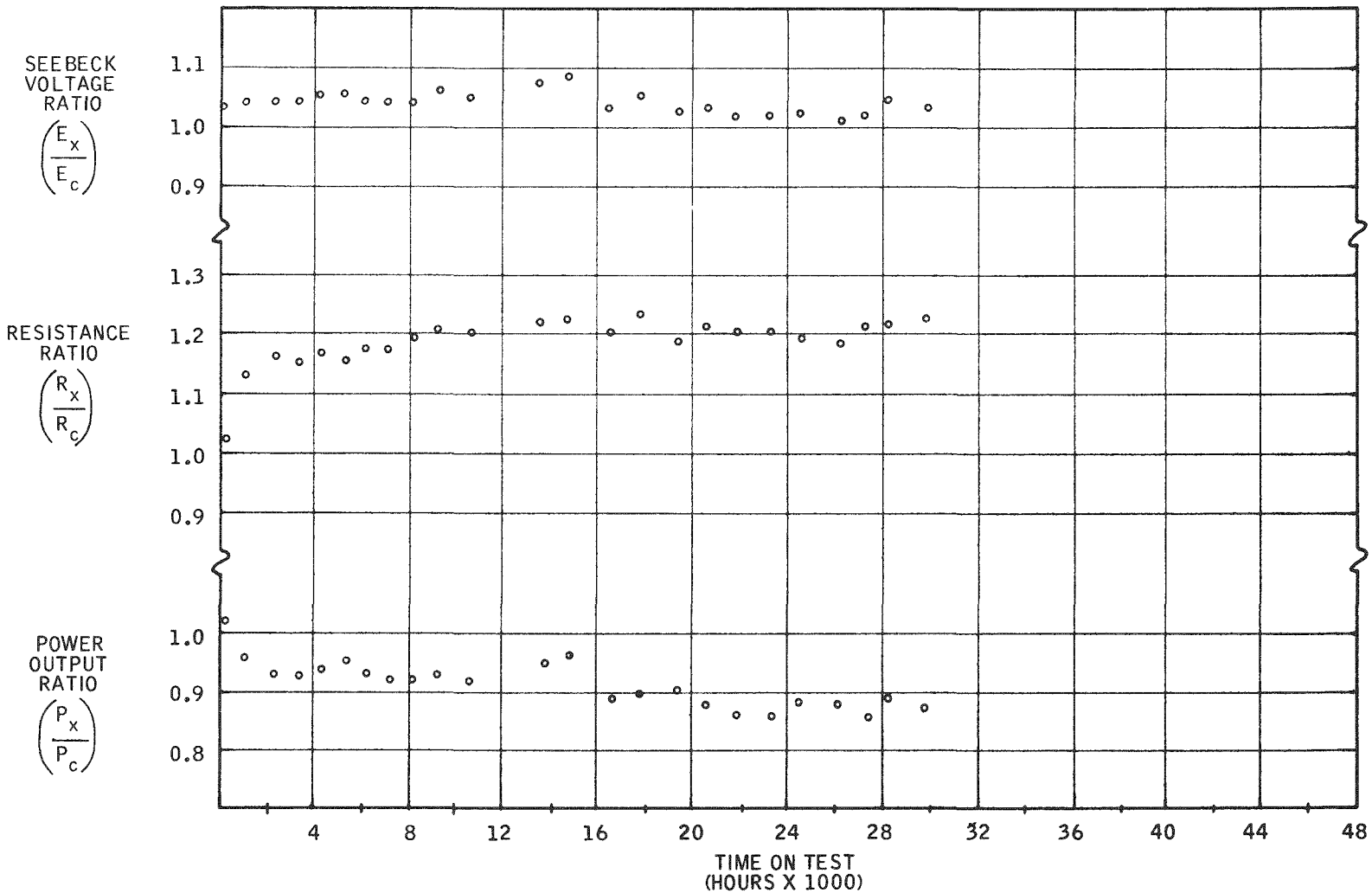

Figure 2-35. SNAP-21B 48-Couple Prototype Generator P6 Performance Ratios (Experimental/Calculated)

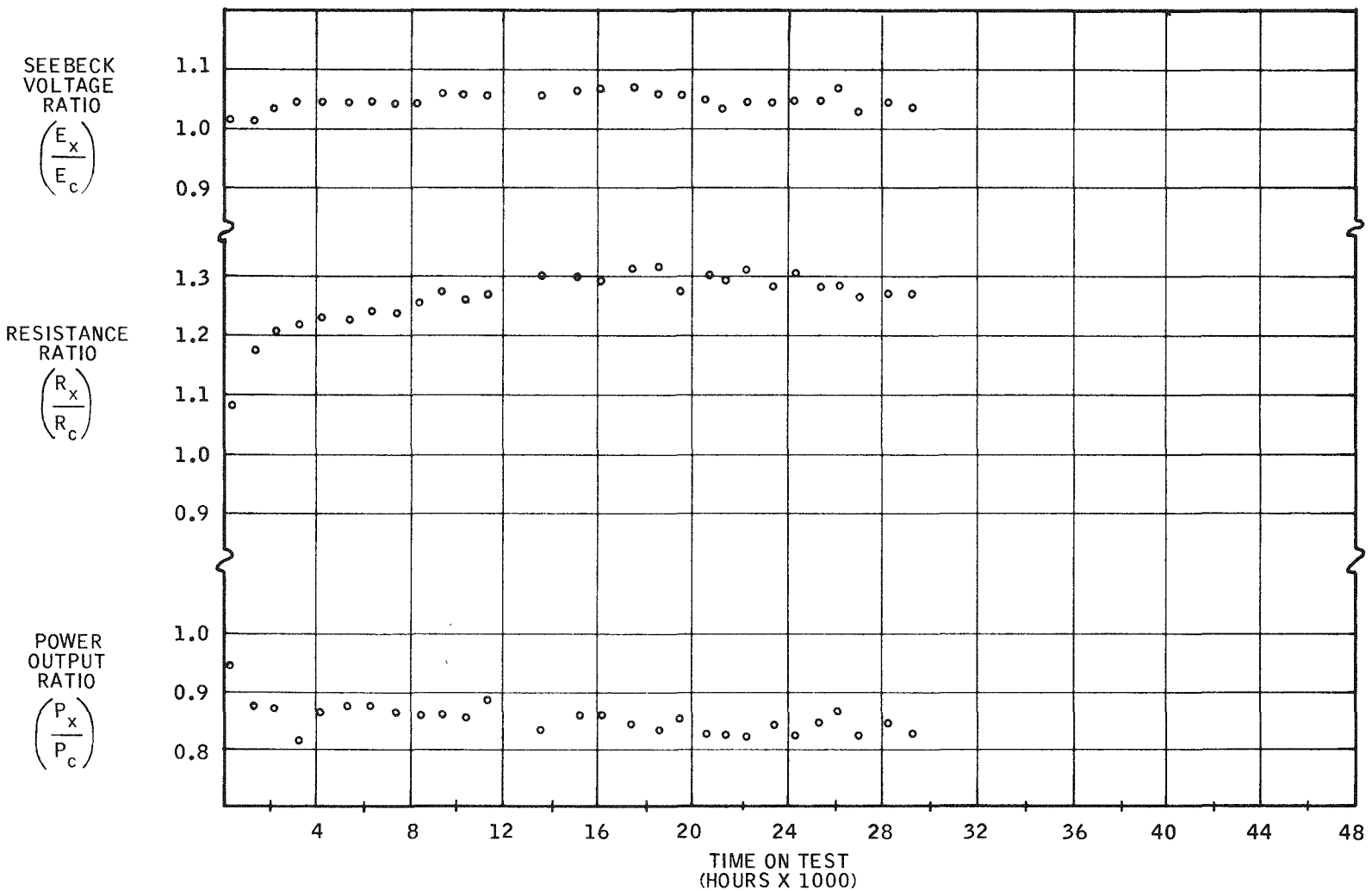

Figure 2-36. SNAP-21B 48-Couple Prototype Generator P7 Performance Ratios (Experimental/Calculated)

the generator was taken off test and placed in a dry box. An anti-collapse collar was installed on the generator at the outer case to prevent collapse or buckling when under vacuum. An attempt was made to leak check and pinpoint the actual location of the leak. No location could be found with probe and plastic bag techniques.

By use of alcohol and pressure in the generator, a leak was found in a solder joint between a Conax fitting and the cold frame. After the valve was taken from the generator, disassembled and leak-checked, a leak was found in the valve assembly. It was the opinion of the engineers working with the leak test that these two leaks were not gross enough to account for the leak as noted in test.

No further leaks could be found by pressurizing the generator with pure helium to 25 psia and pulling a vacuum on the dry box through the leak detector.

A leak check was then performed with a sealed bag of helium (helium was bled into the bag). No additional leaks could be found with this method.

A new valve was installed on the gas inlet line (pinch-off tube). A dam was constructed on the cold frame around the Conax fittings and pinch-off tube fitting. The dam was high enough so that the potting compound would cover the terminal board and Conax fittings. 3M Brand #2216 A/B potting compound was used, and the top of the cold frame was potted. During the leak check and repair procedure, an inert gas above atmospheric pressure was maintained. Whenever the generator was below atmospheric pressure, the atmosphere surrounding the generator was an inert gas or at a vacuum condition in the dry box. This was done in order to prevent air from accidentally entering the generator.

After the potting cure, an extensive leak check (both internal and external) was performed. The leak-check equipment indicated no detectable leaks at room temperature. The generator was replaced in the test station at 15 psig argon-helium. The heaters were activated, the gas pressure was stabilized at temperature, and the valve was closed. At the end of a week of testing at temperature, the test indicated that pressure had dropped approximately 0.25 psi per day. It is suspected that a leak at hot or operating temperature is occurring which is sealed at room temperature.

Later investigation showed that the valve which was put on the thermoelectric generator prior to potting is leaking. A positive pressure ($\approx$25 psia) was put on the outlet side of the valve and appears to have solved the problem.

The thermoelectric generator performance can be found in Figure 2-37. It appears that the power-out from the unit is decreasing. The exact cause for this is not known at this time. Because the testing of this TEG was interrupted to repair a leak, the temperature distribution has changed. And, since the internal thermocouples are shorted out, accurate temperature determination is difficult. It is believed that temperature error accounts for about 3 percent error in the curves shown in Figure 2-37. The temperature distribution will be watched closely during the next quarter. The generator is in no great danger because of this temperature problem.

A10D2

Thermoelectric generator A10D2 continued on test this past quarter. Testing was interrupted on October 22, 1968 for heater replacement. The operating temperatures of the generator are 1080 ± 10°F and 110 ± 10°F for the hot and cold button, respectively.

Figures 2-38 and 2-39 show the normalized Seebeck, resistance and power for this unit. It can be seen that the resistance is increasing. This could be due to sublimation. It appears that the Seebeck voltage is increasing slightly, but this could be due to temperature measurement error. This will be closely monitored during the next quarter. As a result, the power-out for the thermoelectric generator is decreasing.

A10D4

Refer to paragraph 2. 1. 1 (S10D2) for generator performance. Figure 2-40 shows the normalized Seebeck voltage, resistance and power.

A10D6

In the previous quarter, this generator was removed from test to repair a leak in its hermetic seal. After being on test for several hundred hours, it appears that the leak has been sealed.

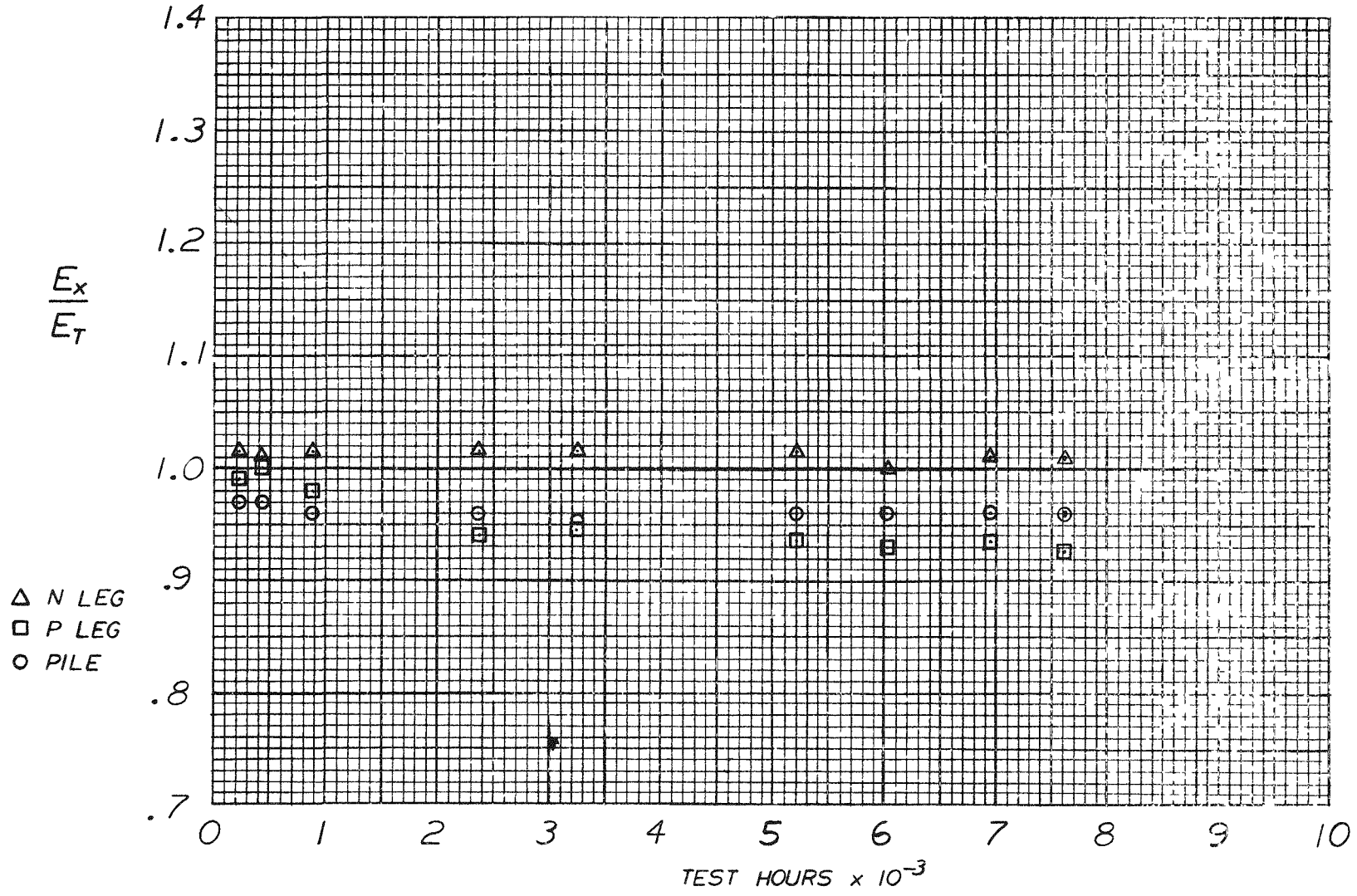

Figure 2-37a. SNAP-21 Thermoelectric Generator A10D1 Normalized Seebeck Voltage Ratio

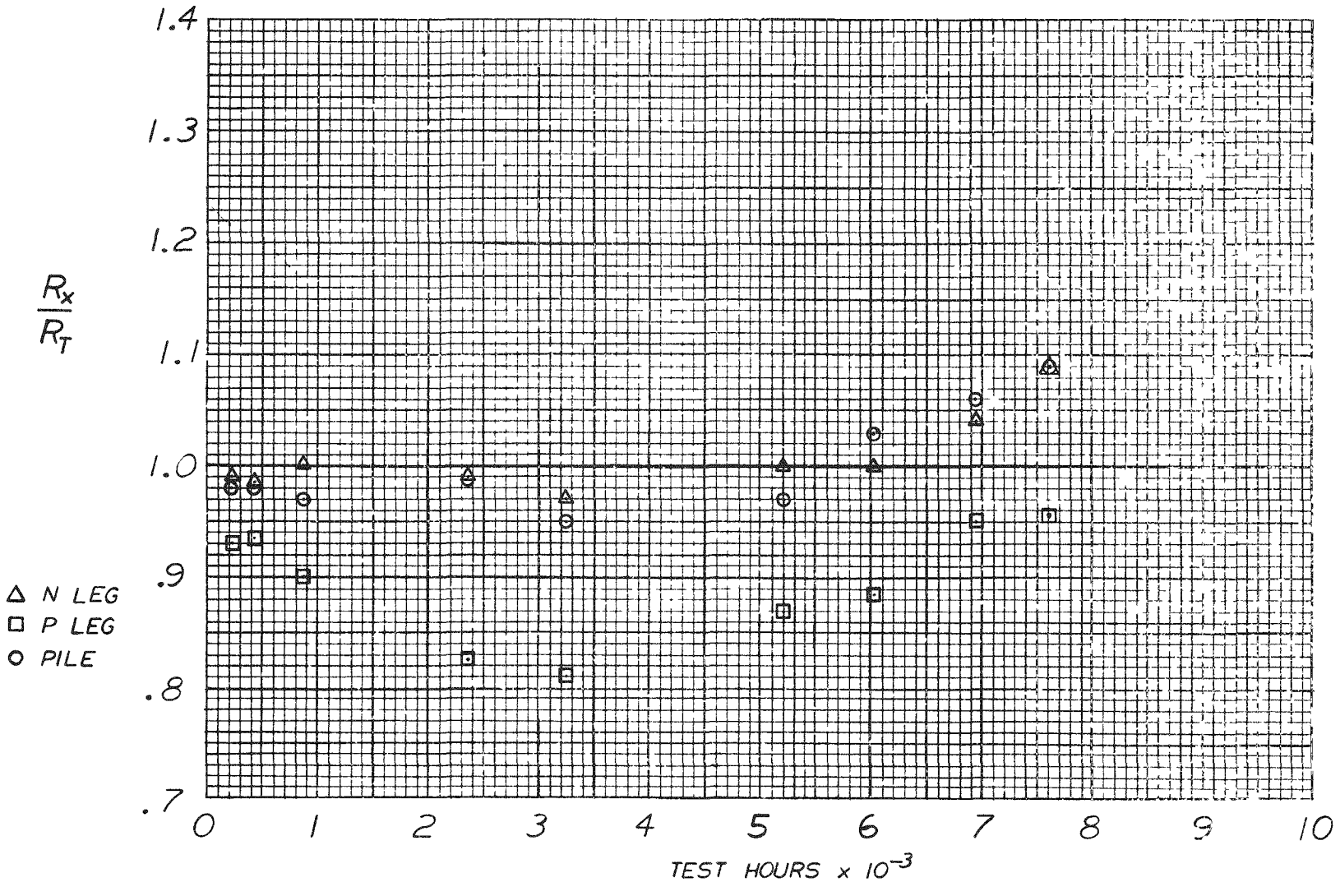

Figure 2-37b. SNAP-21 Thermoelectric Generator A10D1 Normalized Resistance Ratio

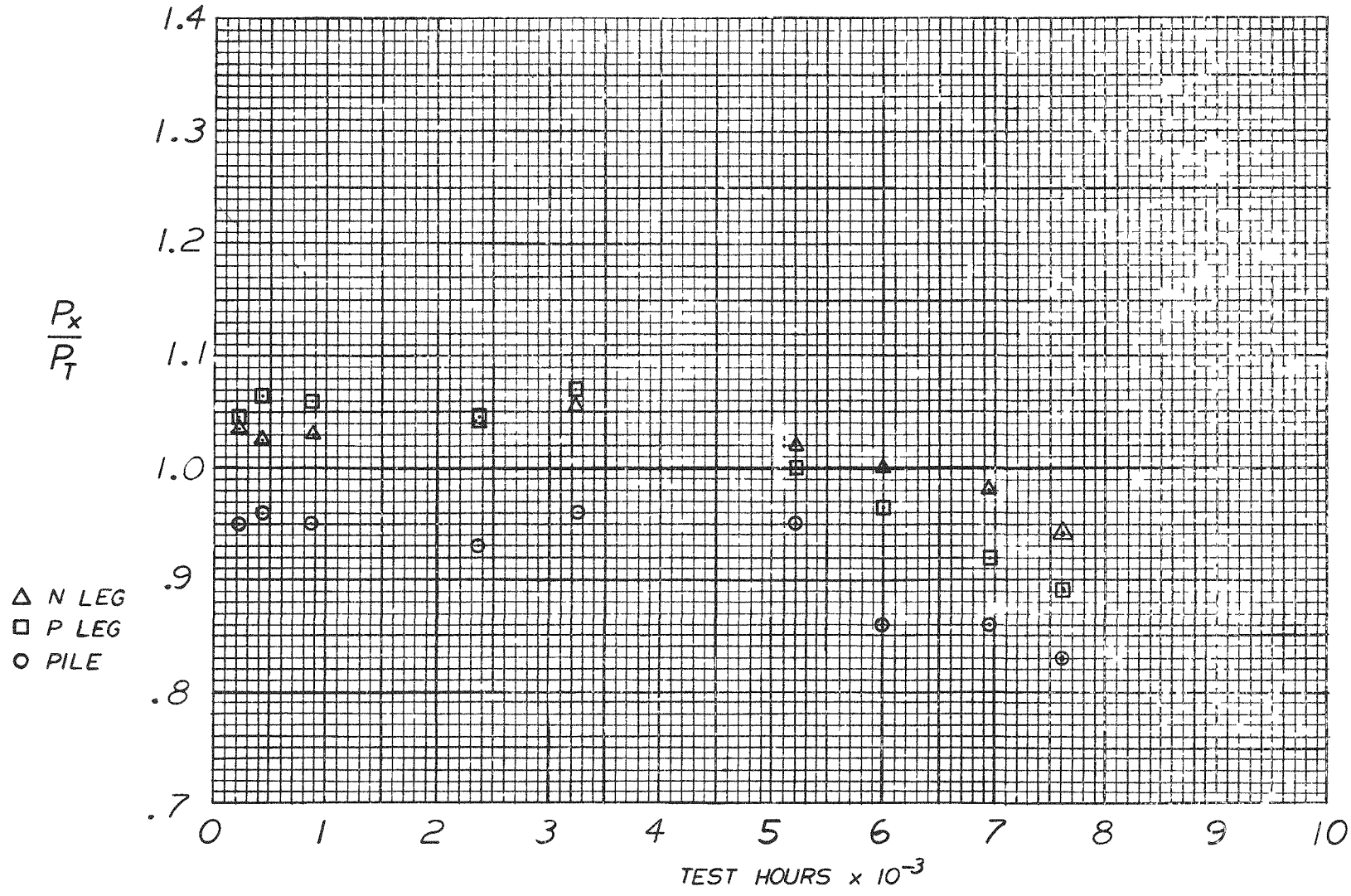

Figure 2-37c. SNAP-21 Thermoelectric Generator A10D1 Normalized Power Ratio

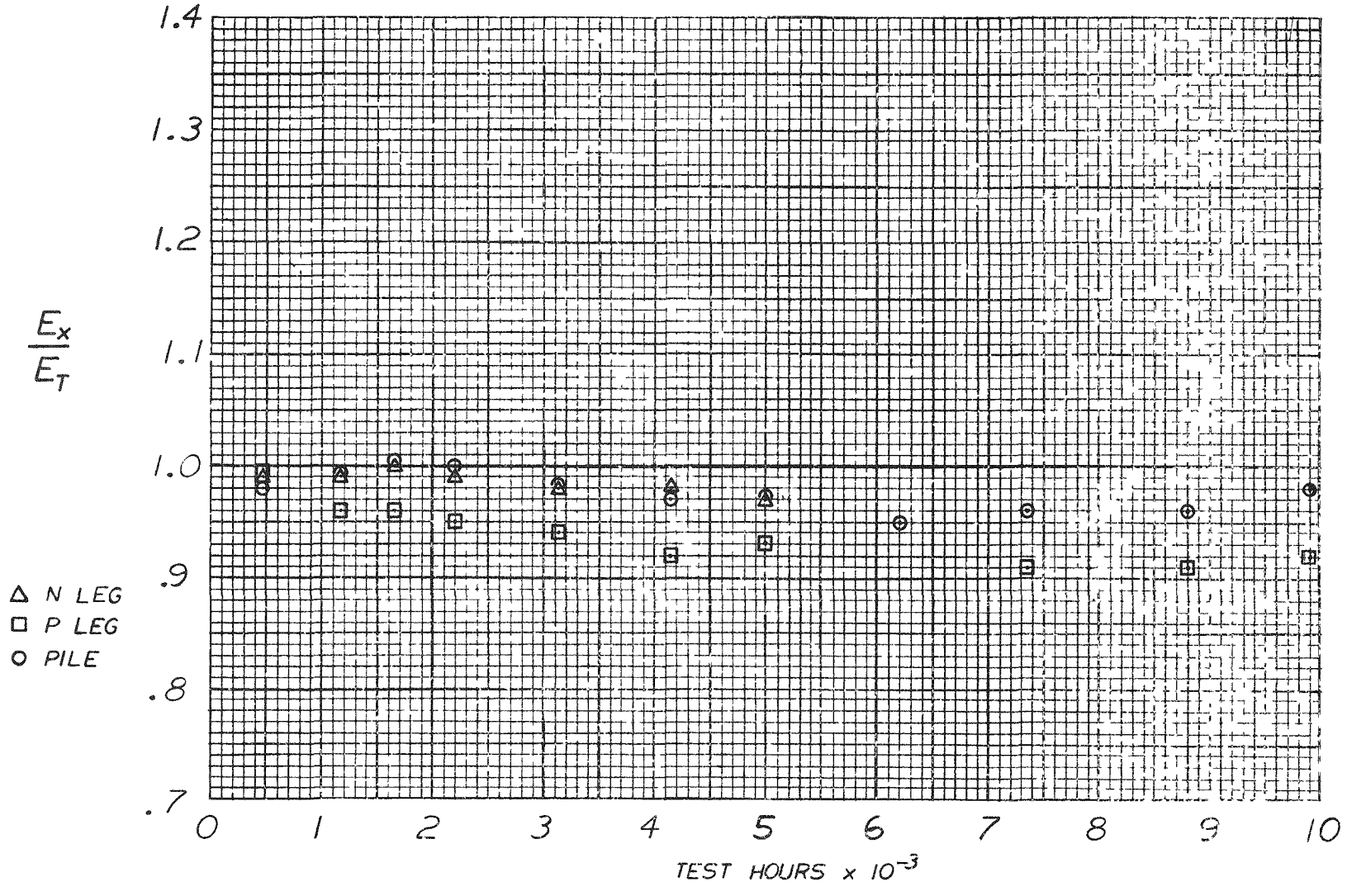

Figure 2-38a. SNAP-21 Thermoelectric Generator A10D2 Normalized Seebeck Voltage Ratio

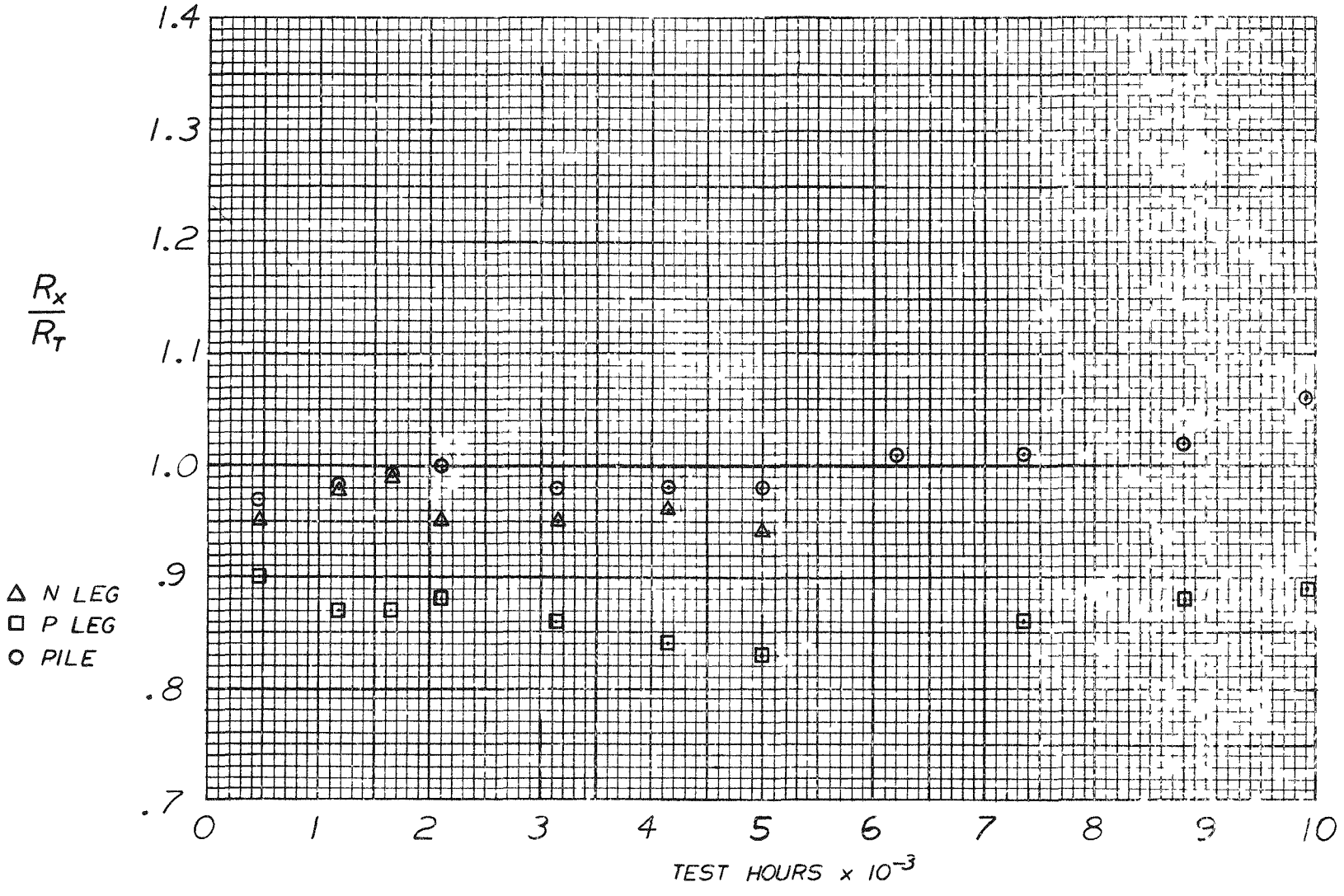

Figure 2-38b. SNAP-21 Thermoelectric Generator A10D2 Normalized Resistance Ratio

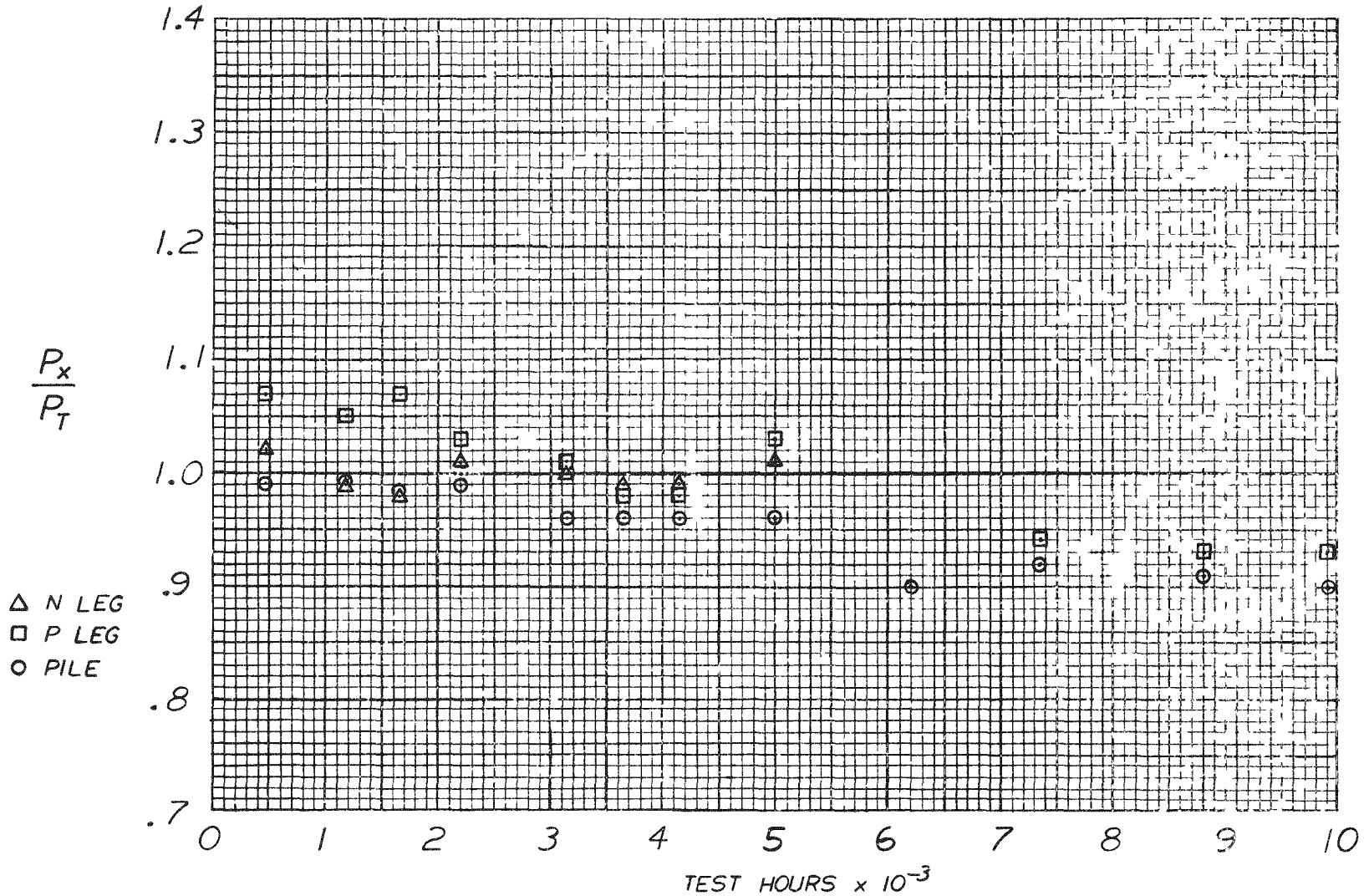

Figure 2-38c. SNAP-21 Thermoelectric Generator A10D2 Normalized Power Ratio

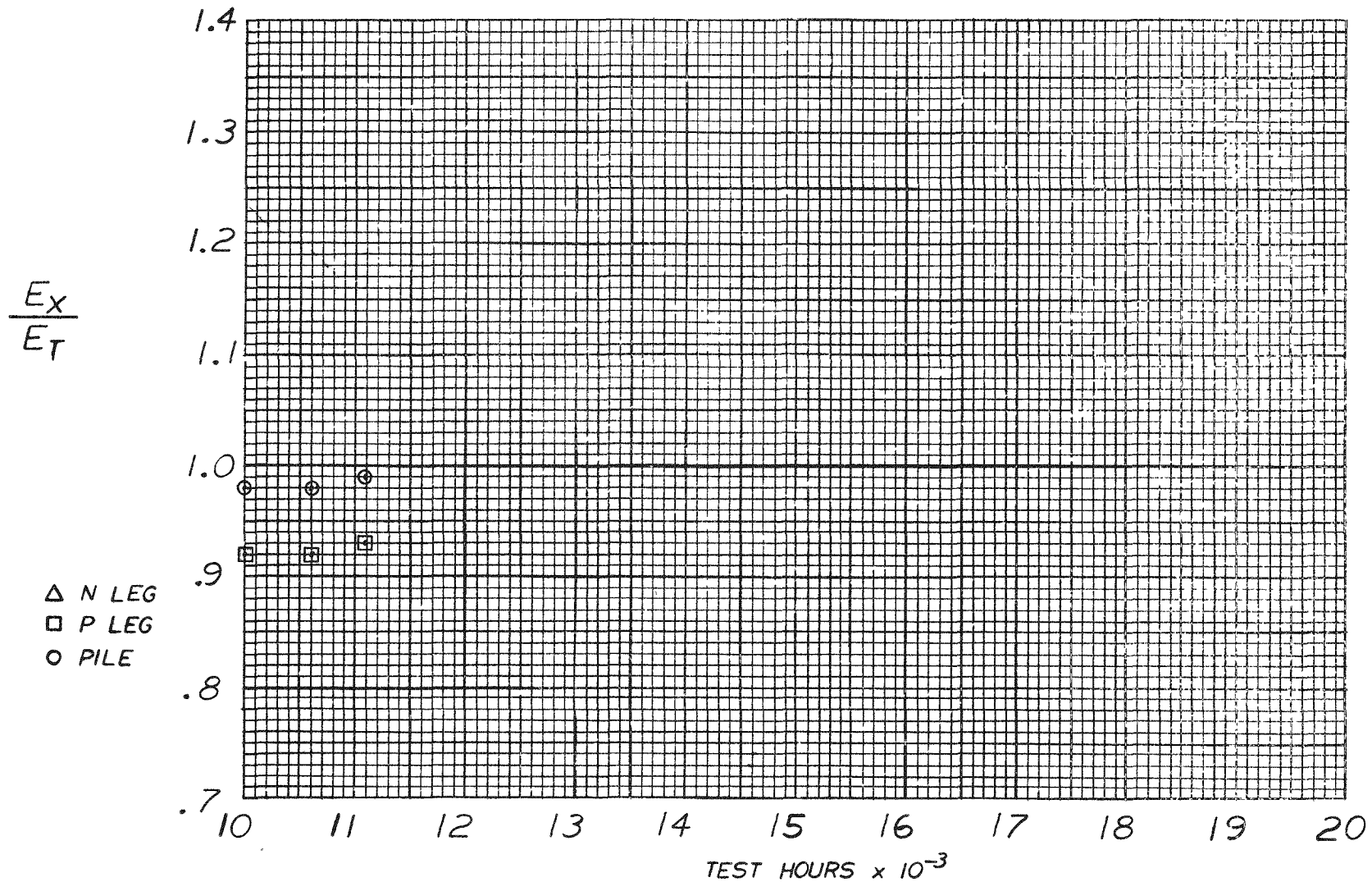

Figure 2-39a. SNAP-21 Thermoelectric Generator A10D2 Normalized Seebeck Voltage Ratio

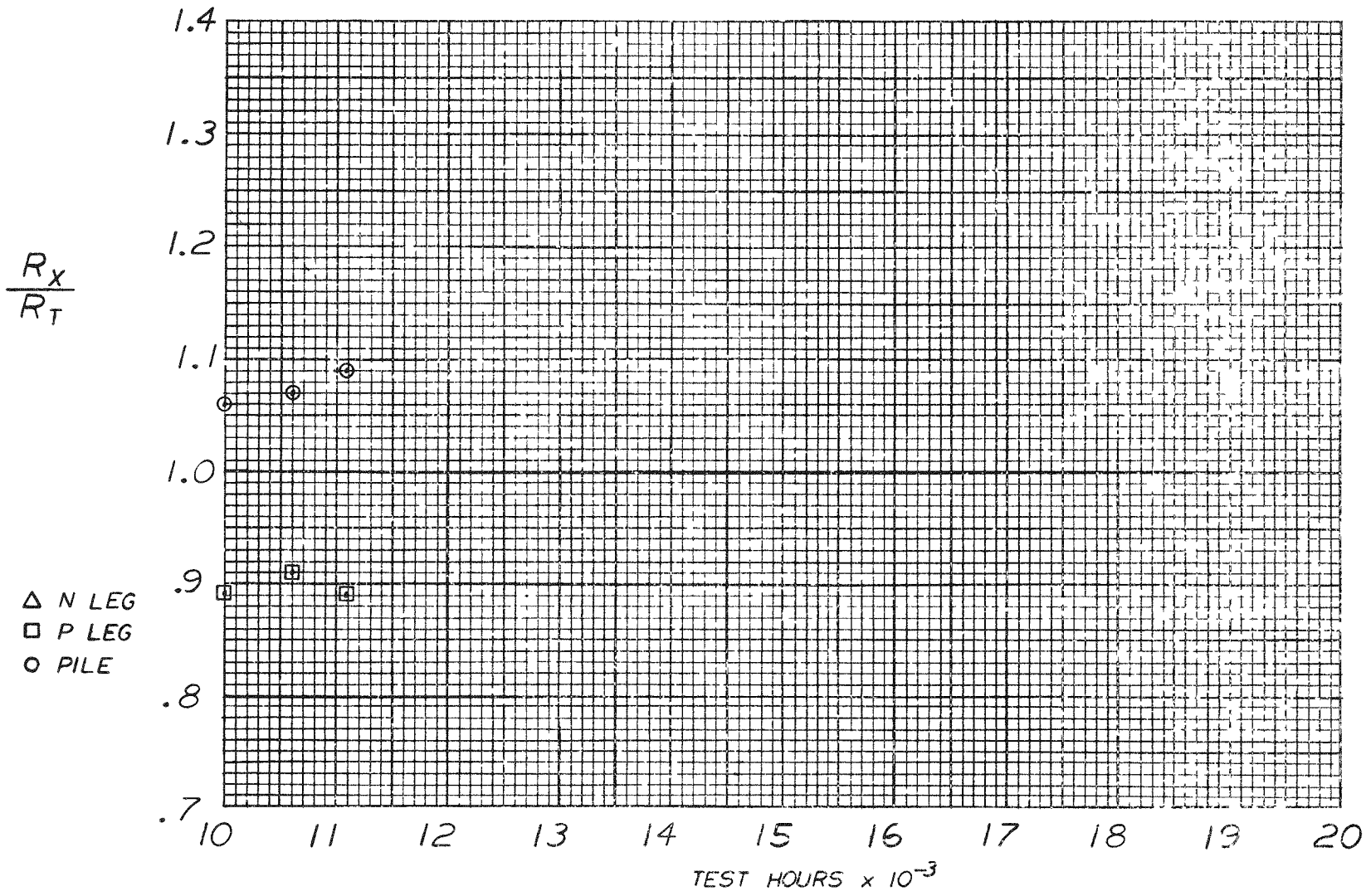

Figure 2-39b. SNAP-21 Thermoelectric Generator A10D2 Normalized Resistance Ratio

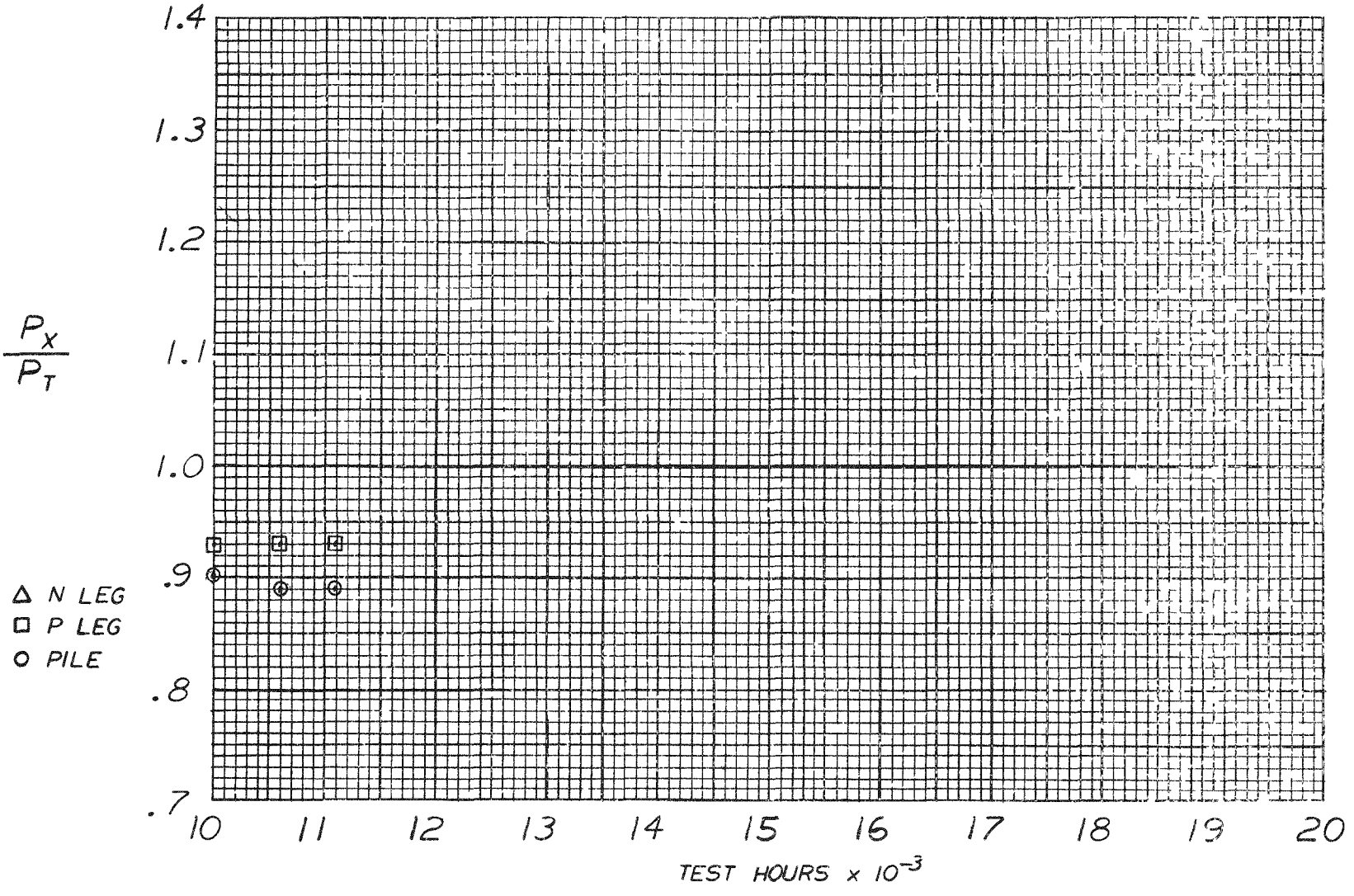

Figure 2-39c. SNAP-21 Thermoelectric Generator A10D2 Normalized Power Ratio

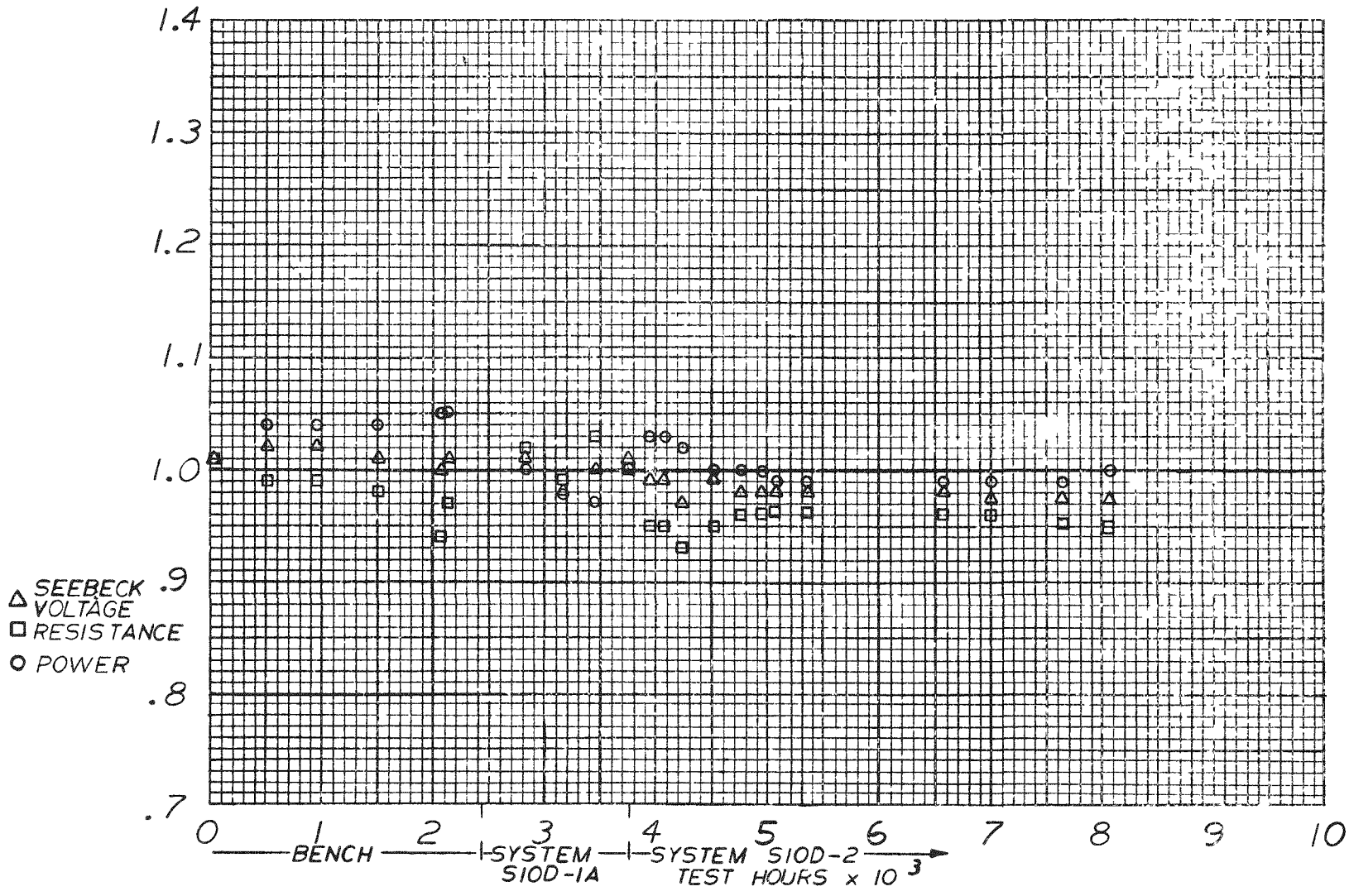

Figure 2-40. SNAP-21 Thermoelectric Generator A10D4 Normalized Data

Figure 2-41 shows the pertinent performance data for this thermoelectric generator. At the beginning of this past quarter, there was a decrease in power output. This was due to fluctuations in Seebeck voltage and resistance of both the P- and N-legs. However, the power output appears to be starting to increase.

A10D7

During the first 5200 hours of life test, this thermoelectric generator experienced an increase in resistance of about 13 percent for the thermopile (Figure 2-42). During this period, the Seebeck voltage was fairly stable. During this past quarter, the resistance decreased about 5 percent from its maximum of 17 percent over design. Also, the Seebeck voltage decreased slightly. Because of these changes in Seebeck voltage and resistance, the power output for the thermoelectric generator has stabilized during this past quarter. The greatest change in resistance appears to be in the P-leg.

A10P1

Generator A10P1 continued on test this past quarter. The SNAP-21 data reduction program was modified to include data from generator A10P1. Prior to this modification the program was unable to handle the temperatures at which A10P1 operates (T_{HB} = 1050 ± 10°F, T_{CC} = 90 ± 10°F). Test results from generator A10P1 indicate stable operation over the first 3000 hours of test (see Table 2-17).

Table 2-17. SNAP-21 Generator A10P1 Normalized Performance Data Expressed in Ratios (Experimental/Calculated)

Test Hours	Thermopile		
	E_x/E_c	R_x/R_c	P_x/P_c
126	0.97	1.03	0.93
527	0.97	1.01	0.93
961	0.97	1.02	0.93
1540	0.96	1.02	0.92
2431	0.97	1.03	0.91
2950	0.97	1.04	0.90

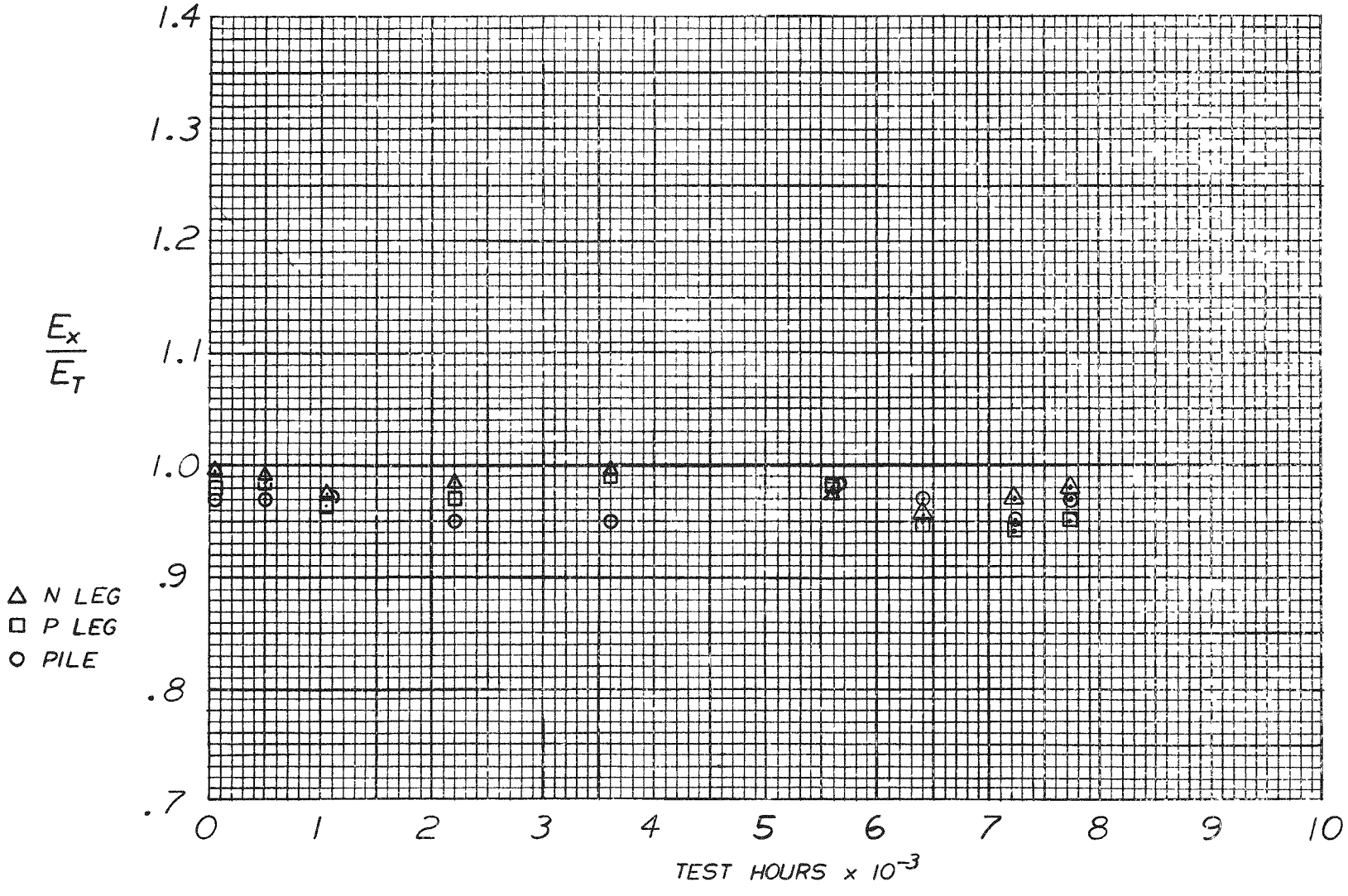

Figure 2-41a. SNAP-21 Thermoelectric Generator A10D6 Normalized Seebeck Voltage Ratio

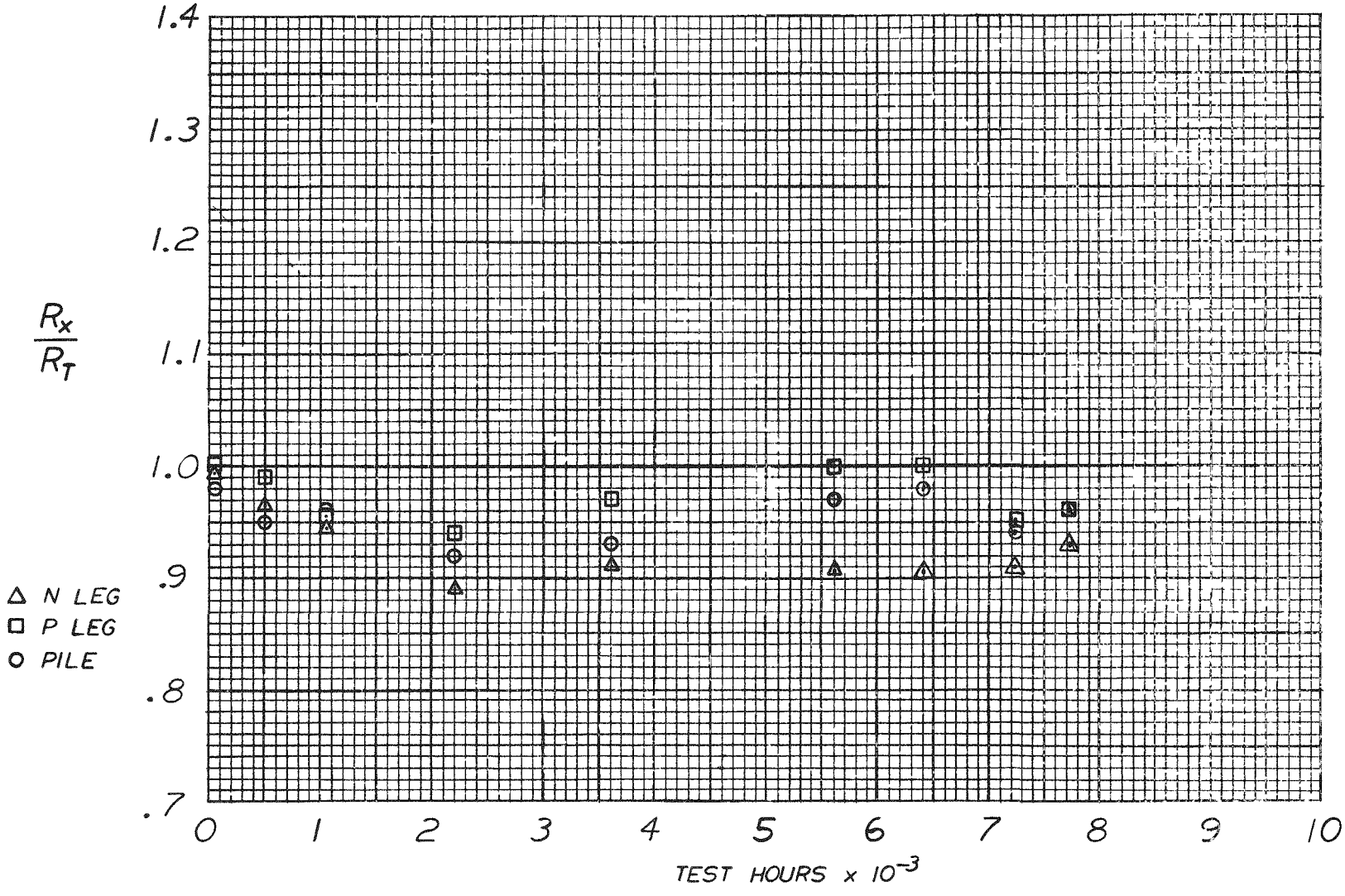

Figure 2-41b. SNAP-21 Thermoelectric Generator A10D6 Normalized Resistance Ratio

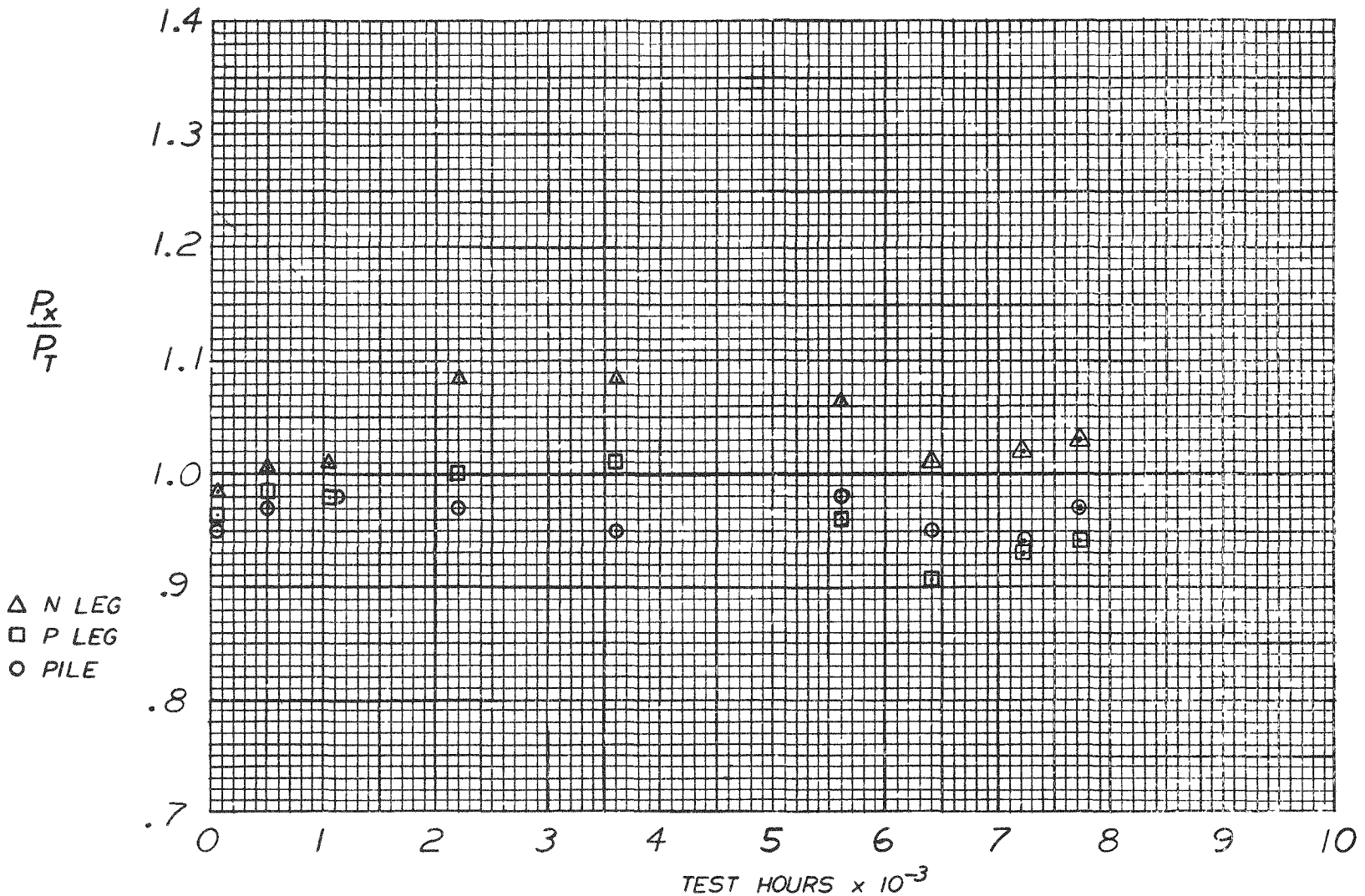

Figure 2-41c. SNAP-21 Thermoelectric Generator A10D6 Normalized Power Ratio

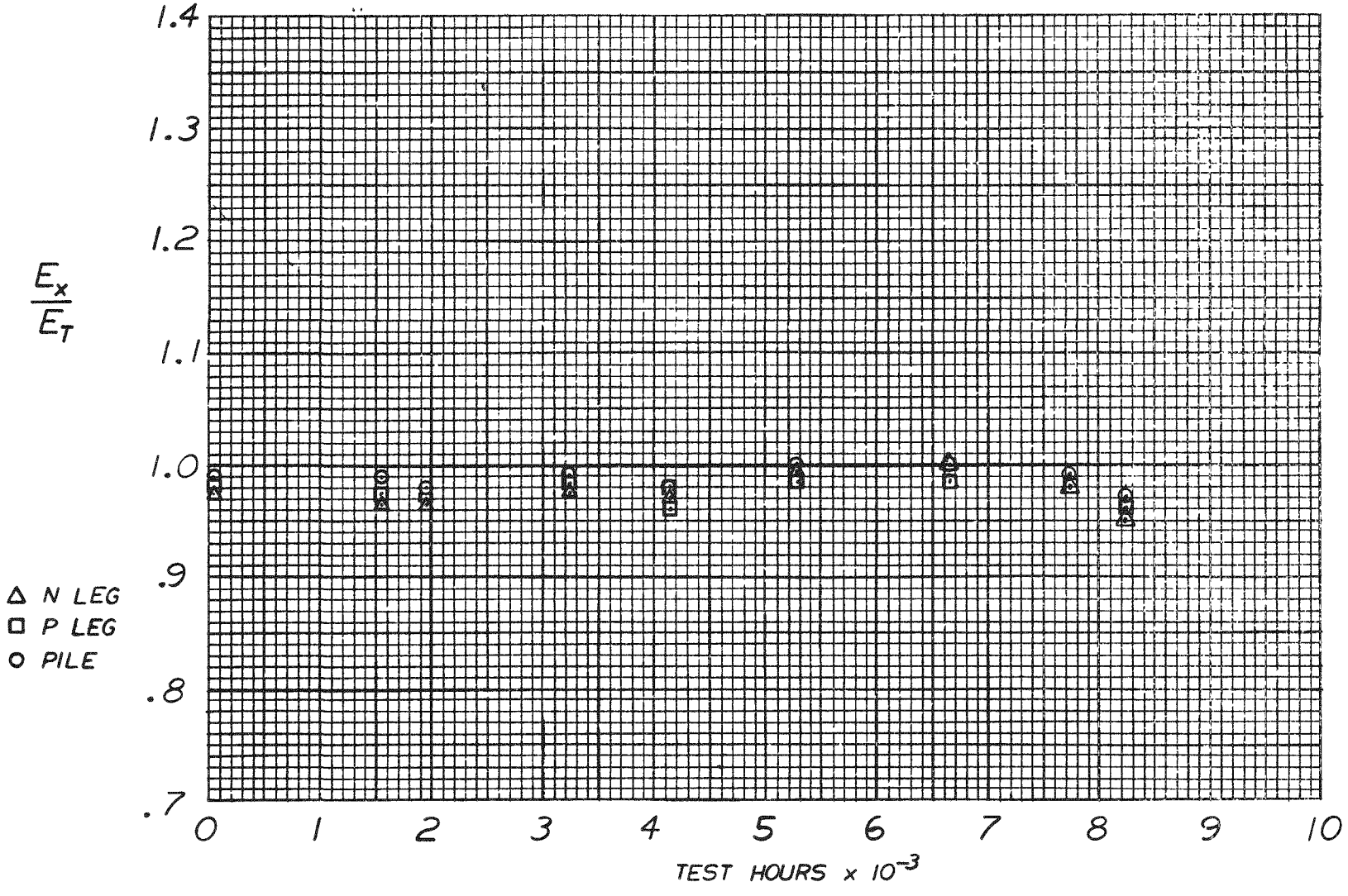

Figure 2-42a. **SNAP-21** Thermoelectric Generator A10D7 Normalized Seebeck Voltage Ratio

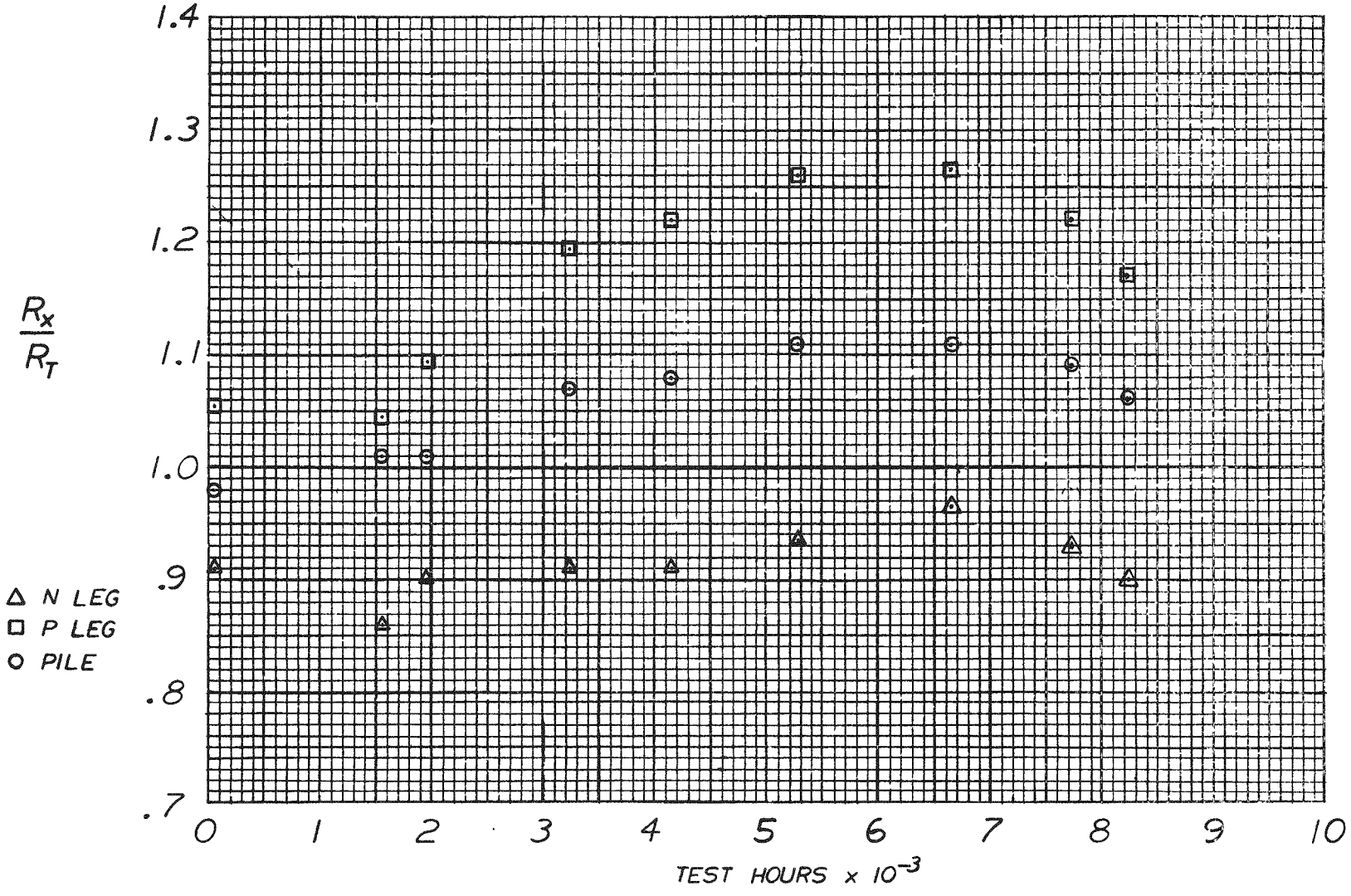

Figure 2-42b. SNAP-21 Thermoelectric Generator A10D7 Normalized Resistance Ratio

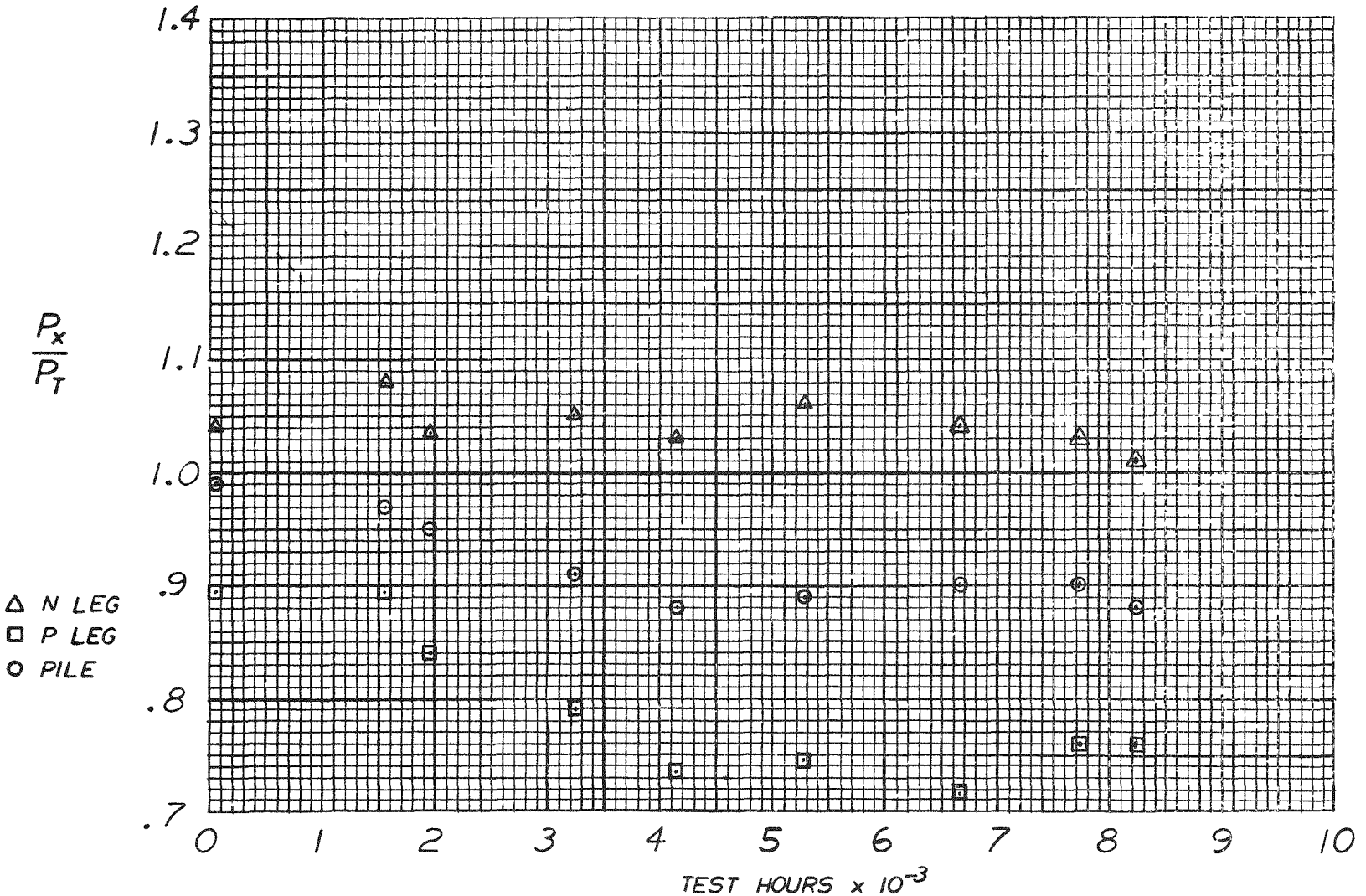

Figure 2-42c. SNAP-21 Thermoelectric Generator A10D7 Normalized Power Ratio

Because of the reversed couple, this generator is essentially a 46-couple generator. Performance parameters, however, are given for an equivalent 48-couple device. This is done by applying the appropriate ratio to the computer calculated results. The Seebeck ratio is multiplied by 48/46. The circuit resistance ratio from the computer is correct as it stands. The power ratio is proportional to E^2/R; thus, the power ratio from the computer is multiplied by $(48/46)^2$

A10P5

Generator A10P5 successfully completed acceptance testing. Table 2-18 summarizes the generator performance as compared to the previously accepted P series generator and design values. As can be seen, the performance from this and other generators is very reproducible.

Table 2-18. Acceptance Test Results: SNAP-21 Thermoelectric Generators

Parameter	A10P2	A10P3	A10P4	A10P5	Design Values
Hot Junction Temperature, T_h (°F)	904	897	897	900	900
Cold Junction Temperature, T_c (°F)	106	104	105	105	105
Open Circuit Voltage, E_o (vdc)	8.26	8.16	8.17	8.15	7.99
Load Voltage, V_L (vdc)	4.73	4.73	4.73	4.73	4.73
Thermopile Resistance, R_1 (ohms)	1.44	1.41	1.45	1.43	1.35
Power Output, P_o (watts)	11.54	11.49	11.18	11.35	11.4
Power Output Ratio, P_x/P_c	1.02	1.02	0.99	0.993	**

**Design requirements for P_x/P_c ratio is a minimum of 0.95.

2.6 POWER CONDITIONERS

2.6.1 Phase I Power Conditioners

Phase I electronic components testing continued this past quarter with the automatic selector switch, power conditioner MP-C and regulators operating satisfactorily. An exception to this is regulator "C" which is fluctuating in performance.

Regulator "C" is a Trio-Lab regulator. There are a total of four such regulators on test (see Table 2-19). The test set-up was examined and it appears that the characteristics of regulator "C" are changing. The regulator will continue on test.

Power conditioner MP-B will not be put back on test. The primary reason is that the experimental tests conducted during design of Phase II power conditioner might have impaired the long-term reliability of some of the components. However, starting characteristics data received from these tests were very helpful in the design of present power conditioners.

Figure 2-43 is a plot of pertinent data for the life testing of this power conditioner. It can be seen that the performance for this conditioner was very stable, and a design objective of an efficiency of 85 percent was exceeded.

Tables 2-19 through 2-22 are the life data for the Phase I electrical units. The performance for all units except regulator "C" has been stable.

2.6.2 Phase II Power Conditioners

Tables 2-23 and 2-24 are the performance data for Power Conditioner H10D3 and H10D6. It appears that the operating temperature has increased. This is probably due to the environment rather than the operation of the conditioners. This should have negligible effects on the performance of the units.

As can be seen, the performance for the modules has been stable.

2.7 ELECTRICAL RECEPTACLE AND STRAIN RELIEF PLUG

No effort was expended on this area during this quarter.

Table 2-19. Phase I Regulator Test Fixture Performance Data

Operating Hours	TRIO-LAB Regulators				High Power Regulator-A HPR-A	
	A Output (vdc)	C Output (vdc)	D Output (vdc)	F Output (vdc)	Output (vdc)	Operating Hours
18,369	21.75	21.86	22.49	21.93	26.78	17,552
18,729	21.72	21.79	22.47	21.90	26.77	17,912
19,257	21.72	21.78	22.46	21.89	26.80	18,440
19,401	21.72	21.78	22.46	21.88	26.81	18,584
19,881	21.54	21.63	22.41	21.88	26.46	19,064
20,265	21.53	21.55	22.42	21.90	26.47	19,448
20,673	21.53	21.46	22.42	21.88	26.51	19,856
21,117	21.49	21.39	22.40	21.84	26.51	20,360
21,161	21.52	21.37	22.39	21.85	26.51	21,344
22,617	21.60	20.79	22.40	21.88	26.48	21,800
23,145	21.46	21.45	22.35	21.82	26.45	22,328
23,769	21.46	21.13	22.31	21.82	26.36	22,952
24,297	21.35	21.52	22.41	21.82	26.31	23,480
24,777	21.43	20.93	22.33	21.76	26.34	23,960
25,137	21.49	21.00	22.36	21.83	26.47	24,320
25,449	21.49	21.00	22.39	21.84	26.53	24,632
25,929	21.50	20.97	22.39	21.83	26.56	25,112
26,381	21.51	20.95	22.40	21.84	26.60	25,564
26,693	21.74	21.81	22.46	21.92	26.93	25,876
28,061	21.52	21.30	22.41	21.83	26.52	27,244
28,541	21.51	21.27	22.38	21.81	26.56	27,724
29,525	21.48	21.00	22.33	21.75	26.52	28,708
30,773	21.46	21.01	22.31	21.75	26.52	29,956
31,733	21.48	20.82	22.32	21.76	26.53	30,916
32,189	21.49	20.28	22.33	21.80	26.51	31,372
33,029	21.51	20.25	22.36	21.78	26.55	32,212
33,941	21.61	21.07	22.39	21.81	26.73	33,124
34,541	21.70	21.73	22.39	21.83	26.78	33,724
35,405	21.70	21.74	22.40	21.85	26.85	34,588

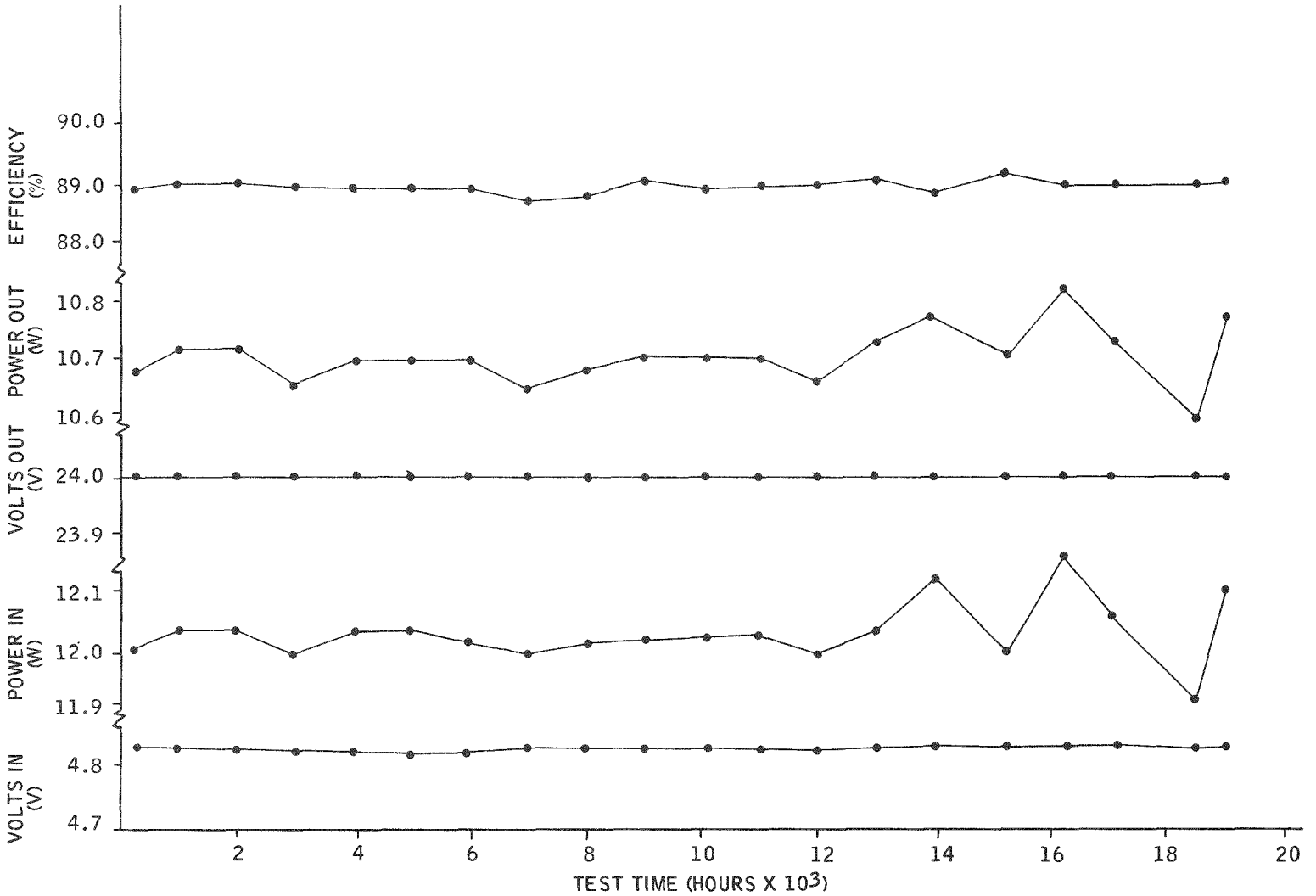

Figure 2-43. Power Conditioner MP-B Performance

Table 2-20. Performance of Phase I Power Conditioner MP-C

Converter Performance Power Conditioner	E_I (volts)	I_I (amps)	P_I (watts)	E_o (volts)	I_o (amps)	P_o (watts)	Efficiency %	Hours on Test	Notes
MP-C	4.913	2.395	11.809	24.00	0.436	10.464	88.61	15,783	
	4.908	2.360	11.606	24.00	0.429	10.296	88.71	16,143	
	4.909	2.374	11 757	24.00	0.432	10.368	88.19	16,671	
	4.910	2.378	11.779	24.00	0.433	10.392	88.22	16,815	
	4.906	2.372	11.740	24.00	0.432	10.368	88.31	17,295	
	4.905	2.374	11.747	24.00	0.432	10.368	88.26	17,679	
	4.904	2.353	11.642	24.00	0.428	10.272	88.23	17,087	
	4.909	2.389	11.831	24.00	0.439	10,416	88.04	18,591	
	4.912	2.395	11 867	24.00	0.436	10.464	88.18	19,575	
	4,913	2.396	11,878	24.00	0.436	10.464	88.10	20,031	
	4.910	2.375	11.764	24.00	0.432	10.368	88.13	20,559	
	4.908	2.371	11.740	24.00	0.431	10.344	88.11	21,183	
	4.909	2.375	11.762	24.00	0.432	10.368	88.15	21,811	
	4.909	2.376	11.767	24.00	0.432	10.368	88.11	22,098	
	4.910	2.375	11.764	24.00	0.432	10.368	88.13	22,485	
	4.912	2.403	11.907	24.00	0.438	10.512	88.28	22,770	
	4.911	2.377	11.776	24.00	0.433	10.380	88.92	23,250	
	4.909	2.357	11.674	24.00	0.428	10.270	87.99	24,066	Note: Unit accidentally shut down. Discovered on 12/22/67. Power restored 12/22/67.
	4.908	2.368	11.725	24.00	0.431	10.344	88.22	25,434	
	4.908	2.368	11.725	24.00	0.430	10.320	88.02	25,914	
	4.908	2.374	11.755	24.00	0.432	10.368	88.21	26,898	
	4.908	2.376	11.764	24.00	0.432	10.368	88.13	28,146	
	4.910	2.378	11.779	24.00	0.433	10.384	88.16	29,106	
	4.910	2.395	11.862	24.00	0.435	10.440	88.01	29,562	
	4.909	2.395	11.860	24.00	0.435	10.440	88.03	30,402	
	4.907	2.375	11.757	24.00	0.432	10.368	88.18	31.314	
	4.905	2.373	11.743	24.00	0.434	10.416	88.70	31,914	
	4.904	2.371	11.730	24.00	0.431	10.344	88.18	32,778	

Table 2-21. Phase I Automatic Selector Switch Performance Data

Notes	Hours	Output Voltage	
		Conditioner MP-A (vdc)	Conditioner MP-D (vdc)
	13,583	24.54	24.59
	13,943	24.55	24.60
	14,471	24.56	24.60
	14,615	24.55	24.59
Note: System turned off from 4/24/67 to 6/6/67	15,095	24.62	24.58
	15,479	24.62	24.58
	15,887	24.50	24.59
	16,343	24.46	24.58
	16,799	24.45	24.57
	17,327	24.47	24.55
	17,951	24.50	24.55
	18,479	24.47	24.59
	18,959	24.47	24.57
	19,319	24.48	24.59
	19,631	24.48	24.58
	20,111	24.47	24.58
	20,687	24.45	24.56
	20,999	24.48	24.56
	22,367	24.49	24.60
Note: At 22,367 hours system shut down to install into cabinet type mount (2/28/67).	22,895	24.49	24.56
	24,119	24.49	24.57
	24,719	24.50	24.57
Note: 8/27/68 unit put back on test.	25,583	24.51	24.58

Table 2-22. Phase I Regulator I Performance Data

Operating Hours	No-Load Voltage (vdc)
15,783	24.54
16,143	24.54
16,671	24.54
16,815	24.53
17,295	24.54
17,679	24.54
18,087	24.53
18,591	24.53
19,575	24.52
20,031	24.52
20,559	24.51
21,183	24.52
21,811	24.52
22,098	24.51
22,485	24.51
22,770	24.50
23,250	24.51
24,066	24.51
25,434	24.49
25,914	24.48
26,898	24.52
28,146	24.52
29,106	24.52
29,562	24.52
30,402	24.51
31,314	24.52
31,914	24.52
32,778	24.52

Table 2-23. Power Conditioner H10D3 Performance Data

E_I Primary (volts)	I_I Primary (amps)	P_I Primary (watts)	E_I Bias (volts)	I_I Bias (amps)	P_I Bias (watts)	E_o (volts)	I_o (amps)	P_o (watts)	Efficiency (%)	Temp (°F)	Test* Hours
5 06	2 17	11 02	0 646	0 132	0 085	23 77	0 424	10 08	90 77	82	1296
5 06	2 17	11 00	0 657	0 132	0 085	23 76	0 423	10 05	90 66	82	1413
5 08	2 18	11 07	0 658	0 134	0 087	23 80	0 422	10 04	89 99	82	1576
5 08	2 18	11 07	0 647	0 132	0 085	23 81	0 422	10 05	90 09	80	1894
5 08	2 18	11 07	0 648	0 132	0 086	23 83	0 422	10 06	90 18	81	2106
5 08	2 18	11 07	0 648	0 134	0 087	23 82	0 422	10 05	90 10	86	2904
5 08	2 18	11 07	0 647	0 134	0 087	23 81	0 422	10 05	90 07	86	3575
5 08	2 18	11 07	0 648	0 134	0 087	23 82	0 422	10 05	90 07	86	4244

*Includes 1241 hours of short-term tests

Table 2-24. Power Conditioner H10D6 Performance Data

E_I Primary (volts)	I_I Primary (amps)	P_I Primary (watts)	E_I Bias (volts)	I_I Bias (amps)	P_I Bias (watts)	E_o (volts)	I_o (amps)	P_o (watts)	Efficiency (%)	Temp (°F)	Test* Hours
4 81	2 35	11 30	0 646	0 122	0 079	24 00	0 430	10 32	90 69	82	1296
4 81	2 35	11 30	0 646	0 122	0 079	24 00	0 430	10 32	90 69	82	1437
4 82	2 35	11 33	0 648	0 122	0 079	24 08	0 425	10 23	89 67	82	1600
4 83	2 35	11 35	0 648	0 122	0 079	24 20	0 430	10 41	91 08	80	1968
4 83	2 35	11 35	0 648	0 122	0 079	24 09	0 425	10 24	89 60	81	2278
4 82	2 35	11 33	0 648	0 122	0 079	24 07	0 425	10 23	89 67	87	2904
4 82	2 35	11 33	0 647	0 122	0 079	24 07	0 425	10 23	89 67	86	3575
4 82	2 35	11 33	0 648	0 122	0 079	24 07	0 425	10 24	89 75	87	4244

*Includes 1271 hours of short-term tests

2.8 PRESSURE VESSEL

Pressure vessel components (body and long and short cover) were reinspected and reidentified to the latest drawing revision.

The pressure vessel cover assemblies and the power conditioners have been completed. The short- and long-cover assemblies were used for fueled systems S10P1 and S10P2, respectively.

3.0 TASK II – 20-WATT SYSTEM

No effort was expended on this subtask during this report period.

4.0 PLANNED EFFORT FOR NEXT QUARTER

- The Final Development Test Plan for SNAP-21 Fueled Systems will be revised and reissued.
- Systems S10P1 and S10P2 will be dynamically tested and hydrostatically tested.
- Systems S10P1 and S10P2 will be completely characterized thermally and electrically; will be shipped to NRDL and will be implanted in the ocean.
- System S10P3 will be fueled, dynamically tested, hydrostatically tested, and completely characterized thermally and electrically.
- Complete Revision 1 of the Final Development Test Plan for SNAP-21 Fueled Systems.
- Complete Final Design Description.
- Complete Final Safety Analysis Report.
- Assist NAVSHIPS R&D Center with assembly of 10-couple module number 5.
- Complete Insulation System B10DL5 and integrate it with system S10P3.
- Rebuild Insulation System B10Q1 into B10DL6 and place it on long-term test.
- Complete development work on hydroformed inner liners and incorporate them into Insulation Systems B10DL7 and B10DL8.

- Initiate Task II planning.
- Initiate design and development of Task II components.
- Complete Operational Safety Analysis.
- Rebuild System S10D3 and place it on long-term test.
- Continue testing Phase I and Phase II thermoelectric generators.
- Continue long-term test of Phase II power conditioners.